Effects of chlorine exposure on physiochemical properties and performance of polyamide membranes

Do, Thanh Van

2013

Do, T. V. (2013). Effects of chlorine exposure on physiochemical properties and performance of polyamide membranes. Doctoral thesis, Nanyang Technological University, Singapore.

https://hdl.handle.net/10356/53527

https://doi.org/10.32657/10356/53527

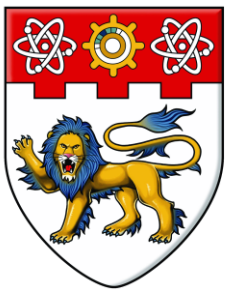

NANYANG TECHNOLOGICAL UNIVERSITY

EFFECTS OF CHLORINE EXPOSURE ON PHYSIOCHEMICAL PROPERTIES AND PERFORMANCE OF POLYAMIDE MEMBRANES

DO THANH VAN

SCHOOL OF CIVIL AND ENVIRONMENTAL ENGINEERING

2013

Effects of Chlorine Exposure on Physiochemical Properties and Performance of Polyamide Membranes

Do Thanh Van

School of Civil and Environmental Engineering

A thesis submitted to the Nanyang Technological University
in partial fulfillment of the requirement for the degree of
Doctor of Philosophy

2013

To my parents

and my little sister

Abstract

In nanofiltration (NF) and reverse osmosis (RO) processes, membranes are prone to biofouling and need to be cleaned periodically using oxidizing biocides, including the most widely used chlorine in different forms. The polyamide-based (PA) separation layer of thin film composite (TFC) membranes can be modified or degraded during contact with those agents. Understanding the effects of chlorine exposure on PA membranes is essential to improving the life span of membranes from both manufacturing and operation perspectives. This research presents a systematic investigation of the effects of chlorine exposure on the physiochemical properties and performance of PA membranes.

To study the degradation of PA NF and RO membranes by sodium hypochlorite, six coated and uncoated fully aromatic (FA) and piperazine (PIP) semi-aromatic PA membranes were treated with hypochlorite solution and analyzed by X-ray photoelectron spectroscopy (XPS) and attenuated total reflection-Fourier transform infrared (ATR-FTIR) spectroscopy. XPS results showed that in chlorine treated FA PA membranes the ratio of bound chlorine to surface nitrogen was 1:1 whereas it was only 1:6 in the case of PIP PA membranes. The surface oxygen of uncoated FA and PIP membranes increased with increasing hypochlorite concentration whereas it decreased for coated FA membranes. High resolution XPS data supported that chlorination increased the number of carboxylic groups on the PA surface, which appeared to form by hydrolysis of the amide bonds (C(O)–N). FTIR data indicated the disappearance of the amide II band (1541 cm^{-1}) and aromatic amide peak (1609 cm^{-1}) in both coated and uncoated chlorinated FA membranes, consistent with the N-chlorination suggested by the XPS results. Furthermore, the surface charge of the chlorinated membranes at low pH (< 6) became negative, consistent with amide-nitrogen chlorination. Chlorination appeared to either increase or decrease membrane hydrophobicity depending on the chlorination exposure conditions, which implied that N-chlorination and hydrolysis may be competing processes. The effects of property

changes on the performance were also observed for the NF90, BW30 and NF270 membranes.

Detailed appraisal of NF and RO membrane performance due to chlorine treatment was carried out by exposing three PA-TFC membranes (NF90, BW30 and NF270) to different concentrations of sodium hypochlorite (NaOCl) at pH 5 for 24 h. The elemental composition obtained from XPS showed that the chlorine content in the PA layer increased with the chlorine concentration. Treatment of membranes with 10 ppm Cl increased the membrane hydrophilicity. In contrast, when treated with 1000 ppm Cl or more, the membranes became less hydrophilic. Water permeability values for all three membrane types declined with increased chlorine concentrations. Filtration of polyethylene glycols (PEGs) with molecular weights of 200, 400 and 600 Daltons (Da) was performed to investigate the influence of chlorine treatment on the membrane molecular weight cut-off (MWCO) and rejection by size exclusion. Treatment with 10 and 100 ppm Cl lowered the MWCO while treatment with higher concentrations increased the MWCO. All chlorinated membranes experienced higher NaCl rejection compared to the virgin ones. The performance of NF90 was tested with respect to the rejection of inorganic contaminants including boric acid (H_3BO_3) and arsenic ($H_2AsO_4^-$). The boron rejection results paralleled the PEG rejection, whereas those for arsenic followed the NaCl rejection patterns. The changes in membrane performance due to chlorine treatment were explained in terms of competing mechanisms: membrane tightening, bond cleavage by N-chlorination and chlorination promoted polyamide hydrolysis.

The effects of chlorine exposure conditions on the physiochemical properties and performance of a polyamide membrane were studied by treating an NF90 membrane with sodium hypochlorite at different concentrations, pH and duration. The changes in membrane elemental composition and bonding chemistry obtained from XPS and ATR-FTIR revealed the impacts of two competing mechanisms: N-chlorination and chlorination promoted hydrolysis. More chlorine was incorporated into the PA matrix at pH < 7, at which HOCl is dominant; while

chlorine promoted hydrolysis was more favorable at pH > 7 with an abundance of hydroxyl groups. The membrane surface became more hydrophobic when chlorination was dominant, which in turn caused the water permeability of the chlorinated membrane to decrease. Meanwhile, the membrane became more hydrophilic and less cross-linked when hydrolysis effects were governing, which made the membrane more permeable for water. Rejection of charged solutes (NaCl, As(V)) improved under most chlorinating conditions due to increased charge density. However, when hydrolysis was severe (≥ 1000 ppm, pH 7 and 9), the enhanced charge repulsion effect could not compensate for the extensive amide bond cleavage, resulting in decreased rejection. The lower rejection of neutral boric acid provided strong evidence of a less cross-linked separation layer.

Acknowledgments

My years pursuing Ph.D have been a very exciting, challenging and rewarding experience and I owe my accomplishments to many people who have offered their support in various ways.

First and foremost, I would like to express my deepest gratitude to my supervisors Associate Professor Tang Chuyang and Professor James O. Leckie for their patience, nurture and endless effort in guiding me throughout this research. I am truly blessed and honored to be your student. Thank you Chuyang for the countless long discussions that have not only made this study a success but also helped to build my confidence and vision for long term career. I am tremendously grateful for your patience and confidence in me during a not so smooth study path and your financial support towards the end. Thank you Jim for many insightful advices and constructive criticism throughout my work and for encouraging me to expand my horizons.

Special and sincere thank to Prof. Martin Reinhard for your inputs and critical reviews on my experiments and publications. It is a privilege to have you as a co-author of my papers. Warm thanks to Prof. William Krantz, whose infectious enthusiasm for science and life has inspired me every time we met. Your personal coaching in technical writing skills will benefit me for a lifetime. I would also like to express my gratitude to Assoc. Prof. Edmond Lo and Assoc. Prof. Adrian Law; your kindness and help during my second year have gone a long way and will never be forgotten.

A token of thanks goes to my current and former research group members (Chuyang's group): Wang Yining, Wei Jing, Gao Yiben, Qi Saren, She Qianhong, Zhang Minmin, Zou Shan, Dr. Li Weiyi, Dr. Qiu Changquan, Dr. Jin Xue, Dr. Ma Ning, Dr. Zhang Zan, Zhao Yang, Liu Xin, Gu Yangshuo, and the late Wang Yichao. All the late nights in the lab, the help with labwork or broken down

equipment, the group meetings and outings… have made precious memories of mine. I also thank my final year project (FYP) students, especially Ho Yung Lin and Lim Siow Kee for their hard work and contribution to experiments.

During my first year of Ph.D. studies in Stanford University, I have benefited greatly from the discussions with many talented members of Jim's group: Kaimin Shih, Young-Nam Kwon, Alexander Robertson (Sandy), Federico Pacheco and Martin's group: Eva Steinle-Darling, Megan Plumlee, Sophie Walewijk, Jennie Lioue. I am thankful for their sharing in many research aspects such as critical thinking, analysis techniques and experimental organizing.

I would like to thank all the technicians in the Environment Laboratory, especially Phang-Tay Beng Choo, Lim-Tay Chew Wang, Aidil bin Md Idris, Tan Han Khiang, Yong Fook Yew and Ong Chee Yung for their assistance in sample analysis and equipment purchase. I have received great help with XPS analysis from Chow Shiau Kee (School of Mechanical and Aerospace Engineering) and ICP-MS measurements from Assoc. Prof. Richard Webster and Bahareh Khezri (School of Physical and Mathematical Sciences). Soo Ching Ng, Manesia Bt. Ahmad, Christiana Tan-Soh and Duc Wong are thanked for their valuable assistance with administrative procedures.

To my friends all over the world, in the basement 4 offices and my SSP classmates, I value our friendship. I would like to cherish Loc Nguyen, Mi Nguyen, Keat Lim, Nguyet Minh Le; no matter what distance, you have always managed to send your care, comfort, giggles and rainbows over. Deep appreciation goes to Chien Nguyen and Thang Nguyen for help with Matlab and other programming. Sincere thanks goes to Ha Le for help with thesis proof-reading and for being my extended family, together with Tuyet Minh Le.

Heartfelt appreciation is next extended to Jewel Chew who has taken me in as a sister, given not only a peaceful home but also lots of care. I can never thank her enough for many fun moments and wise advices and in daily life.

Last but not least, I would like to dedicate this dissertation to my loving Mom and Dad and my precious little sister for their unconditional and continuous support and encouragement. Along the years, I am more aware of and deeply appreciate the immenseness of my parents' love and sacrifice for their children. I am sure only a mom can feel eager and happy to spend her vacation in the lab, helping the daughter with pH control and other tedious measurements. To my sister – my best friend and confidant, you are my source of joy and fire.

This research was financially supported by the Tier 1 Research Grant #RG6/07, Ministry of Education, Singapore and the Singapore Stanford Partnership Program. I would like to acknowledge the Singapore Membrane Technology Centre for lab facility access, and Dow FilmTec and GE Osmonics for providing the membrane samples.

Table of Contents

List of Publications

Van Thanh Do, Chuyang Y. Tang, Martin Reinhard, and James O. Leckie (2012). "Degradation of Polyamide Nanofiltration and Reverse Osmosis Membranes by Hypochlorite." Environmental Science & Technology 46(2): 852-859.

Van Thanh Do, Chuyang Y. Tang, Martin Reinhard, and James O. Leckie (2012). "Effects of Hypochlorous Acid Exposure on the Rejection of Salt, Polyethylene Glycols, Boron and Arsenic (V) by Nanofiltration and Reverse Osmosis Membranes." Water Research 46(16): 5217-5223.

Van Thanh Do, Chuyang Y. Tang, Martin Reinhard, and James O. Leckie (2012). "Effects of Chlorine Exposure Conditions on Physiochemical Properties and Performance of a Polyamide Membrane – Mechanisms and Implications." Environmental Science & Technology 46 (24): 13184-13192.

List of Tables

List of Figures

List of Abbreviations and Symbols

Abbreviations

ATR-FTIR	Attenuated total reflection Fourier transform infrared spectroscopy
BE	Binding energy
DBP	Disinfection-byproduct
FA	Fully aromatic
GPC	Gel permeation chromatography
ICP-MS	Inductively coupled plasma with mass spectrometry
ICP-OES	Inductively coupled plasma with optical emission spectrophotometry
IEP	Isoelectric point
IP	Interfacial polymerization
MF	Microfiltration
MPD	M-phenylene diamine, also 1,3-benzenediamine
MWCO	Molecular weight cut-off
NF	Nanofiltration
NMR	Nuclear magnetic resonance
PA	Polyamide
PEG	Polyethylene glycol
PhAC	Pharmaceutically active compound
PIP	Piperazine
PVA	Polyvinyl alcohol
RO	Reverse osmosis
RSF	Relative sensitivity factors
TFC	Thin-film composite
TMC	Trimesoyl chloride
TMP	Trans-membrane pressure
UF	Ultrafiltration
XPS	X-ray photoelectron spectroscopy

Symbols

A	Water permeability coefficient
A_m	Membrane area
B	Solute permeability coefficient

C_b	Solute bulk concentration
C_f	Solute feed concentration
Cl_T	Total free chlorine
C_p	Solute permeate concentration
J	Flux
J_w	Water flux
K_a	Acidity constant
ΔP	Applied filtration pressure difference
Q_p	Water volumetric flow rate
R	Solute rejection
R_g	Universal gas constant
R_m	Total hydraulic resistance of the membrane

Greek letters

$\Delta\pi$	Osmotic pressure difference
ε	Permittivity
ζ	Zeta potential
η	Permeate viscosity
κ	Conductivity of solution
θ	Contact angle

Chapter 1

Introduction

1.1 Problem statement

The 21st century has been named the "century of water shortage" to raise the public awareness about this manifesting global crisis (Mehdizadeh, 2006). Since 1900, rapid population growth, together with intensified agriculture and industry has sent water demand soaring six-fold (FAO, 2009). Meanwhile, sustainable fresh water supplies are constantly and significantly depleted due to pollution and changing climatic patterns. Lower quality water sources (wastewater, brackish and sea waters) are now in the research spotlight as attractive options (Wintgens et al., 2005; Gray et al., 2011). However, these alternatives put stress on process technologies to treat their associated contaminants of new and wider variation and higher concentration to meet the increasingly stringent health regulations (e.g., lower maximum contaminant levels and more regulated chemicals) (Zhou and Smith, 2001). Nanofiltration (NF) and reverse osmosis (RO) processes that mainly employ polyamide-based (PA) thin film composite (TFC) membranes have become the leading technology to address the above challenges, offering several significant advantages such as cost effective and high quality water product, smaller footprint, easier up-scaling, operation and maintenance (Lee et al., 2010; Fane et al., 2011; Gray et al., 2011).

A major issue in membrane processes is fouling by colloids, inorganic and organic substances and microorganisms (Antony et al., 2011) which requires chemical cleaning (Watanabe and Kimura, 2011). However, exposure of PA membranes to cleaning agents, among which chlorine in different forms and its derivatives are most common, will gradually degrade performance and shorten their life span (Glater et al., 1994). It has been reported that exposure to chlorine

can cause the flux to decline (Glater et al., 1981; Koo et al., 1986; Soice et al., 2003; Kwon and Leckie, 2006b; Kwon et al., 2006; Kang et al., 2007; Simon et al., 2009; Ettori et al., 2011) and either increase (Kwon and Leckie, 2006b; Kwon et al., 2006; Simon et al., 2009) or decrease (Glater et al., 1981; Koo et al., 1986; Soice et al., 2003; Kwon and Leckie, 2006b; Kwon et al., 2006; Kang et al., 2007; Simon et al., 2009; Ettori et al., 2011) the salt rejection. Nonetheless, certain chlorine exposure conditions can improve flux and salt rejection of PA membranes, and are employed as a post-treatment in membrane manufacturing (Glater et al., 1981; Jons et al., 1999; Kwon and Leckie, 2006b; Kwon et al., 2006; Kang et al., 2007; Zhai et al., 2011). Factors that influence the chlorination impacts on membranes were identified to be exposure chlorine concentration, pH and duration and chemistries of the PA layer (Lowell et al., 1987; Glater et al., 1994; Soice et al., 2003; Ettori et al., 2011).

A great deal of effort has been put into understanding the chlorine attack pathways on PA membranes, for which several mechanisms were proposed. N-chlorination occurs when active chlorine binds with the lone electron pair of the amide N atom to become N-chloroamide (Challis and Challis, 1970; Glater et al., 1994; Jensen et al., 1999; Kwon et al., 2008). Ring chlorination mechanism suggests that chlorine can attach to the amide aromatic ring via direct electrophilic substitution (Shafer, 1970; Glater and Zachariah, 1985) or via intra-molecular rearrangement from N-chloroamide (Orton and Jones, 1909; Orton et al., 1928; Kawaguchi and Tamura, 1984a). Based on these mechanisms, a number of physical and chemical processes were proposed to explain the opposing observations of chlorine exposure impacts on membrane performance, which are hydrophobicity changes (Koo et al., 1986), more rigid polymer conformation (Avlonitis et al., 1992; Soice et al., 2004; Kwon and Leckie, 2006a; b), polyamide chain cleavage (Glater et al., 1981; Glater et al., 1983; Koo et al., 1986), or physical separation of the PA rejection layer from its polysulfone support (Soice et al., 2004). However, these propositions still could not explain the opposing observations consistently. More investigations and possibly additional mechanisms

are required to obtain insight into the various membrane degradation processes by chlorination.

While the data about the influence of membrane chlorination on flux and NaCl rejection are well-documented, studies of the effects of membrane chlorination on the passage of other solutes through NF and RO membranes are limited. Investigation on rejection of trace organic compounds by chlorinated NF and RO membranes suggested that changes in rejection are the results of complex interactions between modified membrane properties and the nature of the solutes under filtration conditions (Urase and Sato, 2007; Simon et al., 2009). Studies on inorganic boron rejection of chlorinated membranes by Taniguchi et al. (2001) and Zhai et al. (2011) focused on the correlation between the rejection of NaCl and boron and the effects of feed pH and hypochlorite concentrations on rejection rather than on explaining the rejection mechanism. The passage of trace organic and inorganic compounds, such as pharmaceutically active compounds or boron and arsenic through membranes affected by chlorine is an important issue and requires more research because these contaminants are of great concern in desalination and wastewater reclamation (Gray et al., 2011; Leverenz and Asano, 2011).

1.2 Objectives

The overall focus of this research was to systematically investigate the mechanisms that are involved in changes in physiochemical properties and performance of membranes due to chlorine exposure. NF and RO membranes of different PA chemistries were exposed to sodium hypochlorite at different concentrations, pH and durations. Changes in chemical bonding and composition, surface charge and functional groups and wettability of the PA layers were evaluated. The performance of chlorine exposed membranes was appraised in terms of water permeability, rejection of charged solutes (NaCl, arsenic (V) anion) and neutral solutes (polyethylene glycols – PEGs and boric acid). The specific objectives were:

1. To systematically characterize changes in chemical structure and composition, surface charge and wettability of different PA chemistries under different chlorine concentrations and exposure durations at constant pH.

2. To interpret the above changes consistently using available mechanisms or incorporating new propositions.

3. To elucidate the impacts of chlorine exposure on different rejection mechanisms (size exclusion and charge repulsion) of RO and NF membranes using charged and neutral solutes at constant pH.

4. To assess the effects of chlorine concentrations, pH and exposure durations on changes in membrane physiochemical properties and performance.

1.3 Hypotheses and investigative approach

1.3.1 Hypotheses

This research proposed and examined the following hypotheses:

1. The effects of chlorination on different membrane chemistries are dissimilar:
   - binding of chlorine to secondary amide happens more readily than to tertiary amide
   - membrane coating layer can prevent chlorine from binding to the PA layer

2. Incorporation of chlorine into PA matrix can simultaneously promote hydrolysis of PA layer. The existence of hydrolysis results in:
   - an increase oxygen content of the PA layer
   - a more negatively charged and more hydrophilic membrane surface due to addition of carboxylic groups

3. The pHs of chlorine solutions determine the concentrations of HOCl OCl^- and OH^- species; therefore, pH directly affects the extent of both chlorination and chlorination promoted hydrolysis of the PA layer:
   - incorporation of chlorine into the PA layer increases as pH reduces, due to the domination of HOCl, which is a stronger chlorinating agent than OCl^-
   - hydrolysis happens more readily at higher pHs due to abundant OH^- groups

4. Chlorination and chlorination promoted hydrolysis produce competing effects on the following aspects of the physiochemical properties and performance of the membranes:
   - PA structure
   - membrane hydrophilicity
   - membrane surface charge
   - rejection by size exclusion
   - rejection by charge repulsion

1.3.2 Investigative approach

The experimental approach involved the study of state-of-the-art membranes representing semi-aromatic piperazine and fully aromatic (with and without coating layer) PA chemistries. Commercial membranes (NF270, HL, NF90, XLE, BW30 and SW30HR) were chosen owing to their well-documented and stable physiochemical properties and performance. The investigated parameters for chlorine treatment conditions included concentration, pH and treated duration. Sodium hypochlorite, NaOCl was used as chlorinating agent because it is most commonly used in membrane bio-cleaning and safe to handle. Chlorine concentrations range from 1 and 10 ppm Cl, which mimic common practice in plant operation, to 100, 1000 and 2000 ppm Cl, which accelerate the degradation process in the laboratory. Since NaOCl has a $pK_a \sim 7.5$, the treatment pHs were set at 5, 7 and 9 to achieve different chlorine speciation.

X-ray photoemission spectroscopy (XPS) and attenuated total reflection-Fourier transform infrared (ATR-FTIR) spectroscopy provided data for chemical composition and bonding at the membrane surface and bulk. The changes in the membrane surface charge and wettability were determined using zeta potential and sessile drop contact angle measurements.

The performance of virgin and treated membranes was evaluated in terms of water permeability, rejection of charged (NaCl, arsenic (V) anion) and neutral (polyethylene glycols – PEGs and boric acid) solutes.

1.4 Scope and outline

This thesis contains seven chapters and four appendices. **Chapters 1-3** and **Chapter 7** present the introduction, literature review, experimental materials and methods and conclusions, respectively. The major results and discussion are presented in Chapters 4-6. Chapter 4 and Chapter 6 have been published in Environmental Science & Technology Journal. Chapter 5 has been published in Water Research Journal. The contents of Chapters 4-6 and appendices are summarized below in brief.

Chapter 4 presents evidences that chlorine treatment of different PA chemistry based NF and RO membranes leads to the uptake of chlorine and oxygen by PA membranes. Changes in the membrane surface and bulk chemistry as well as surface charge and wettability imply that subsequent reactions with hypochlorite appear to hydrolyze the amide C–N bond of the PA layer.

Chapter 5 assesses the performance changes of NF and RO membranes due to hypochlorite exposure. Changes in rejection by size exclusion are investigated by filtration of neutral solutes (PEGs and boron) while changes in rejection by charge repulsion are studied with NaCl and As(V). The importance of chlorination-promoted hydrolysis in Chapter 4 on both major solutes (NaCl), PEGs and trace contaminants (boron and As(V)) is discussed in detail.

Chapter 6 systematically investigates the chlorination effect on compound rejection. Factors that were considered included chlorination promoted hydrolysis, changes in membrane physioproperties and the influence of treatment conditions (chlorine concentration, pH and exposure duration) on membrane permeability and compound rejection. In addition, to highlight the effects of chlorine exposure, the rejection of inorganic contaminants was evaluated with boron and arsenic (V) representing neutral and charged solutes, respectively.

The appendices provide additional information to the main chapters. Appendix A consists of the calibration curve for determination of PEG concentration determination by gel permeation chromatography. Appendices B, C and D provide supplemental data for Chapters 4, 5, and 6, respectively.

Chapter 2

Background and Literature Review

2.1 Pressure-driven processes overview

The heart of membrane separation processes is the semi-permeable thin film that allows the passage of water yet retains other solutes or particles (Mulder, 1996). Pressure-driven membranes in water processes are mainly classified according to their pore size and rejection properties as microfiltration (MF), ultrafiltration (UF), nanofiltration (NF) and reverse osmosis (RO). Table 2-1 presents an overview of the properties of each membrane category.

Table 2-1. Characteristics of pressure-driven membranes (Mulder, 1996; Fane et al., 2011).

	Microfiltration	**Ultrafiltration**	**Nanofiltration**	**Reverse osmosis**
Pore size (nm)	50–10 000	1–100	~ 2	< 2
Operating pressure (bar)	0.1–2.0	1.0–5.0	2.0–10	10–100
MWCO (Da)	Not applicable	1000–300 000	> 100	> 20
Targeted contaminants	Bacteria, algae, suspended solids, turbidity	Bacteria, viruses, colloids, macromolecules	Di- and multivalent ions, natural organic matter	Dissolved monovalent ions, small molecules
Membrane materials	Polymeric, inorganic, metallic	Polymeric, some inorganic	TFC PA, cellulose acetate, other materials (Schäfer et al., 2005)	TFC PA, cellulose acetate

TFC PA: Thin-film composite polyamide

Low pressure MF and UF membranes are commonly employed to remove suspended solids, colloids, bacteria, and viruses in water and wastewater treatment or to concentrate valuable solutes such as proteins and dyes in biomedical and industrial applications. They are also used as a pretreatment step prior to NF and RO processes and are often operated in dead-end (or frontal) configuration, in which the feed water passes perpendicularly through the membrane (Fane et al., 2011; Watanabe and Kimura, 2011).

Non-porous RO membranes are the key in the desalination process of seawater and brackish water owing to their efficiency in removing monovalent ions and most other contaminants. NF membranes, which are more permeable and require less operating energy than RO membranes, are used to remove impurities down to the size of divalent ions, such as salts, hardness, pathogens, turbidity, disinfection-byproduct (DBP) precursors, pesticides and other potable water contaminants (Childress and Elimelech, 2000; Schäfer et al., 2005). NF and RO processes are typically configured in the cross-flow mode, which is illustrated in Figure 2-1. Feed water flows through the unit in parallel to the membrane surface at a cross-flow velocity. Trans-membrane pressure is the driving force for water to pass through the membrane as permeate while dissolved solutes are retained and discharged as retentate/concentrate.

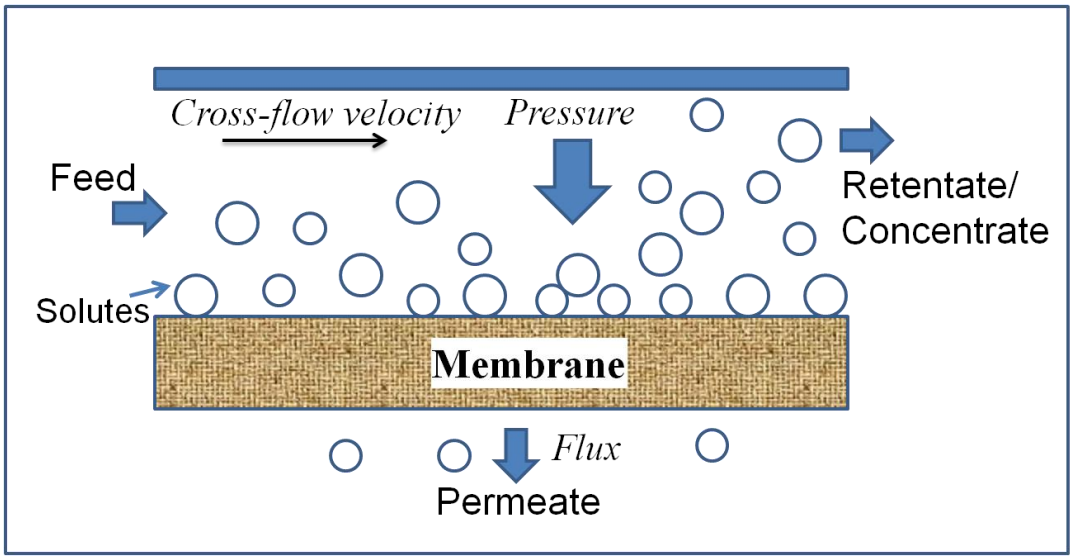

Figure 2-1. Schematic operation of a cross-flow filtration unit.

The permeate flux, J (volumetric), is related to the applied pressure difference, ΔP, and the osmotic pressure difference, $\Delta\pi$, across the membrane, permeate viscosity, η, and total hydraulic resistance, R_m of the membrane and fouling layer, if any, through the following equation (Schäfer et al., 2005):

$$J = \frac{\Delta P - \Delta\pi}{\eta R_m} \tag{2-1}$$

The membrane water flux (J_w), which is one of the main parameters to evaluate membrane performance, is obtained from the water volumetric flow rate, Q_p, that permeates through the membrane area, A_m, by:

$$J_w = \frac{Q_p}{A_m} \tag{2-2}$$

The water permeability coefficient, A is determined from the water flux, J_w, following the phenomenological Darcy's law (Mulder, 1996; Fane et al., 2011):

$$A = \frac{J_w}{\Delta P - \Delta\pi} \tag{2-3}$$

For dilute solute concentrations, the osmotic pressure difference, $\Delta\pi$ can be reliably estimated using the following equation. In case of more concentrated solutions, the $\Delta\pi$ can significantly deviate from the true value and should be calculated using more sophisticate approaches or software.

$$\Delta\pi = iR_gT(C_b - C_p) \tag{2-4}$$

where i is the dimensionless van't Hoff factor

R_g is the universal gas constant

T is the absolute temperature

C_b and C_p are the bulk and permeate salt concentrations, respectively.

The apparent solute rejection, R is determined from the solute concentrations of the permeate, C_p and of the feed, C_f by:

$$R = 1 - \frac{C_p}{C_f} \tag{2-5}$$

The solute permeability coefficient, B is determined from rejection test results by (Mulder, 1996; Fane et al., 2011):

$$B = J_w \times (\frac{1}{R} - 1) \tag{2-6}$$

2.2 Structures and chemistries of NF and RO PA membranes

An ideal membrane for a successful separation process requires thermal and chemical stability, good mechanical durability, and low production cost. The two main groups of NF and RO membranes are integrally skinned asymmetric ones formed by a phase inversion process and thin film composite (TFC) ones achieved via interfacial polymerization (IP) (Schäfer et al., 2005). Although phase inversion offers a one-step preparation of membranes at lower cost by "the controlled transformation of a cast polymeric solution from a liquid into a solid phase", it is limited to soluble polymers (Schäfer et al., 2005). Meanwhile, in IP process, the thickness of the separation layer can be reduced down to hundreds of nanometers by polymerization reaction that occurs between monomers at the interface of two immiscible liquid phases (Mulder, 1996). The multilayer approach by IP allows easy optimization of the individual layers and the functional layer to be fabricated out of different materials from those of the support.

TFC membranes typically consist of an ultrathin barrier layer cast on a thick, porous and nonselective supporting layer as illustrated in Figure 2-2 (Fane et al., 2011). The support layers usually include a nonwoven polyester web as reinforcing fabric, coated with an anisotropic microporous material, which is

frequently polysulfone (Figure 2-3) owing to its good mechanical strength, thermal stability and chemical resistance (Cadotte and Petersen, 1980; Petersen, 1993).

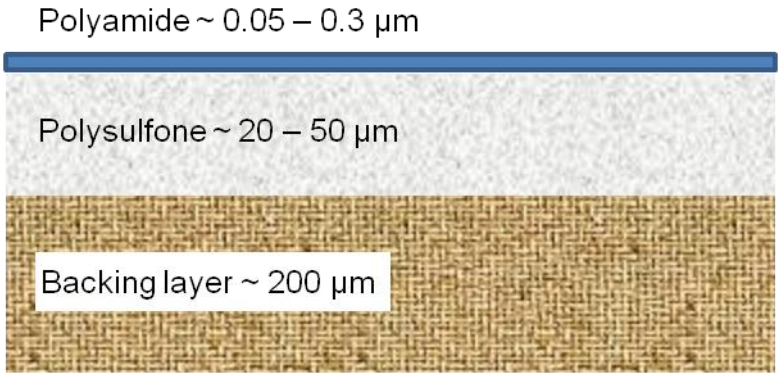

Figure 2-2. Typical structure of thin film composite polyamide membrane (Fane et al., 2011).

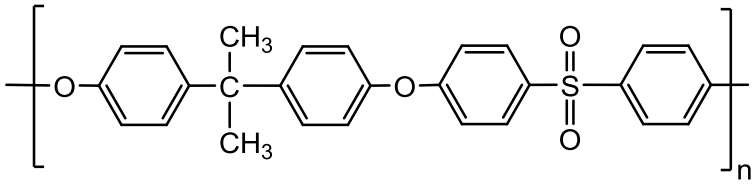

Figure 2-3. Polysulfone chemistry.

The chemistry of the active layer of a TFC membrane is critical in determining its physiochemical properties, such as surface charge, wettability and morphology and the permeation characteristics, such as molecular weight cut-off (MWCO) and permeation rate (Cadotte and Petersen, 1980). The most well-known and commonly used formula for the selective layer is the fully aromatic (FA) polyamide (PA) formed by interfacial polymerization of trimesoyl chloride (TMC) and 1,3-benzenediamine (also known as *m*-phenylene diamine, MPD) to obtain a three-dimensional cross-linked rejection layer (Figure 2-4a) (Petersen, 1993; Tang et al., 2009a). Since its invention in 1970s by Cadotte and co-workers, this membrane recipe was developed and commercialized by FilmTec under the name FT-30 and has become the principal chemistry for most commercial NF and RO membranes available today (Cadotte, 1985; Petersen, 1993). Polyamide from this

formula has a typically rough ridge-and-valley surface structure and carboxyl functional groups introduced by the TMC (Petersen and Cadotte, 1990; Petersen, 1993; Tang et al., 2006). A common replacement of MPD is piperazine (PIP), which results in a semi-aromatic PA (Figure 2-4b) with a smoother membrane surface (Petersen and Cadotte, 1990; Tang et al., 2009b).

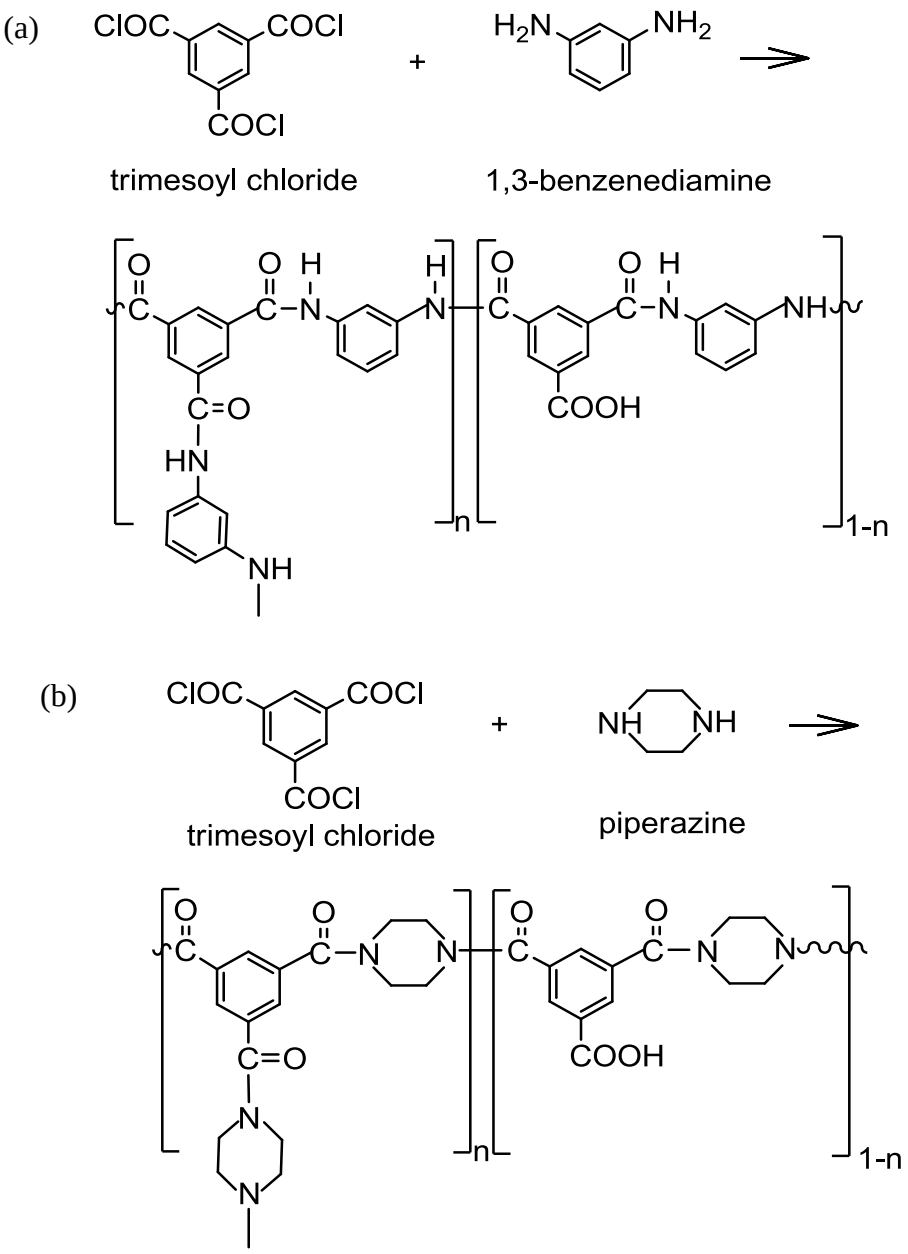

Figure 2-4. Typical chemistries of polyamides formed by interfacial polymerization: (a) Fully aromatic polyamide based on trimesoyl chloride (TMC) and 1,3-benzenediamine and (b) Semi-aromatic polyamide based on trimesoyl chloride (TMC) and piperazine.

The degree of polyamide cross-linking is indicated by the value of *n*, which is in the range of 0 – 1 and the O/N ratio in the range of 1 – 2. A linear aromatic PA (*n* = 0) has one free carboxyl group for every two amide groups, which results in the molecular formulas: $C_{15}H_{10}O_4N_2$ and $C_{13}H_{12}O_4N_2$ for FA and PIP PA, respectively, and the O/N ratio = 2. For a fully cross-linked aromatic PA (*n* = 1), each repeating unit shares an additional half of the amide ring of the inter-chain cross-link, which results in the molecular formulas: $C_{18}H_{12}O_3N_3$ and $C_{15}H_{15}O_3N_3$ for FA and PIP PA, respectively; and all O and N atoms form amide groups, hence the O/N ratio = 1 (Tang et al., 2007; 2009a).

In order to further enhance the membrane performance, reduce fouling and protect the membrane against oxidation, surface modifications are often employed to change the pore structure and wettability and introduce functional groups. Besides plasma treatment, polymer grafting and classical organic reactions, surface coating has proved to be an effective method (Schäfer et al., 2005). Neutral hydrophilic coatings, such as polyvinyl alcohol (PVA) can reduce the surface charge, hydrophobicity and roughness of the membranes (Ariza et al., 2000a; Tang et al., 2007; 2009a; b), which can mitigate foulant deposition on the surface.

2.3 Membrane rejection mechanisms

2.3.1 Rejection models

There have been several mechanistic and mathematical models developed to describe the passage of water and retention of solutes in NF/RO membranes. Two widely accepted mechanistic models, which were both initiated in the second half of twentieth century, are the solution-diffusion model and the pore-flow model (Wijmans and Baker, 1995).

2.3.1.1 Solution-diffusion model

The solution-diffusion model, proposed by Lonsdale et al. (1965), which is outlined in Figure 2-5, is widely accepted to explain the separation process in RO

membranes (Wijmans and Baker, 1995). Solutes and solvent dissolve into and diffuse through the homogenous and nonporous active layer of the RO membrane. The diffusion of solutes and solvent is uncoupled and driven by their individual chemical potential gradients across the membrane following Fick's law. The separation is governed by the difference in quantities of solutes or solvent that can dissolve in and the rates that they diffuse through the membrane matrix (Lonsdale et al., 1965; Soltanieh and Gill, 1981; Wijmans and Baker, 1995). In addition, compounds can be adsorbed onto the membrane surface and internal matrix, which results in their slower initial passage rates until all the sorption sites are saturated (Ng and Elimelech, 2004; Nghiem et al., 2004).

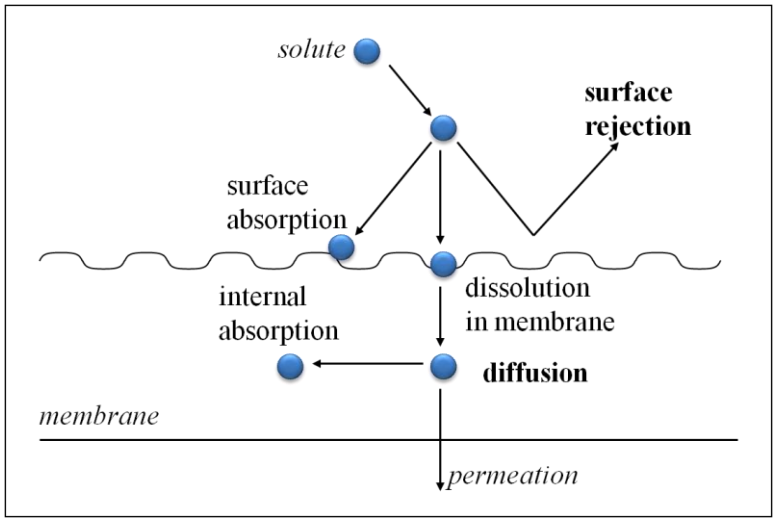

Figure 2-5. Separation processes in the solution-diffusion model (Steinle-Darling, 2008).

2.3.1.2 Pore-flow model

In contrast to the solution-diffusion model, the pore-flow model (Figure 2-6) describes the membrane as a nano-porous material and is applicable for NF membranes (Bowen and Doneva, 2000). Solutes convectively pass through the membrane matrix by means of solvent flow in the pores. Rejection is achieved when solutes are retained by the membrane pores. Both convection and diffusion account for the transport of water and solutes (Sourirajan and Matsuura, 1985; Wijmans and Baker, 1995).

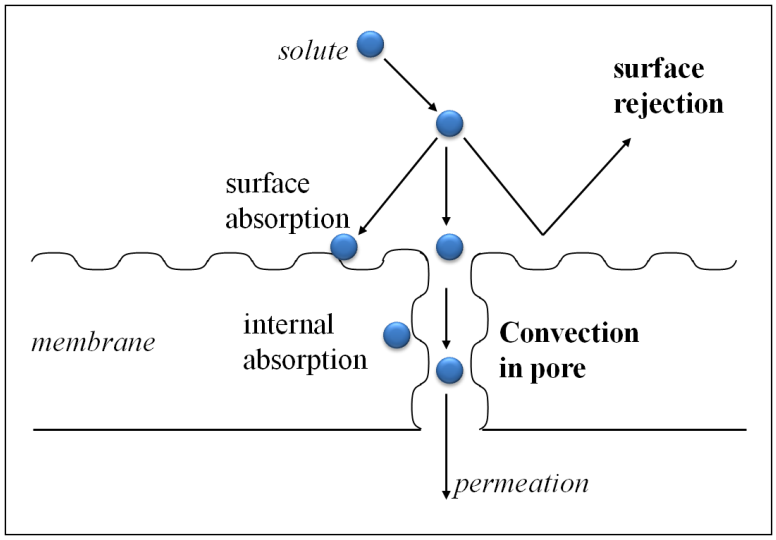

Figure 2-6. Separation processes in the pore-flow model (Steinle-Darling, 2008).

2.3.2 Factors affecting rejection

Although the aforementioned models have different assumptions about the structure of the membranes, they both agree that there are many additional factors affecting the separation process, especially in case of trace organic compounds, such as charge, size, hydrophobicity, polarity (Van der Bruggen et al., 2003; Bellona et al., 2004; Nghiem et al., 2004). These factors are further discussed in the following sections.

2.3.2.1 Steric interaction – size exclusion

Size exclusion considers that retention of a contaminant molecule is based only on its steric hindrance. This model can be visualized as a "sieving phenomenon, except that in membrane filtration, pores neither have a uniform pore size nor are the solutes of a uniform size" (Nghiem and Schäfer, 2005). Molecular weight cut-off (MWCO) is an indicator that uses the relationship between molecule size and weight to gauge membrane separation. MWCO, which usually has the unit of the Dalton (Da), is the weight of the lightest solute that is retained by more than 90% by the membrane (Van der Bruggen et al., 2003). Uncharged solutes that are commonly used as the molecular probe for the MWCO include polyethelyne glycol

PEG (Braghetta et al., 1997; López-Muñoz et al., 2009), saccharides (Seidel et al., 2001; Nghiem et al., 2004) and dyes. However, it should be noted that the MWCO does not precisely represent the actual size, rigidity or geometry of a molecule.

2.3.2.2 Electrostatic repulsion

As most of available membranes have a negatively charged surface, charge interaction between solutes and membranes plays an essential role in a separation process. Negatively charged molecules have been reported to experience electrostatic repulsion from membrane surfaces, and consequently are retained more than other non-charged compounds of the similar size (Kimura et al., 2003b). Since the charge of both the membrane and ionic compounds depends on pH, solution pH can greatly affect their repulsive interaction, and hence their rejection efficiency (Bellona and Drewes, 2005; Mänttäri et al., 2006; Nghiem et al., 2006).

2.3.2.3 Other factors

The polar organic compound separation process by RO/NF membranes is more complicated due to intervention of other factors such as polarity and hydrophobicity. These factors can alter the partitioning of solutes between the bulk solution and membrane surface (Nghiem and Schäfer, 2005). Van der Bruggen et al. (1998) have proposed that the dipole moment of solute molecules will cause their oppositely charged side to be attracted to the membrane surface. Hence, the dipole moment of compounds will enhance their passage through membranes.

Hydrophobicity can be another factor in the rejection of organic compounds. Most of the available PA-based NF and RO membranes have hydrophobic surfaces. Studies have indicated that hydrophobic compounds are adsorbed more by hydrophobic membranes (Kiso et al., 2001; Nghiem et al., 2002; Kimura et al., 2003a; Kimura et al., 2003b).

2.4 Chemistry of chlorine species

One of the major obstacles in membrane processes is fouling, which is defined as the accumulation of substances on a membrane surface and/or within the membrane pores (Schäfer et al., 2005). The four main categories of foulants are: 1. colloidal and particulate matter; 2. inorganic salts that cause scaling; 3. organic macromolecules; and 4. microorganisms that cause biofouling (Goosen et al., 2004; Bartels and Wilf, 2005). Fouling causes a decline in the permeate flux or an increased trans-membrane pressure, resulting in either loss of water throughput or additional energy consumption. Besides the physical membrane cleaning methods such as hydraulic backwashing, air scrubbing, sponge ball and brush cleaning, disinfection chemicals are employed to combat organic and biofouling (Mulder, 1996). In membrane operation, chlorine and its derivatives are widely used as cleaning agents and also as disinfectants to control biofouling for RO upstream (Glater et al., 1994; Gray et al., 2011; Watanabe and Kimura, 2011).

The earliest use of chlorine for water disinfection, which was in form of hypochlorite salt, dates back in 1850. It was later observed that it can achieve the same result as that of chlorine gas (White, 2010). Today, sodium hypochlorite – NaOCl is most commonly used in water disinfection and membrane cleaning because it is relatively safe to handle and cost-effective (Glater et al., 1994; White, 2010). Hypochlorite is usually prepared at 25 – 100 ppm total residual chlorine for membrane cleaning or dosed into the feed water of water/wastewater treatment plants (e.g., NEWater Factory in Singapore) at ~ 2.0 – 2.5 ppm at pH ~ 5 – 6 to restrain microorganism growth, reduce scale and other deposits on membranes (Wilf and Alt, 2000; Bartels and Wilf, 2005; Gray et al., 2011).

The disassociation of NaOCl in water at a pH above 2 gives major active chlorine species as follows:

$$NaOCl \leftrightarrow Na^{+} + OCl^{-} \quad (2\text{-}7)$$

$$OCl^{-} + H^{+} \leftrightarrow HOCl \quad (2\text{-}8)$$

The composition of the species depends on the solution pH and follows the equations (Benjamin, 2002):

$$[HOCl] = \frac{Cl_T [H^+]}{K_a + [H^+]} \quad (2\text{-}9)$$

$$[OCl^-] = \frac{Cl_T K_a}{K_a + [H^+]} \quad (2\text{-}10)$$

where: Cl_T is the free chlorine, which is defined as the sum of species containing the chlorine atom in the 0 or +1 oxidation state that are not combined with ammonia or organic nitrogen (White, 2010).

K_a is the acidity constant of hypochlorous acid, = 2.9×10^{-8} (Kwon and Leckie, 2006a; Silberberg, 2006).

Other trace chlorine species can be formed under specific conditions, such as:

$$HOCl\ (aq) + Cl^- + H^+ \leftrightarrow Cl_2\ (aq) + H_2O\ (l) \qquad \log K_1 = 3.43 \quad (2\text{-}11)$$

$$2HOCl\ (aq) \leftrightarrow Cl_2O\ (aq) + H_2O\ (l) \qquad \log K_2 = -2.06 \quad (2\text{-}12)$$

It was documented by White (2010) that HOCl is a more effective disinfectant than OCl^- because HOCl is uncharged and can penetrate the negatively charged walls of bacteria cells more readily. For example, HOCl is 80 times more effective than OCl^- for inactivation of *Escherichia coli* (Fair et al., 1948). Based on the oxidation/reduction potentials in Table 2-2, the oxidation strength of these species is established as: Cl_2 ~ HOCl > OCl^- (White, 2010). However, the electrophilic reactivity with the aromatic ring or "chlorination strength" of the species is established as $Cl_2 > Cl_2O \gg HOCl \gg OCl^-$ (Voudrias and Reinhard, 1988a; b; Sivey and Roberts, 2012).

Table 2-2. Half reactions and standard redox potentials (at 25 ^{o}C) for selected chlorine compounds (White, 2010).

Half-reaction	E^0 (V)
$Cl_2(aq) + 2e^- \rightarrow 2Cl^-$	+1.396
$HOCl + H^+ + 2e^- \rightarrow Cl^- + H_2O$	+1.482
$OCl^- + H_2O + 2e^- \rightarrow Cl^- + 2OH^-$	+0.81

2.5 Chlorination mechanisms

Chemical cleaning is an effective and indispensable method to mitigate the inevitable fouling problem in filtration processes, but it is also aggressive to PA membranes, causing membrane deterioration and performance loss. It is essential in both membrane manufacturing and operation to fully understand the causes of membrane degradation under chemical exposure, especially the commonly used chlorine in different forms. Numerous researches have tackled this issue and suggested several mechanisms for chlorine to attack the PA rejection layer as outlined in Figure 2-7.

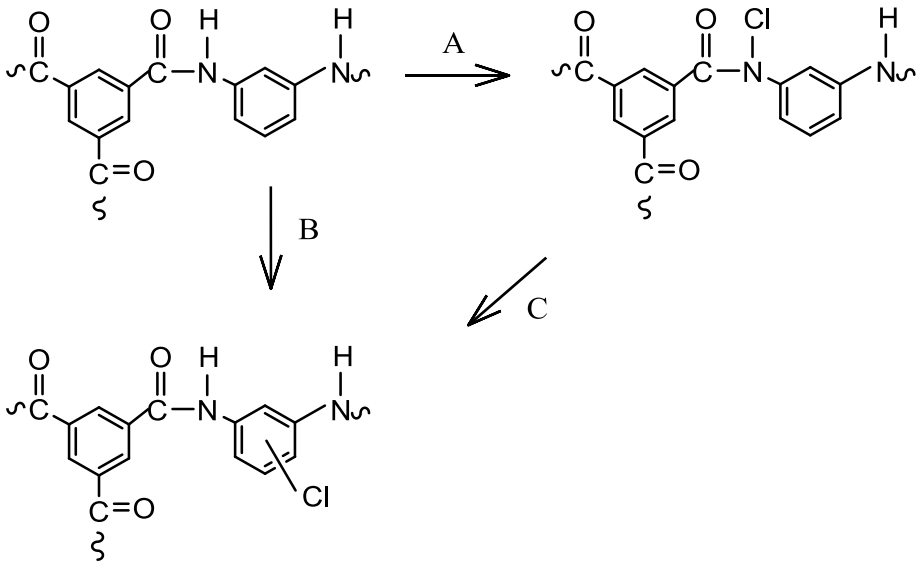

Figure 2-7. Chlorination mechanisms of fully aromatic polyamide (FA PA) membranes. (A) N-chlorination; (B) direct ring chlorination; (A) and (C) indirect ring chlorination by Orton rearrangement (Glater et al., 1994).

The secondary amide group of the FA PA has two typical resonance structures as shown in Figure 2-8, which account for its enhanced stability and diminished basicity of the N atom (Wade, 2006). The N-chlorination mechanism (Figure 2-9) proposed that active chlorine species having a partial positive charge can bind with the lone electron pair of either the N or O atom of the amide group and rearrange to become N-chloroamide (Hardy and Robson, 1967; Challis and Challis, 1970; Glater et al., 1994; Singh, 1994; Jensen et al., 1999; Kwon et al., 2008). It was observed from NMR (Kawaguchi and Tamura, 1984a; Jensen et al., 1999) and FTIR spectra (Kang et al., 2007) that chlorine attachment to the N atom can be reversed by treating with sulfite or alkaline solution. It was reported that the nitrogen of the tertiary amide in semi-aromatic PA (Figure 2-4) is not susceptible to chlorine attack due to the absence of an amide proton (Kawaguchi and Tamura, 1984a; b; Soice et al., 2003).

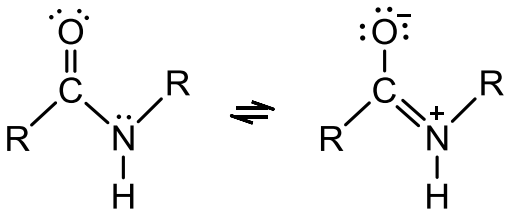

Figure 2-8. Resonance structures of amide bond (Wade, 2006).

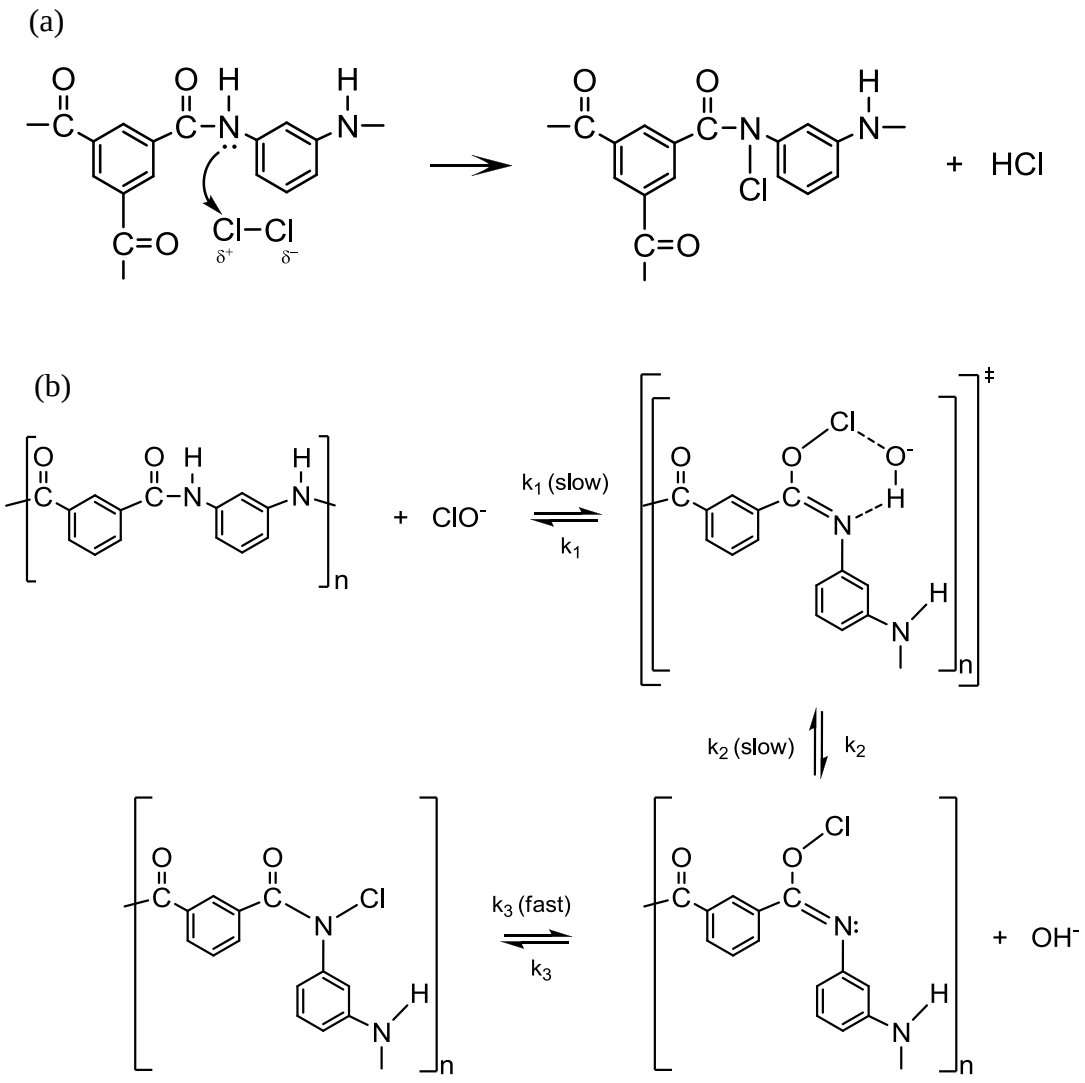

Figure 2-9. Mechanism of N-chlorination via (a) N atom (Kwon, 2005) and (b) O atom of amide group (Barassi and Borrmann, 2012).

In FA PA structure, N–H is an electron releasing group, hence it activates the ring reactivity while C=O is a ring deactivating group due to its electron withdrawing effect (Glater et al., 1994). The direct ring mechanism (Figure 2-10) suggested that chlorine is incorporated into the PA layer through electrophilic substitution at the aromatic ring of m-phenylene diamine, mostly observed at the *para*-position (Shafer, 1970; Glater and Zachariah, 1985). Using bromine as halogenating agents, Glater and Zachariah (1985) observed multiple ring bromination. However, Soice et al. (2003) only observed single chlorine addition to the ring and explained that chlorine can deactivate the ring from further

substitution owing to its electron withdrawing. They also suggested a "saturation point" for ring chlorination, implying that reaction sites are limited.

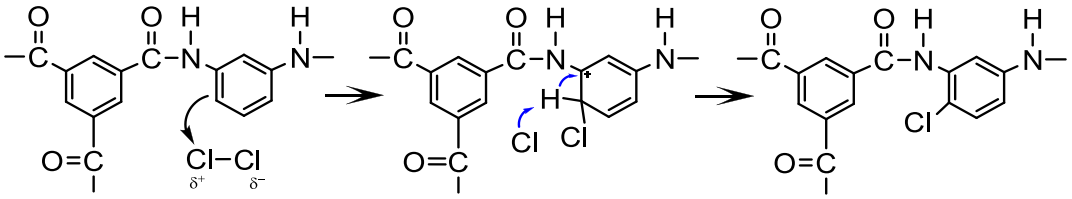

Figure 2-10. Mechanism of direct aromatic chlorination by electrophilic substitution (Kwon, 2005).

Indirect ring chlorination via N-chloroamide (Figure 2-11) was first observed by Mills in 1860 and later the Orton rearrangement mechanism was proposed by Orton and Jones (1909) and supported by others (Kawaguchi and Tamura, 1984a; b; Soice et al., 2003). The first step involves dechlorination of N-chloroamide and generation of elemental chlorine (Cl_2) in acid solution in the presence of chloride anions (Orton and Jones, 1909; Orton et al., 1928). Irreversible ring chlorination via electrophilic substitution by chlorine subsequently occurs at either the *para*- or *ortho*-position (Ingold, 1953; Kawaguchi and Tamura, 1984a).

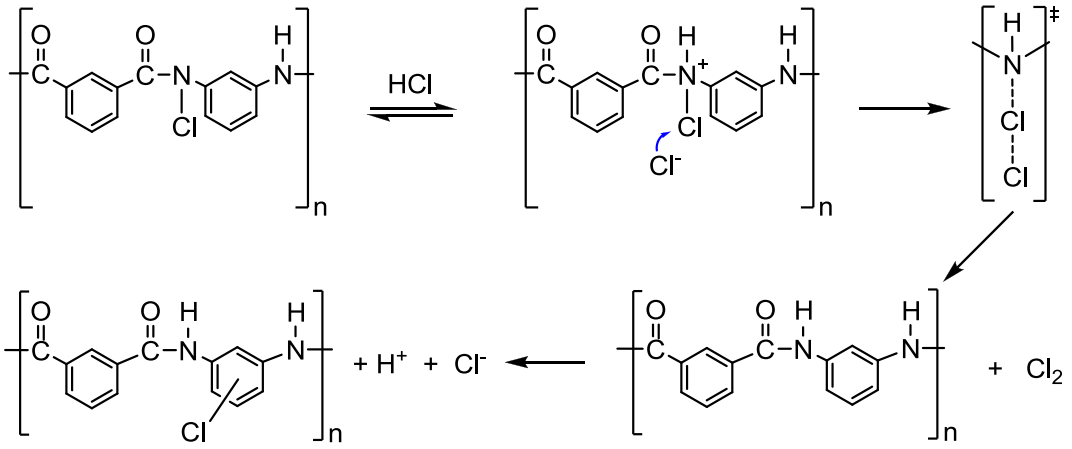

Figure 2-11. Indirect ring chlorination - Orton rearrangement (Barassi and Borrmann, 2012).

Addition of chlorine into the PA layer causes polymer deformation and is believed to be responsible for changes in membrane properties. At a more severe degree of chlorination, amide bond cleavage can occur when chlorine attacks the nitrogen or the ring of the amide group, thus leading to depolymerization. Koo et al. (1986) proposed that the cleavage was followed by benzene ring oxidation and resulted in substituted quinone derivatives. The pH of chlorine exposure was reported to affect the extent to which PA membranes are degraded by chlorination (Lowell et al., 1987; Soice et al., 2003; Ettori et al., 2011). Studies have shown that chlorine is more reactive with PA at low pH, at which HOCl is the dominating active chlorine species (Lowell et al., 1987; Avlonitis et al., 1992; Soice et al., 2003). Using simple model compounds, Soice et al. (2003; 2004) reported that OCl^- may not react directly with the amide and aromatic rings and suggested that a different unknown degradation mechanism occurs at pH 9 and above. Hoffman degradation was suggested by Avlonitis et al. (1992) where amide bond cleavage at high pH formed primary amines and carbon dioxide through loss of the carbonyl group. However, Hoffman degradation happens in alkaline condition, which is not applicable to wastewater treatment. Further studies are required to gain to insight into chlorination degradation at high pH.

Studies in the literature have favored chlorination by Orton rearrangement, but still not been able to rule out N-chlorination or direct ring chlorination (Glater et al., 1994). Although some studies have proposed that N-chlorination and direct ring chlorination can happen simultaneously and independently (Orton et al., 1928; Ingold, 1953; Bieron and Dinan, 1970; Antony et al., 2010), other studies seemed to only support either of them. For example, Glater and Zachariah (1985) only reported direct ring chlorination and still observed N–H bonding using IR and NMR spectral analysis. However, ring chlorination mechanisms alone cannot adequately explain certain phenomena consistently observed in PA chlorination such as the disappearance of the FTIR characteristic peaks associated with the N–H bond or the enhanced negative charge on membrane surface after chlorine exposure (Kwon and Leckie, 2006a; b; Kang et al., 2007; Simon et al., 2009; Ettori et al., 2011). Moreover, almost all previous studies have focused on the

incorporation of chlorine into the membrane matrix, but systematic studies on oxygen composition changes and the role of chlorine in promoting amide hydrolysis as a significant competing degradation reaction have not been emphasized or reported (Glater et al., 1994).

2.6 Effects of chlorination on membrane performance

2.6.1 Changes in water flux and NaCl rejection

Studies on the effects of chlorine exposure on membrane performance in terms of water permeability and NaCl rejection have led to divergent observations and numerous explanations based on the chlorination mechanisms in Section 2.5 and other processes. It has been reported that exposure to chlorine can cause the flux to decline and to either increase or decrease the salt rejection (Glater et al., 1981; Koo et al., 1986; Soice et al., 2003; Kwon and Leckie, 2006b; Kwon et al., 2006; Kang et al., 2007; Simon et al., 2009; Ettori et al., 2011). Nonetheless, certain chlorine exposure conditions can improve the flux and salt rejection of PA membranes, and are patented as a post-treatment in membrane manufacture (Cadotte, 1981; Uemura et al., 1988; Uemura et al., 1991; Jons et al., 1999). Generally, the performance changes depend on the chlorine exposure conditions such as concentration, pH and duration (Glater et al., 1994). A summary of profound studies on the performance of chlorinated PA membranes is presented in Table 2-3 and discussed in more detail below.

Table 2-3. Summary of typical chlorinated PA membrane performance.

References	Observations	Membrane chemistry (commercial name /company)	[Cl]* × h (pH)
Koo et al., 1986	Initial F↓ but ↑ with time, R↓ as F↑	FA PA (FT-30/Dow FilmTec)	100 ppm × 24, 48, 72 h (pH 7)
Glater et al., 1981	• FT-30: 3 ppm: F & R↑ (pH 5.8 & 8.6); F & R↓ (pH 3) • B-9: 3 ppm: F & R↓ (pH 8.6); F↑ & R↓ (pH 3 & 5.8)	• FA PA (FT-30/Dow FilmTec) • homogeneous aromatic PA (Aramid B-9/Dupont)	Use Cl_2 gas 3, 30 ppm × 40 h (pH 3, 5.8, 8.6)
Kwon and Leckie, 2006b	• pH 4: F↓; R↑ (100 ppm), R↓ (>500 ppm) • pH 9: F↑, R↑ (100 ppm), R↓ (>500 ppm)	FA PA (LFC1/ Hydranautics)	100, 500, 1000, 2000 ppm × 1 h (pH 4, 9)
Kwon et al., 2006b	• pH 4: F↓; R↑ (100, 500 ppm), R↓ (>1000 ppm) • pH 9: F↑, R unchanged (<500 ppm), R↓ (>1000 ppm)	LE (FA PA/Dow FilmTec)	100, 500, 1000, 2000 ppm × 1 h (pH 4, 9)
Kang et al., 2007	• pH 4 & 7: F & R↓ • pH 10: F & R↑ (<36 h), but F & R↓ (>36 h)	FA PA (RO/Hangzhou Beidouxing Membrane Co.Ltd, China)	10, 100 ppm × 10 h (pH 4, 7, 10)
Buch et al., 2008	F & R↓	AC PA (NF/Lab-cast)	1, 3, 5 ppm × 24 h (pH 7)
Simon et al., 2009	• F↓ in all cases • NF90, BW30 & NF270: R↑ slightly at 500 ppm, R↓ at 2000 ppm • TFC-SR2: R↓ at 500 ppm	• FA PA (NF90, BW30 /Dow FilmTec) • SAP PA (NF270/Dow FilmTec) • N.A. (TFC-SR2/Koch Membrane Systems)	500, 2000 ppm × 18 h (pH 10.5)
Antony et al., 2010	F↑ & R↓	FA PA (BW30-FR/Dow FilmTec)	25, 62.5, 250, 625 ppm × 16 h (pH 6)
Raval et al., 2010	F↑ for all exposure times & pH R↑ for pH 10, 12 R↓ for pH 8.5 & 12.5	FA PA (RO/Lab-cast)	4000 ppm × 15, 30, 45 mins (pH 8.5, 10, 12, 12.5)
Ettori et al., 2011	<400 ppm, pH 6.9, 8: F↑, R↓ slightly >400 ppm, pH 6.9, 8: F↓, R↓	FA PA (SW30HR-400/ Dow FilmTec)	40, 100, 400, 4000 ppm × 1 h (pH 5, 6.9, 8, 12)
Zhai et al., 2011	F↑ except slight F↓ at 2000 ppm R↑ in all cases	• Aromatic PA (Merlin & AG/GE Osmonics) • FA PA (BW30LE/Dow FilmTec)	1000, 2000, 4000 ppm × 0.25, 0.5, 0.75 h (pH 9)

Note: *: chlorine is in the form of NaOCl unless specified otherwise
F: water flux, R: NaCl rejection
↑: increase, ↓: decrease
FA PA: fully aromatic polyamide, SAP PA: semi-aromatic piperazine polyamide, and AC PA: aromatic-cycloaliphatic polyamide
N.A.: not available

The decline in water flux after membrane chlorination has been attributed to the presence of chlorine in the PA layer that causes an increase in membrane hydrophobicity (Koo et al., 1986). "Membrane tightening" due to chlorine addition (Glater et al., 1981; Glater et al., 1983) or formation of azo-compounds in the PA layer (Soice et al., 2003) or an increased degree of cross-linking (Avlonitis et al., 1992) were proposed to be the cause to a reduced flux and increased rejection. Alternatively, Kwon et al. suggested that the loss of hydrogen bonds between amidic hydrogen and the carbonyl groups in the polymer chains due to chlorination can lead to chain compaction and restricted water passage (Kwon and Leckie, 2006b; Kwon et al., 2006). It was consistently observed that chlorinated membranes experience enhanced surface negative charge, which can improve charged solute rejection due to Donnan effects, despite the weakened polymeric structure (Kwon and Leckie, 2006a; Simon et al., 2009).

In contrast, the observed increase in flux is usually accompanied by a decrease in salt rejection (Glater et al., 1981; Glater et al., 1983; Koo et al., 1986; Soice et al., 2004; Kwon and Leckie, 2006b; Kwon et al., 2006; Simon et al., 2009; Raval et al., 2010; Ettori et al., 2011). The most supported mechanism for this observation is polyamide chain cleavage at the amide bond (Glater et al., 1981; Glater et al., 1983; Koo et al., 1986; Singh, 1994; Taniguchi et al., 2001). However, in their study on model compounds, Soice et al. (2003; 2004) did not observe chain scission due to chlorination, and suggested that physical separation of the PA rejection layer from its polysulfone support could be responsible for the impaired performance. Avlonitis et al. (1992) investigated the physical properties of chlorinated polymeric membranes and proposed that acidic chlorination can decrease the intermolecular forces (i.e., hydrogen bonding) of the PA and transform its crystallized structure into an amorphous state that allows more solutes and solvent passage; and Hoffman rearrangement is the cause for membrane degradation during chlorination under basic conditions. Kwon et al. postulated that dislodging of hydrogen bonding between the carbonyl and amine due to chlorine attack introduces unbalanced dipole moments to the membrane surface and increases the hydrophilicity as well as the water flux (Kwon and Leckie, 2006b;

Kwon et al., 2006). Hydrogen bond dislodging also increases the rotational freedom or flexibility of the polymer chains and eases their self-rearrangement into stable positions, causing a systematic increase in flux.

The complex effects of chlorine exposure on membrane performance have resulted in contradicting phenomenological observations that were rationalized by various proposed mechanisms and processes. However, to obtain a consistent explanation by these mechanisms is still difficult. Therefore, further study and possibly additional mechanisms are required to obtain more insight into the membrane degradation process by chlorination.

2.6.2 Changes in rejection of trace contaminants

While data about the changes in membrane flux and NaCl rejection due to chlorine exposure are well-documented, studies on the effects of membrane chlorination on the passage of other trace organic and inorganic compounds through NF and RO membranes are limited. Inorganic contaminants, such as boron (in the form of boric acid and borate ion) and arsenic (commonly existing as arsenate (V) anion) are contaminants of concern in desalination (Macedonio and Drioli, 2008). A study by Taniguchi et al. (2001) focused on the mathematical correlation between the permeation of NaCl and boron for the chlorinated cross-linked fully-aromatic PA UTC-80 membranes (Toray Industries, Japan). The increase in boron permeation due to membrane chlorination at 10, 20 and 40 mg/L NaOCl, 24 h and pH 7 is attributed to bond cleavage proposed by Koo et al. (1986) without further explanation. Zhai et al. (2011) reported that hypochlorite treated PA RO membranes at pH 9 experienced enhanced boron rejection. However, the study focused on the effects of hypochlorite concentrations and filtration feed pH on rejection rather than on any explanation for the rejection mechanism.

Investigation on rejection of pharmaceutically active compounds (PhACs) by chlorinated NF and RO membranes suggested that changes in rejection are the result of complex interaction between modified membrane properties and the

nature of the solutes at filtration conditions (Urase and Sato, 2007; Simon et al., 2009). It was observed without mechanistic explanations in the study of Urase and Sato (2007) that a loose NF membrane was more sensitive to chlorine exposure than a tight one and both experienced an increase in pore size. However, their membranes were chlorinated at a fixed chlorine concentration (1250 ppm) without pH control. Moreover, the focus of their study was on the filtration conditions (e.g., pH, type of membranes, filtrated compounds) rather than chlorination conditions. Simon et al. (2009) presented a more detailed study on NF and RO membranes and explained the increased and decreased rejection of PhACs due to chlorine exposure using available mechanisms; their chlorination tests were conducted at 500 and 2000 ppm NaOCl at fixed pH 10.5.

Obviously, very few compounds have been used in rejection tests for chlorinated membranes; yet, the complex properties of inorganic and organic compounds, such as arsenic, surfactants, endocrine disruptors, etc., can involve a very different interaction with chlorinated membranes. It is of considerable basic and practical interest to bridge this knowledge gap. To the best of my knowledge, there is no report in the literature that has focused on the MWCO of chlorinated membranes determined by PEGs. The effect of chlorination pH on trace contaminant rejection is also lacking in the literature.

2.7 Summary of knowledge gaps

Polyamide based membranes are widely employed in desalination, water treatment and wastewater reclamation using nanofiltration and reverse osmosis processes. The inevitable contact of membranes with chlorine as biocidal agent results in their degraded performance and shortened life span. In order to develop chlorine-resistant membranes, it is crucial to obtain a more comprehensive understanding of the attack of chlorine on the membranes by bridging the following knowledge gaps:

- Chlorine has been proposed to attack the FA-PA separation layers via three mechanisms: (1) substitution of amide nitrogen, (2) direct amide ring

substitution and (3) indirect amide ring substitution via intermolecular rearrangement. However, the mechanism whereby chlorine attacks semi-aromatic PA membrane is poorly understood. Chlorination mechanisms of the tertiary amide nitrogen of the semi-aromatic PA are expected to differ from the secondary amide nitrogen of the FA-PA.

- A drawback of direct and indirect ring chlorination mechanisms is that they alone cannot adequately explain the disappearance of N–H bonds of the PA layer or the enhanced negative charge on membrane surface after chlorine exposure.

- The studies of chemical composition and bonding are mainly focus on chlorine incorporation; oxygen composition change has not been reported.

- The role of chlorine in promoting amide hydrolysis as a significant competing degradation reaction has not been systematically investigated.

- The hydrophilicity of the chlorinated membrane surface was reported to either increase or decrease, which is not clearly explained using the available mechanisms.

- The complex performance changes of chlorinated membranes (increased or decreased water permeability coupled with increased or decreased salt rejection) have not been consistently explained by the current studies.

- The molecular weight cut-offs of the chlorinated membranes have not been assessed.

- The existing researches mainly focus on the rejection of NaCl by chlorinated membranes. Studies on rejection of other solutes such as trace inorganic and organic contaminants are limited.

Chapter 3

Methodology

3.1 Materials and chemicals

3.1.1 Membranes

The commercial thin film composite (TFC) cross-linked PA membranes investigated in the current study include three RO membranes (SW30HR, BW30, and XLE) and three nanofiltration membranes (NF90, NF270, and HL). According to our previous characterization work (Tang et al., 2007; 2009a), NF270 and HL membranes have the semi-aromatic PIP PA chemistry; the other four membranes are of the FA PA chemistry. In addition, the FA PA membranes SW30HR and BW30 are coated with a polyvinyl alcohol (PVA) surface coating. The physiochemical properties of these membranes are provided in the Table 3-1. Membranes were provided by Dow FilmTec (Minneapolis, MN, USA), except the HL, which was from GE Osmonics (Minnetonka, MN, USA). All membranes were preserved as received at 4 ^{o}C in the dark until used.

Table 3-1. Membrane physiochemical properties. Data were extracted from Tang et al. (2009b) and Fane et al. (2011), except the MWCO data were from López-Muñoz et al. (2009).

	Membrane		Company	Type	MWCO (Da)[a]	RMS roughness (nm)	Contact angle (^{o})	Zeta potential (mV)[b]	Permeability ($L/m^2.hr.bar$)[c]	NaCl rejection (%)
Fully aromatic	Uncoated	XLE	FilmTec	RO	-	142.8 ± 9.6	46.4 ± 3.3	-27.8	6.04 ± 0.64	96.5
		NF90	FilmTec	NF	180	129.5 ± 23.4	44.7 ± 1.9	-37.0	11.2 ± 0.64	94.4 ± 1.5
	Coated	SW30HR	FilmTec	RO	-	54.4 ± 9.1	30.9 ± 3.6	-1.7	0.85	99.6
		BW30	FilmTec	RO	-	68.3 ± 12.5	25.9 ± 4.7	-10.1	3.96 ± 0.31	97.9 ± 0.4
Piperazine based	Uncoated	HL	GE Osmonics	NF	-	7.2 ± 2.6	27.5 ± 4.3	-26.0	12.8 ± 0.18	21.3
		NF270	FilmTec	NF	340	9.0 ± 4.2	32.6 ± 1.3	-41.3	14.5 ± 1.1	56.9 ± 3.8

[a] MWCO was determined by cross-flow filtration of polyethylene glycol (PEG) (López-Muñoz et al., 2009).

[b] Zeta potential was measured at pH 9, with 10 mM NaCl as the background electrolyte.

[c] Permeability was evaluated using MilliQ water. The rejection was determined using a 10 mM NaCl solution at pH 7. The applied pressure was 1380 kPa (200 psi).

3.1.2 Chemicals

Unless specified otherwise, all reagents and chemicals were of analytical grade with a purity over 99%. Sodium thiosulfate ($Na_2S_2O_3$) used in the chlorine titration, sodium hypochlorite (~ 10% NaOCl, reagent grade) used in the membrane degradation and boric acid (H_3BO_3) used in the filtration tests were purchased from Sigma Aldrich (St. Louis, MO, USA). Disodium hydrogen arsenate heptahydrate ($Na_2HAsO_4 \cdot 7H_2O$) was obtained from Alfa Aesar (Ward Hill, MA, USA). Polyethylene glycol - PEG standards for the calibration curves were obtained from Varian Inc. (Santa Clara, CA, USA). PEGs used for the rejection tests, calcium chloride dehydrate ($CaCl_2 \cdot 2H_2O$) used in the reaction with membrane functional groups, sodium chloride (NaCl) and concentrated hydrochloric acid (HCl) were purchased from Merck (Darmstadt, Germany). MilliQ water (Millipore, Billerica, MA, USA) was used in all preparations and experiments.

3.2 Membrane chlorination protocol

The chlorination solutions were prepared from NaOCl stock solution with their pHs adjusted by adding concentrated HCl or NaOH not more than 24 h before use. The total chlorine concentration – Cl_T, which is defined as the sum of all active chlorine species (White, 1986), was determined from iodometric titration with sodium thiosulfate and reported as ppm of Cl equivalent (Eaton et al., 1995). The titration involves the following main chemical reactions:

$$HOCl + 2I^{-1} \rightarrow Cl^{-1} + I_2^{0} + OH^{-} \quad (3\text{-}1)$$

or

$$Cl_2^{0} + 2I^{-1} \rightarrow 2Cl^{-1} + I_2^{0} \quad (3\text{-}2)$$

$$I_2^{0} + 2S_2O_3^{2-} \rightarrow S_4O_6^{2-} + 2I^{-} \quad (3\text{-}3)$$

Before the chlorination tests, the membrane coupons were rinsed and soaked in MilliQ water for 24 h to remove surface impurities and preservatives. The coupons were pre-soaked in NaOCl solutions at the same test conditions for 1 min to remove excess water on the surface and then immersed in 0.5 L Wheaton

bottles containing NaOCl solutions of different Cl_T and pH for different predetermined durations. The bottles with PTFE-lined caps were wrapped in aluminum foil to prevent radical reactions and photochemical degradation of the chlorine, and were constantly shaken at room temperature (~ 21 ^oC). After the exposure tests, the average chlorine depletion of the soaking solutions was less than 10%, and was within the range reported in the literature (Ettori et al., 2011).

3.3 Membrane characterization

After the chlorine exposure tests, the samples were thoroughly rinsed with MilliQ water. For XPS, FTIR and contact angle measurements, the membranes were vacuum dried whereas the zeta potential measurement was performed immediately after chlorination.

3.3.1 Carboxyl functional groups identification by calcium cation

A virgin membrane was prepared by soaking for 24 h in advance; freshly chlorinated membranes were thoroughly rinsed of chlorine solution. Membrane coupons were immersed in $CaCl_2$ 0.1 mM solution twice, each time for 10 min. The reaction pH was adjusted to 7 by adding appropriate amounts of 0.1 M HCl or NaOH. The coupons were then rinsed with a 0.001 mM $CaCl_2$ solution at pH 7 four consecutive times (5 min each) to remove calcium ions that were not bound to the membrane surface (adapted from Coronell et. al (2008; 2009)). In order to prevent Ca^{2+} precipitation due to absorption of atmospheric carbon dioxide and maintain a stable pH of the solution, the reactions were performed in 500 mL cylindrical gas-washing bottles, which allowed nitrogen gas to be continuously purged in order to blanket the solution. The coupons were dried with nitrogen gas and kept in a vacuum desiccator. The composition of Ca^{2+} on the membrane surface was determined by XPS.

3.3.2 X-ray Photoelectron Spectroscopy (XPS)

To obtain information about composition and bonding chemistry for the surface layer (top 1 to 5 nm sample thickness), XPS analysis was carried out on a Kratos AXIS Ultra spectrometer (Shimadzu, Columbia, MD, USA) with a monochromatic aluminum Kα X-ray source at 1486.7 eV. To compensate for membrane surface charging, the electron flood gun was operated at 3.6 eV. Survey spectra were recorded 3 times per sample, over the range of 0 – 1000 eV at 1 eV resolution. The high-resolution spectra had a resolution of 0.1 eV. Calibration for the elemental binding energy (BE) was done based on the reference for carbon 1s at 285 eV (Beamson and Briggs, 1992). Data were processed using standard software with Shirley background. The elemental BE and the relative sensitivity factors (RSF) are summarized in Table 3-2. From 2 to 5 replicates analyses were done at each chlorination condition for the NF90, BW30 and NF270 membranes.

Table 3-2. XPS elemental binding energy (BE) and relative sensitivity factors (RSF).

Element	O 1s	C 1s	N 1s	Cl 2p	S 2p	Ca 2p
RSF	0.78	0.278	0.477	0.891	0.668	1.833
BE (eV)	531	285	400	200	168	347

3.3.3 Attenuated total reflection-Fourier transform infrared (ATR-FTIR)

The bonding chemistry of the chlorinated membranes was obtained using an FTIR (IRPrestige-21, Shimadzu, Columbia, MD, USA) with 45^{o} multi-reflection HATR ZnSe flat plate crystal (PIKE Technologies, Madison, WI, USA) as the ATR element. Each spectrum was averaged for 50 scans over the range of 650 – 4000 cm^{-1} at a resolution of 2 cm^{-1}. Baselines were corrected for atmospheric CO_2 and water vapor. One replicate was done for each sample. The assignments for the membrane characteristic peaks are summarized in Table 3-3.

Table 3-3. Peak assignment for FTIR spectra (Tang et al., 2009a).

	FTIR peaks	Peak assignments
Fully aromatic polyamide	1663 cm^{-1}	Amide I band (C=O stretching – dominant contributor, C–N stretching, and C–C–N deformation vibration in a secondary amide group)
	1609 cm^{-1}	Aromatic amide (N–H deformation vibration or C=C ring stretching vibration)
	1541 cm^{-1}	Amide II band (N–H in-plane bending and N–C stretching vibration of a –CO–NH– group)
Semi-aromatic poly(piperazin-amide)	1630 cm^{-1}	Amide I band for poly(piperazin-amide)
Polysulfone	~ 1587, 1504, and 1488 cm^{-1}	Aromatic in-plane ring bend stretching vibration
	1385 – 1365 cm^{-1}	C–H symmetric deformation vibration of $>C(CH_3)_2$
	1350 – 1280 cm^{-1}	Asymmetric SO_2 stretching vibration
	~ 1245 cm^{-1}	C–O–C asymmetric stretching vibration of the aryl–O–aryl group
	1180 – 1145 cm^{-1}	Symmetric SO_2 stretching vibration
	~ 830 cm^{-1}	In-phase out-of-plane hydrogen deformation of para-substituted phenyl groups
Others	3330 cm^{-1}	N–H and O–H stretching
	3100 – 3000 cm^{-1}	Aromatic =C–H stretching
	3000 – 2900 cm^{-1}	Aliphatic C–H stretching

3.3.4 Zeta potential

Membrane surface charge was measured using a SurPASS electrokinetic analyzer (Anton Paar GmbH, Graz, Austria) with an adjustable gap cell. The cell channel height was adjusted to ~ 110 ± 5 μm. NaCl (10 mM) was used as the electrolyte solution. The solution pH was automatically titrated from 3 to 9 using 0.1 M HCl and 0.1 M NaOH. The zeta potential, ζ was calculated from the

streaming potential using the Helmholz-Smoluchowski equation (Elimelech et al., 1994; Childress and Elimelech, 1996):

$$\zeta = \frac{\Delta U_s}{\Delta P}\frac{\eta}{\varepsilon\varepsilon_0}\frac{L}{A}\frac{1}{R} \tag{3-4}$$

where ΔU_s: streaming potential

ΔP: applied pressure

$\Delta Us/\Delta P$: slope of the streaming potential versus applied pressure curve

η: dynamic viscosity of the solution

ε: permittivity of the test solution

ε_0: permittivity of free space

L, A, R: length, cross-sectional area and electrical resistance of the channel

For solutions with low surface conductivity (i.e., electrolyte concentration > 10^{-3} M), the L/A ratio was determined from the solution conductivity, κ, using the Fairbrother–Mastin approach (Fairbrother and Mastin, 1924):

$$\frac{L}{A} = \kappa R \tag{3-5}$$

Thus Eq. 3-4 becomes:

$$\zeta = \frac{\Delta U_s}{\Delta P}\frac{\eta}{\varepsilon\varepsilon_0}\kappa \tag{3-6}$$

3.3.5 Contact angle

The wettability of a membrane can be assessed via a contact angle measurement, whereby a lower contact angle indicates that the surface is more hydrophilic or more polar. Contact angle measurements were performed with an OCA Goniometer (Dataphysics Instruments, Filderstadt, Germany) by the sessile drop method (Kwon and Leckie, 2006a; Tang et al., 2009b). A syringe with a needle diameter of 0.525 mm was used to place a MilliQ water droplet of 10 µL on

the membrane. A static image of the droplet in equilibration with the membrane surface was taken with a CCD camera. A circular profile of the droplet was generated and the contact angle, θ, which is formed by tangent line to the droplet and the liquid-solid interface, was computed by the SCA20 software (Figure 3-1). The reported contact angle of each membrane sample was the average of 40 measurements (2 independent membrane coupons and 20 different locations for each sample) with errors indicated by the standard deviations.

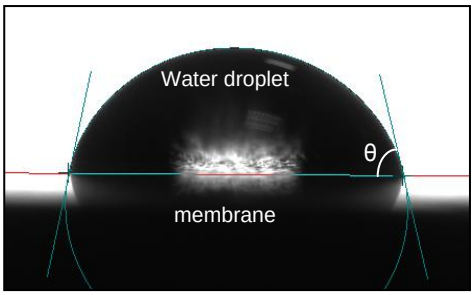

Figure 3-1. Illustration of contact angle measurement by sessile drop method.

3.4 Membrane performance evaluation

3.4.1 NF/RO filtration system design

The laboratory-scale high pressure filtration system in Figure 3-2 consists of identical cross-flow CF042 cells (Delrin Acetal, Sterlitech, Kent, WA, USA) in parallel arrangement. Each cell houses 42 cm^2 (4.6 cm × 9.2 cm) of active membrane area and has maximum operating pressure of ~ 6.89 MPa (~ 1000 psi). Diamond-patterned feed spacers of 1.2 mm thickness from GE Osmonics (Minnetonka, MN, USA) were used for all filtration tests to minimize the effect of concentration polarization. Both permeate and concentrate were re-circulated back to a 30-L stainless steel feed tank by a variable-speed diaphragm pump (HydraCell, Minneapolis, MN). The temperature of the feed solution was controlled at about 21 ± 1 ^oC by a submerged stainless steel heat exchange coil connected to a chiller (Polysciene, Niles, IL, USA). The pressure inside each membrane cell was maintained at the target pressure using flow-control valve and pressure relief valves (Swagelok, USA), and its value was monitored using a pressure gauge. The

cross-flow velocity was adjusted with a needle valve. Both digital pressure and flux readings were recorded with a computer data logging system.

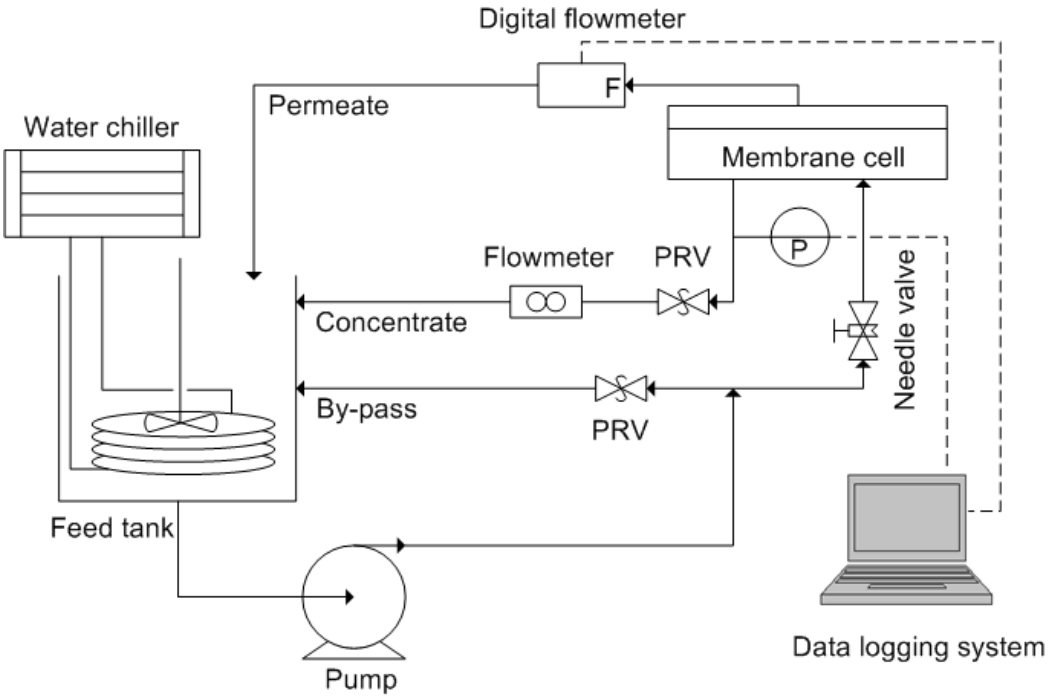

Figure 3-2. Schematic diagram of the NF/RO filtration system. PRV: pressure relief valve, P: pressure gauge.

3.4.2 Water permeability and sodium rejection test

Prior to the permeability and rejection (performance) tests, virgin membranes (soaked in MilliQ water for 24 h) and freshly chlorine-treated membranes were rinsed thoroughly with MilliQ water. The feed solution containing 10 mM NaCl in MilliQ water was circulated in the system at about 21 ± 1 ^{o}C and pH ~ 6.5. For all performance tests (including the PEG rejection in Section 3.4.3 and boron and arsenic rejection in Section 3.4.4), the cross-flow velocity of the system was set at 1 L/min; corresponding to a superficial velocity of 22.6 cm/s. Operating pressures for the NF90, BW30 and NF270 membranes were set at 0.69, 1.79 and 0.48 MPa (~ 100, 260 and 70 psi), respectively, to obtain similar water fluxes (at around 1.4 to 1.7 × 10^{-5} m/s) for the virgin membranes. The reported water permeability and NaCl rejection were recorded after 24 h of

membrane compaction. The permeate flux, J_w was determined by a gravimetric method. The salt rejection was calculated from the permeate and tank conductivity measured using a Ultrameter II conductivity meter (Myron L Company, Carlsbad, CA, USA). At least two separate runs were performed for each treatment.

3.4.3 PEG rejection

After 24 h of membrane compaction described in Section 3.4.2, the system was flushed with MilliQ water for 5 min and the feed was switched to one of three PEG solutions with average molecular weights of 200, 400 and 600 g/mol, each with a concentration of 5.5 g/L. For each PEG feed, 10 mL of PEG samples of both permeate and feed were taken after 10 min filtration. After each PEG run, the system was flushed with fresh MilliQ water for 15 min to clean the setup. At least 1 replicate was made for each test condition.

PEG concentrations were determined by gel permeation chromatography (GPC) performed on a Varian Inc. PL-GPC 50 Plus system (Santa Clara, CA, USA) with a refractive index detector. The system used PL Aquagel-OH 20 GPC column (Varian Inc.) with a packing material of 5 µm diameter, MilliQ water as the solvent and was set at 30 ^{o}C. Details for the calibration curves are provided in Appendix A-1.

3.4.4 Boron and arsenic (V) rejection

After 24 h of membrane compaction described in Section 3.4.2, boric acid and disodium hydrogen arsenate heptahydrate were added to achieve a feed concentration of 20 mg B/L and 150 mg As/L. Concentrated HCl and NaOH were used to adjust the feed pH to 7. The reported rejection was determined after treating boron and arsenate solutions continuously for 24 h. The boron concentration was determined using a Perkin Elmer Optima 2000 inductively coupled plasma – optical emission spectrometer (ICP-OES) (Zaventem, Belgium). The arsenic concentration was analyzed by Agilent 7700 inductively coupled plasma – mass spectrometer (ICP-MS) (Tokyo, Japan).

Chapter 4

Degradation of Polyamide Nanofiltration and Reverse Osmosis Membranes by Hypochlorite

4.1 Introduction

Polyamide-based thin film composite (TFC) membranes are the most widely used reverse osmosis and nanofiltration membranes today, mainly because of their high selectivity and water permeability (Lee et al., 2010). The basic types of membrane structures and chemistries are illustrated in Figure 4-1. The fully-aromatic (FA) polyamide (PA) membrane is formed by interfacial polymerization of m-phenylene diamine and trimesoyl chloride (TMC) to obtain a three-dimensionally cross-linked rejection layer, where the degree of cross-linking, *n*, ranges from 0 (fully linear) to 1 (fully cross-linked) (Tang et al., 2007). The semi-aromatic PA membrane is similarly synthesized by piperazine (PIP) and TMC. Additional surface coating with polyvinyl alcohol (PVA) is used for some commercial membranes to improve the membrane fouling resistance (Tang et al., 2007; 2009a).

A drawback of PA membranes is that they are degraded by chlorine, which is commonly added in form of sodium hypochlorite as a disinfectant to control biofouling or as a membrane cleaning agent (Glater et al., 1994). Addressing the need for chlorine resistant membranes requires a mechanistic understanding of the interactions between chlorine and the PA rejection layer of the membrane and how these effects impact membrane performance. A critical review of prior studies was reported by Glater et al. (1994). The mechanisms that have been identified to explain the properties and performance changes of chlorinated polyamide membranes are summarized in Figure 2-7. Chlorination of the amide nitrogen occurs when active chlorine species (i.e., hypochlorous acid) attack the lone

electron pair of either the N or O atom of the amide group and rearrange to the N-chloroamide (Challis and Challis, 1970; Glater et al., 1994; Jensen et al., 1999; Kwon et al., 2008). A direct ring chlorination mechanism has also been proposed: the aromatic ring of m-phenylene diamine is attacked by active (electrophilic) chlorine species and substitution occurs preferentially at the para position (Shafer, 1970; Glater and Zachariah, 1985). Indirect ring chlorination (termed Orton rearrangement) can be initiated by rapid N-chlorination followed by an intra-molecular rearrangement in which chlorine migrates to the ring (Orton and Jones, 1909; Orton et al., 1928; Kawaguchi and Tamura, 1984a). Most previous studies have focused on the incorporation of chlorine into the membrane matrix, but systematic studies on oxygen composition changes and the role of chlorine in promoting amide hydrolysis as a significant competing degradation reaction are not reported (Glater et al., 1994).

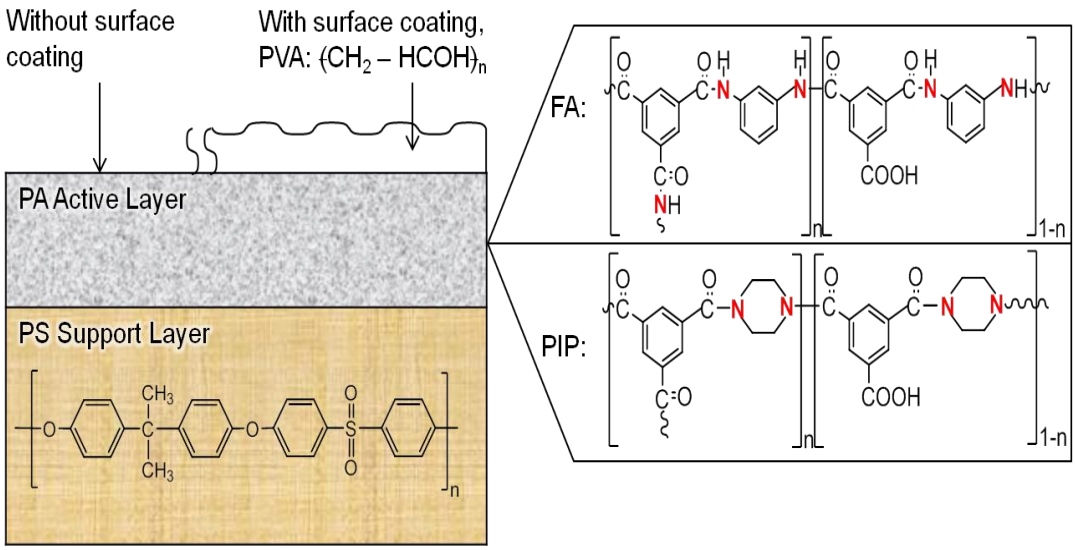

Figure 4-1. Schematic diagram of basic membrane structures and chemistries. Diagram is not to scale.

The effects of chlorination on membrane performance have been reported in the literature but findings appear to be inconsistent. The decline in water flux after membrane chlorination (Glater et al., 1981; Glater et al., 1983; Koo et al., 1986; Soice et al., 2004; Kwon and Leckie, 2006b; Kwon et al., 2006; Simon et al.,

2009; Ettori et al., 2011) has been attributed to an increase in membrane hydrophobicity caused by chlorine attachment (Koo et al., 1986), "membrane tightening" (Glater et al., 1981; Glater et al., 1983), or a more rigid polymer conformation (Avlonitis et al., 1992; Soice et al., 2004; Kwon and Leckie, 2006a; b). In contrast, a brief exposure to chlorine at high pH is used to treat PA RO membranes after fabrication to improve performance (Cadotte, 1981; Jons et al., 1999). The observed increase in flux is usually accompanied by a decrease in salt rejection (Glater et al., 1981; Glater et al., 1983; Koo et al., 1986; Soice et al., 2004; Kwon and Leckie, 2006b; Kwon et al., 2006; Simon et al., 2009; Raval et al., 2010; Ettori et al., 2011) and proposed to be the result of polyamide chain cleavage (Glater et al., 1981; Glater et al., 1983; Koo et al., 1986), or physical separation of the PA rejection layer from its polysulfone support (Soice et al., 2004). Meanwhile, better salt rejection of chlorine-treated membranes has been attributed to the result of membrane tightening (Glater et al., 1981; Glater et al., 1983), or enhanced PA chain cross-linking due to the formation of azo-compounds or quinone-like species (Soice et al., 2003; Soice et al., 2004). Opposite trends are observed in membrane surface charges and wettability as well. The membrane zeta potential is observed to generally become more negative after chlorination (Kwon and Leckie, 2006a; Simon et al., 2009). This change in surface charge does not seem to be adequately explained by ring chlorination or the Orton rearrangement mechanism. The hydrophobicity of chlorinated membranes is reported to both increase and decrease depending on the chlorine concentration, soaking pH and duration (Kwon and Leckie, 2006a; Simon et al., 2009). To explain these observations by a single mechanism is difficult. Therefore, further studies and possibly additional mechanisms are required to obtain insight into the membrane degradation process by chlorination.

This paper presents evidence that chlorine treatment leads to the uptake of chlorine and oxygen by PA membranes. Changes in the membrane surface and bulk chemistry as well as surface charge and wettability are interpreted to infer that subsequent reactions with hypochlorite appear to hydrolyze the amide C–N bond

of the PA layer. These results show that chlorine treatment can significantly modify the membrane properties.

4.2 Materials and methods

4.2.1 Chemicals and materials

The commercial thin film composite cross-linked PA membranes investigated in the current study include three RO membranes (SW30HR, BW30, and XLE) and three nanofiltration membranes (NF90, NF270, and HL). According to our previous characterization work (Tang et al., 2007; 2009a), the NF270 and HL membranes have the semi-aromatic PIP PA chemistry; the other four membranes are of the FA PA chemistry. In addition, the FA PA membranes SW30HR and BW30 are coated with a polyvinyl alcohol (PVA) surface coating. The physiochemical properties of these membranes are given in Table 3-1. The membranes were provided by Dow/FilmTec (Minneapolis, MN, USA), except the HL, which was from GE Osmonics (Minnetonka, MN, USA).

Sodium hypochlorite (~ 10% NaOCl, reagent grade) was obtained from Sigma Aldrich (St. Louis, MO, USA). Exact concentrations for the soaking solutions were determined by a standard titration method using sodium thiosulfate (Eaton et al., 1995). All other reagents and chemicals were of analytical grade with a purity over 99%. MilliQ water (Millipore, Billerica, MA, USA) was used in all preparations and experiments.

4.2.2 Membrane chlorination procedures

Membrane coupons, which were preserved as received at 4 ^{o}C, were cleaned and soaked in MilliQ water for 24 hours before the chlorination experiments. The membranes were pre-soaked in NaOCl solutions at the same testing conditions for 1 min to remove excess water on the surface before being soaked in NaOCl solutions with concentrations of 10, 100, 1000 and 2000 ppm for either 1 or 24 h to accelerate the laboratory degradation process (Kwon and Leckie,

2006b; Simon et al., 2009; Ettori et al., 2011). Since acidification is typically performed in NF/RO plants for scaling control (Bartels and Wilf, 2005), soaking solutions were adjusted to pH 5 by the addition of HCl or NaOH so that HOCl was the main species (Ettori et al., 2011). Samples were contained in sealed 0.5 L Wheaton glass bottles with PTFE-lined caps, covered with aluminum foil (to protect the chlorine from sunlight degradation), and constantly mixed on a shaker at room temperature (~ 21 ^{o}C). After the exposure tests, the average chlorine depletion of the soaking solutions was less than 10%, which was within the magnitude reported in the literature (Ettori et al., 2011).

After soaking, the samples were thoroughly rinsed with MilliQ water. For XPS, FTIR and contact angle measurements, the membranes were vacuum dried, whereas the zeta potential measurements were performed on wet samples immediately after chlorination.

4.2.3 X-ray Photoelectron Spectroscopy (XPS)

To obtain information about the composition and bonding chemistry for the surface layer (top 1 to 5 nm of the sample thickness), XPS analysis was carried out on a Kratos AXIS Ultra spectrometer (Shimadzu, Columbia, MD, USA) with a monochromatic aluminum Kα X-ray source at 1486.7 eV. To compensate for membrane surface charging, the electron flood gun was operated at 3.6 eV. Survey spectra were recorded 3 times per sample, over the range of 0 – 1000 eV at 1 eV resolution. The high-resolution spectra had a resolution of 0.1 eV. Calibration for the elemental binding energy was done based on a carbon 1s reference at 285 eV (Beamson and Briggs, 1992). Data were processed using standard software with Shirley background and relative sensitivity factors (RSF) of 0.78, 0.477, 0.278 and 0.891 for the O 1s, N 1s, C 1s and Cl 2p peaks, respectively. From 2 to 5 replicate analyses were done at each chlorination condition for the NF90, BW30 and NF270 membranes.

4.2.4 Attenuated total reflection-Fourier transform infrared (ATR-FTIR)

Bonding chemistry of the chlorinated membranes was obtained using an FTIR (IRPrestige-21, Shimadzu, Columbia, MD, USA) with a 45^{o} multi-reflection HATR ZnSe flat plate crystal (PIKE Technologies, Madison, WI, USA) as the ATR element. Each spectrum was averaged for 50 scans over the range of 650 – 4000 cm^{-1} at a resolution of 2 cm^{-1}. Baselines were corrected for atmospheric CO_2 and water vapor. One replicate was done for each sample.

4.2.5 Zeta potential and contact angle measurement

The membrane surface charge was measured using a SurPASS electrokinetic analyzer (Anton Paar GmbH, Graz, Austria) with an adjustable gap cell using 10mM NaCl as the electrolyte solution. The cell channel height was adjusted to ~ 110 ± 5 µm. The solution pH was automatically titrated from 3 to 9 using 0.1M HCl and NaOH. The zeta potential was calculated from the streaming potential using the Fairbrother–Mastin formula (Elimelech et al., 1994).

Contact angle measurements were performed with an OCA Goniometer (Dataphysics Instruments, Filderstadt, Germany) by the sessile drop method. A syringe with a needle diameter of 0.525 mm was used to place a water droplet of 10 µL on the membrane. Tangent lines to both sides of the droplet static image were generated and averaged using the SCA20 software. The reported contact angle of each membrane sample was the average of 40 measurements (2 independent membrane coupons and 20 different locations for each sample) with errors indicated by the standard deviations.

4.2.6 Membrane performance tests

The laboratory-scale NF/RO filtration system consisting of four identical cross-flow test cells (CF042, Sterlitech, Kent, WA, USA) is illustrated and described in Figure 3-2. Each cell houses 42 cm^2 (4.6 cm × 9.2 cm) of active membrane area. Spacers of 1.2 mm thickness from GE Osmonics (Minnetonka, MN, USA) were used for all filtration tests.

Membrane performance tests were conducted for the NF90, BW30 and NF270 membranes. Prior to each filtration test, virgin membranes (soaked in MiliQ water for 24 h) and freshly degraded membranes were cleaned thoroughly with MiliQ water. Feed solution containing 10 mM NaCl at 21 ^{o}C and natural pH (pH ~ 6) was re-circulated through the system for 24 h at a 1 L/min cross-flow velocity, corresponding to a superficial velocity of 22.6 cm/s. The operating pressures for NF90, BW30 and NF270 were set at 0.69, 1.79 and 0.48 MPa (~ 100, 260 and 70 psi), respectively, to obtain similar virgin membrane fluxes (around 1.2 to 1.5 m/day). The permeate flux was determined by a gravimetric method. The salt rejection was calculated from the permeate and tank conductivity measured using an Ultrameter II conductivity meter (Myron L Company, Carlsbad, CA, USA). The equations to determine the water permeability coefficient, A (m/s.Pa) and the solute permeability coefficient, B (m/s) are provided in Section 2.1.

4.3 Results and discussion

4.3.1 Chlorine and oxygen on membrane surfaces – elemental changes after chlorination

Six membranes with 3 different chemistries were exposed to 1000 ppm NaOCl solutions for 1 h at pH 5. In addition, the NF90, BW30 and NF270 membranes were treated at 2000 and 1000 ppm for 24 h. The results from the XPS survey scan show that the amount of chlorine attached onto the PA surface decreased in the order: uncoated FA > coated FA > PIP membranes. The correlations between the chlorine (%) uptake of the surface layer and the nitrogen atomic percentage are presented in Figure 4-2. The chlorine to nitrogen atomic ratios (Cl/N ratio) of uncoated FA membranes (NF90 and XLE) cluster around the 1:1 ratio line, which suggests that chlorine attaches to the nitrogen of the secondary amide via the N-chlorination mechanism. The chlorine and nitrogen atomic percentages of the coated FA membranes were 1:1 at 1000 ppm NaOCl × 1 h; however, both percentages increased significantly at 1000 and 2000 ppm NaOCl × 24 h. The average surface nitrogen content was ~ 6% at 1000 and 2000 ppm × 24 h, which is higher than the nitrogen content of the virgin BW30 membrane (Tang

et al., 2007). This is further accompanied with a significant reduction in the oxygen content (Appendix B-1 and B-2). These observations suggest that the PVA coating was likely partially detached under the severe chlorination conditions employed. In addition, elevation of the Cl/N ratio from 1 to 1.56 and 2.3 suggests that chlorine also binds to the PVA coating layer. The observation that the PIP membranes NF270 and HL had Cl/N ratios much less than 1 is consistent with the fact that tertiary nitrogen is not chlorinated, as reported in the literature (Kawaguchi and Tamura, 1984a; Jensen et al., 1999; Soice et al., 2003). The absence of amide protons accounts for the low chlorine incorporation into the PIP membranes (Kawaguchi and Tamura, 1984a; Glater et al., 1994). Chlorination might still occur at the non-crosslinked nitrogen atoms, which are sparse. In spite of the small chlorine uptake, the performance of the chlorinated PIP membranes is reported to be impaired by chlorine exposure (Simon et al., 2009). This phenomenon requires a different explanation for the attack of chlorine on the PIP PA structure.

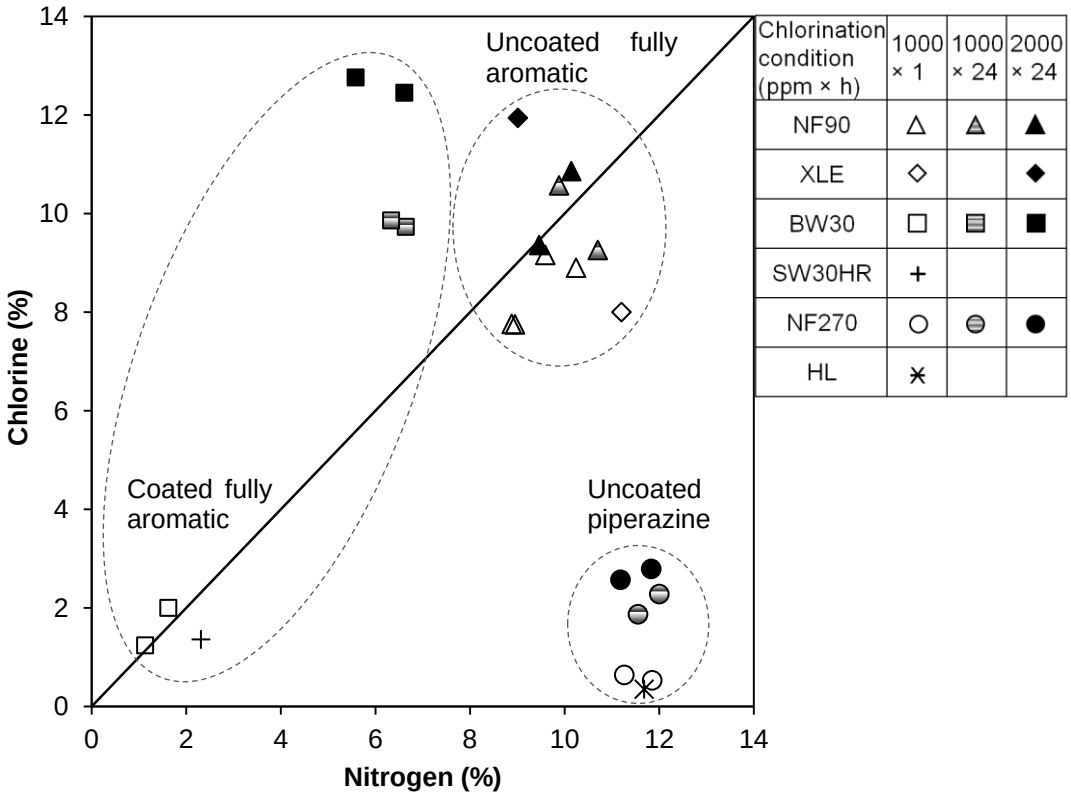

Figure 4-2. Atomic percent of chlorine and nitrogen of chlorinated uncoated fully aromatic (NF90 and XLE), PVA coated fully aromatic (SW30HR and BW30) and uncoated poly(piperazinamide) (HL and NF270) membranes at pH 5; 2000 ppm × 24 h, 1000 ppm × 24 h and 1000 ppm × 1 h.

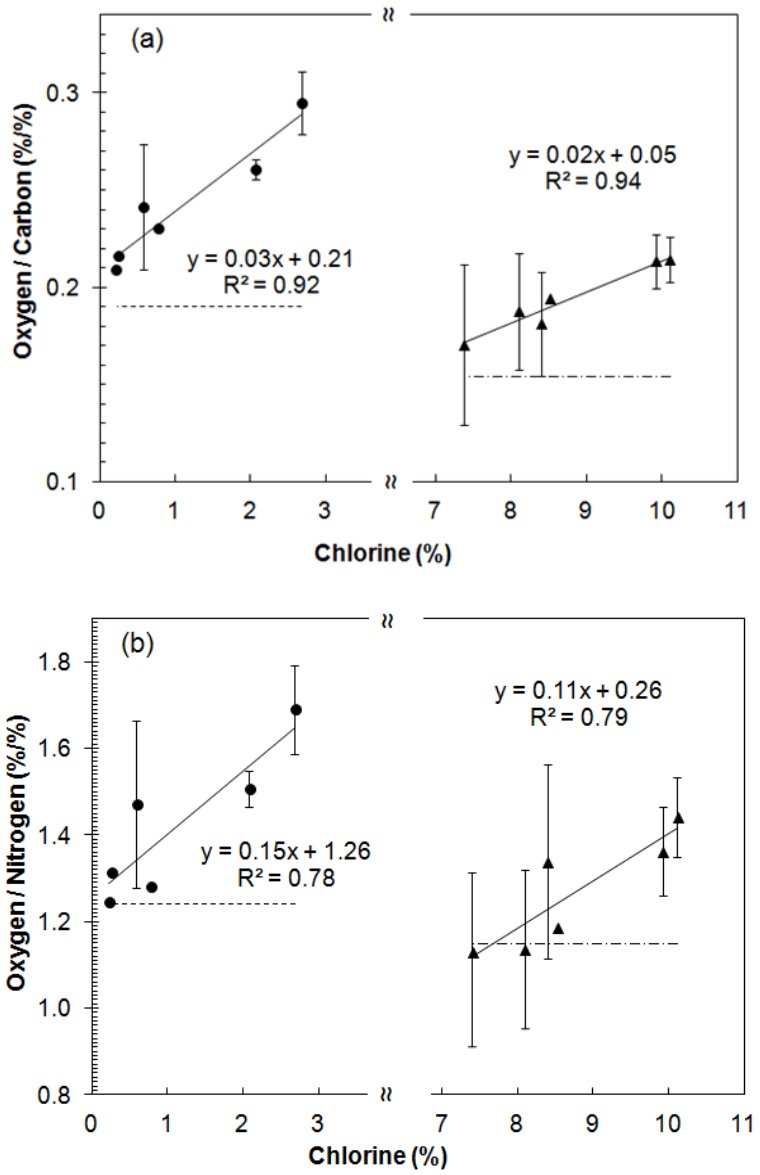

Figure 4-3. Ratio of (a) oxygen to carbon and (b) oxygen to nitrogen as a function of the atomic percent of bound chlorine for (●) NF270 and (▲) NF90 membranes at pH 5 and different chlorination concentrations and durations. The dotted and dashed lines represent the (a) O/C and (b) O/N ratio for virgin NF270 and NF90 membranes, respectively. The error bar indicates the measurement range obtained from 2 to 5 samples.

The XPS results revealed that chlorination increased the O/C ratio on the uncoated membrane surfaces (Figure 4-3a). This ratio increased from 0.2 (virgin) to 0.3 (2000 ppm × 24 h) for the NF270 membrane and from 0.15 (virgin) to 0.21 (2000 ppm × 24 h) for the NF90 membrane. The O/N ratio, which indicates the

degree of PA cross-linking, was plotted against the chlorine content (Figure 4-3b). Theoretically, the O/N ratio is 1:1 for a fully cross-linked PA layer (n = 1, Figure 4-1) and is 2:1 for a linear PA layer (n = 0) (Tang et al., 2007). The O/N ratio of NF90 increased from 1.15 for virgin membrane to 1.44 for the membrane treated with 2000 ppm for 24 h. The NF270 membrane experienced the same increase in O/N ratio from 1.24 to 1.69, which means that the chlorine treated membranes were less cross-linked and that more C–N bonds were broken. The increase of oxygen content and decrease in the number of C–N bonds are hypothesized to result from C–N bond hydrolysis, which leads to additional carboxylic acid groups. Mechanistically, facilitated hydrolysis of the chlorinated C–N bond may be explained by the polarization of the amide carbon due to chlorine substitution at the nitrogen, which makes the carbon more susceptible to nucleophilic attack by hydroxide. Additional evidence for chlorination promoted hydrolysis is presented in Sections 4.3.2 and 4.3.3.

4.3.2 Changes in membrane chemistry due to chlorination

The high resolution XPS spectra for O, C, N and Cl of virgin and chlorinated (at 2000 ppm × 24 h) NF90 membranes are shown in Figure 4-4. Changes in chemical bonding at the surface of the PA layer can be understood through analysis of the shifts in the binding energy (BE) of the deconvoluted peak spectra. The assignments for deconvoluted peaks are summarized in Table 4-1 (Briggs, 1998; Ariza et al., 2000b; Boussu et al., 2007). Only the chlorine peak representing covalent bonding (~ 200.7 eV) is discussed. After chlorination, the second deconvoluted peak of O 1s (~ 532.6 eV) corresponding to H···**O**=C–N, O=C–**O** bonds was shifted upward by about 0.6 eV; the second deconvoluted C 1s (~ 286.2 eV) peak, which is assigned to **C**–O**,** **C**–N and **C**–Cl bonds, was shifted upward by about 0.13 eV. For NF270; an increase in peak intensity was observed for the second O 1s peak (~ 532.6 eV, Appendix B-3). Although these shifts are not sufficiently distinctive to deconvolute and assign new peaks, they may indicate an increase in the number of carboxylic groups due to the chlorine-promoted C–N bond hydrolysis.

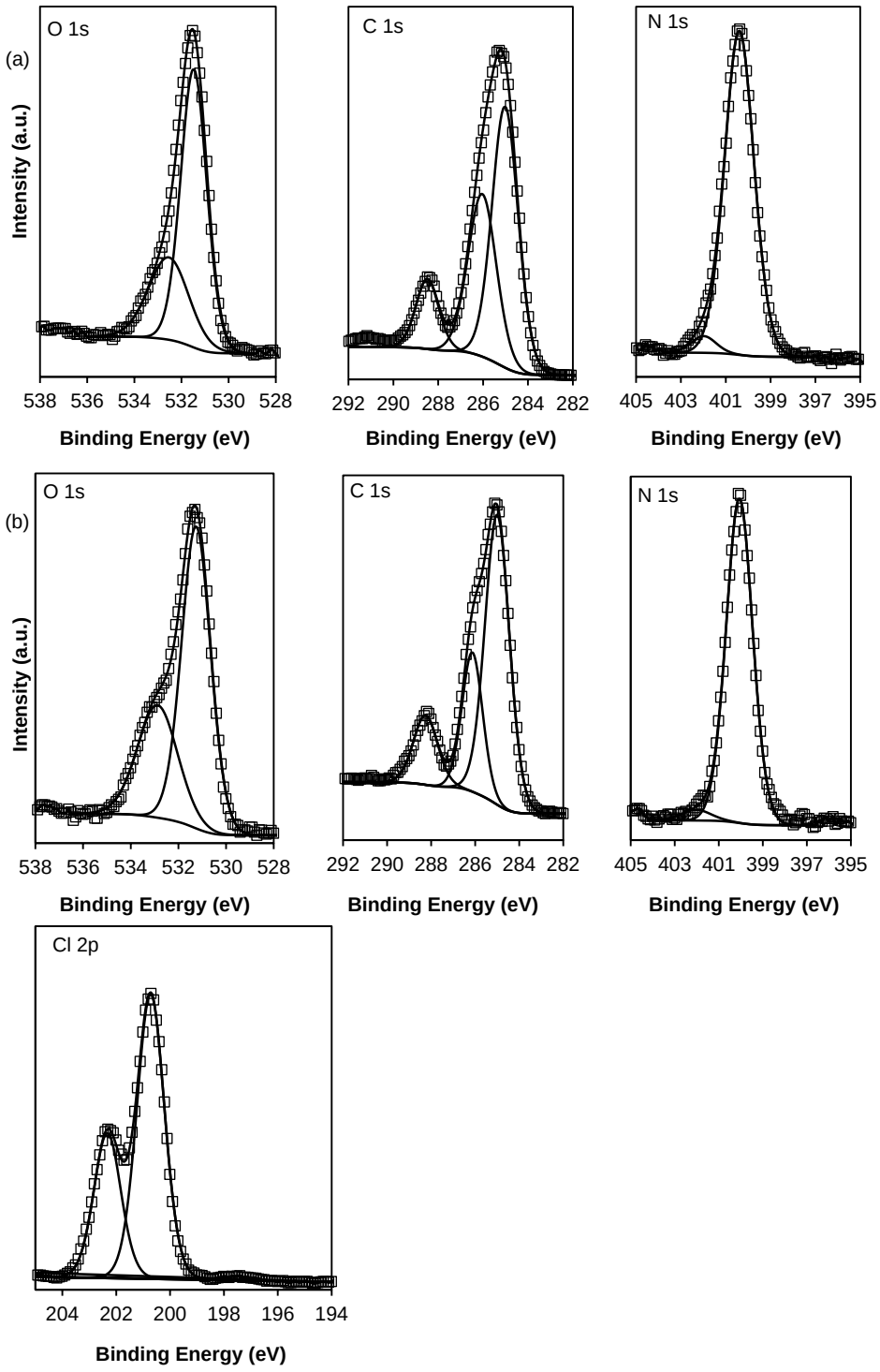

Figure 4-4. High resolution XPS spectra and deconvoluted peak assignments of (a) O 1s, C 1s, N 1s for virgin and (b) O 1s, C 1s, N 1s, Cl 2p for chlorinated NF90 membranes (2000 ppm × 24 h, pH 5). The Cl 2p peak of different bonding states is deconvoluted into Cl 2p3/2 and Cl 2p1/2. The peak intensity ratio of Cl 2p3/2 over Cl 2p1/2 is constant (= 2) and the binding energy of the Cl 2p3/2 peak was used to identify chemical bonding.

Table 4-1. XPS deconvolution peak assignments.

	BE (eV)	Peak Assignment
O 1s	531.2	**O**=C–N, C=**O**, C–**O**
	532.6	H···**O**=C–N, O=C–**O**
C 1s	285.0	**C**–C, **C**=C
	286.2	**C**–O**, C**–N, **C**–Cl
	288.1	O=**C**–N, **C**=N, **C**=O
N 1s	400.0	C–**N**, C=**N**, O=C–**N**
	401.2	–$\mathbf{N}H_3^+$, –$\mathbf{N}H_2R^+$
Cl 2p3/2	197.6	**Cl**$^-$
Cl 2p1/2	199.2	
Cl 2p3/2	200.7	C–**Cl**
Cl 2p1/2	202.3	

Bulk chemistry changes due to chlorination in both the polysulfone and PA layers were obtained from the FTIR spectra for virgin and chlorinated NF90, BW30 and NF270 membranes (Figure 4-5). Peak assignments for the FTIR spectra of these PA membranes were reported in detail elsewhere (Tang et al., 2009a). The FA amide signature peaks at wave numbers of 1541, 1609 and 1663 cm^{-1} experienced prominent changes in the case of the NF90 and BW30 membranes, consistent with literature data (Kwon and Leckie, 2006b; Kang et al., 2007; Buch et al., 2008; Kwon et al., 2008; Ettori et al., 2011). The disappearance of the amide II band (1541 cm^{-1}) for the N–H in-plane bending and N–C stretching vibration and aromatic amide peak (1609 cm^{-1}) for N–H deformation vibration and C=C ring stretching vibration (Tang et al., 2009a) strongly suggests that chlorine replaced the hydrogen of the amide nitrogen via electrophilic substitution in N-chlorination. This FTIR information is consistent with the Cl/N ratio from the XPS results in Figure 4-2. It was observed that the amide I band (1663 cm^{-1}), which represents the C=O stretching (major contributor) and C–N stretching and C–C–N deformation vibrations, was shifted to a higher wave number. Since the C=O stretching of benzoic acid is at 1680 cm^{-1} (Roeges, 1994; Ettori et al., 2011), it can be hypothesized that the breakage of hydrogen bonds between the C=O and N–H groups (Kwon and Leckie, 2006b; Ettori et al., 2011) and additional carboxyl groups by hydrolysis have contributed to this shift.

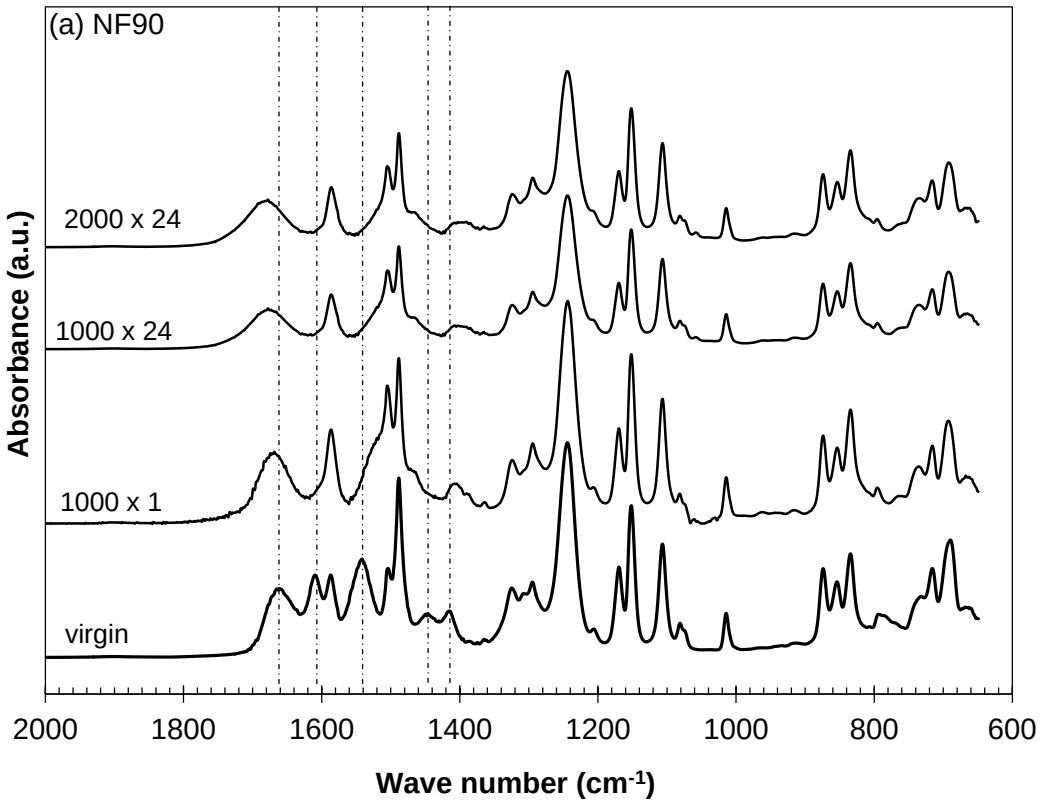

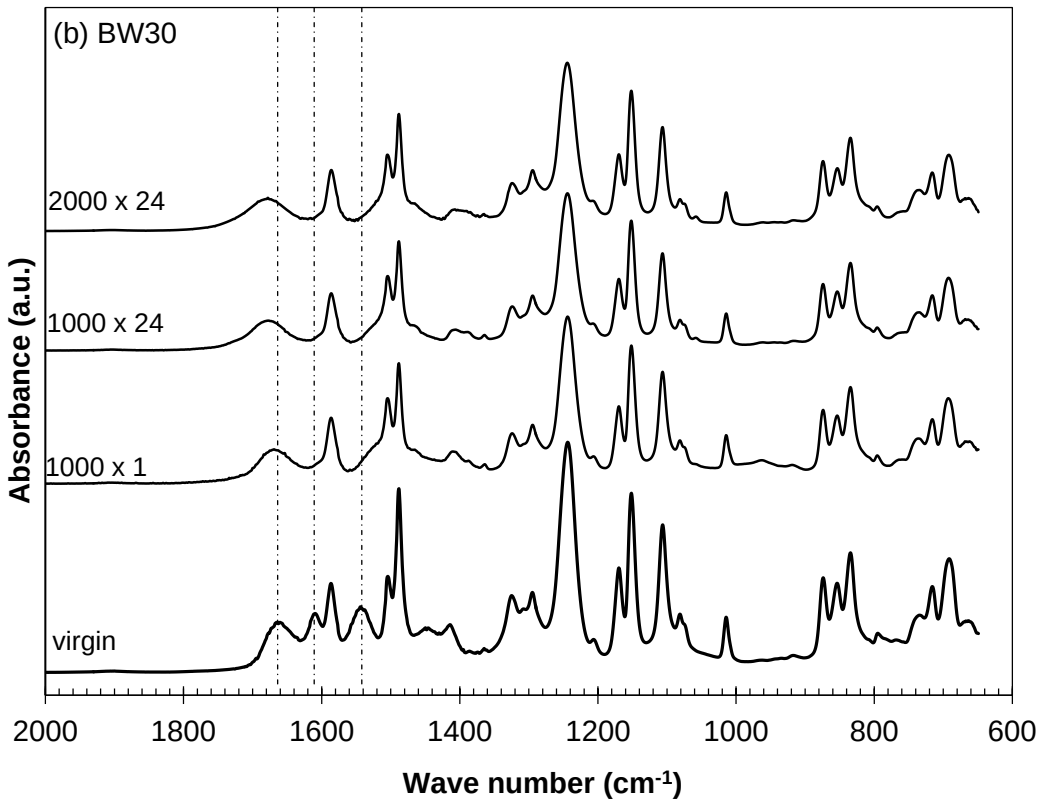

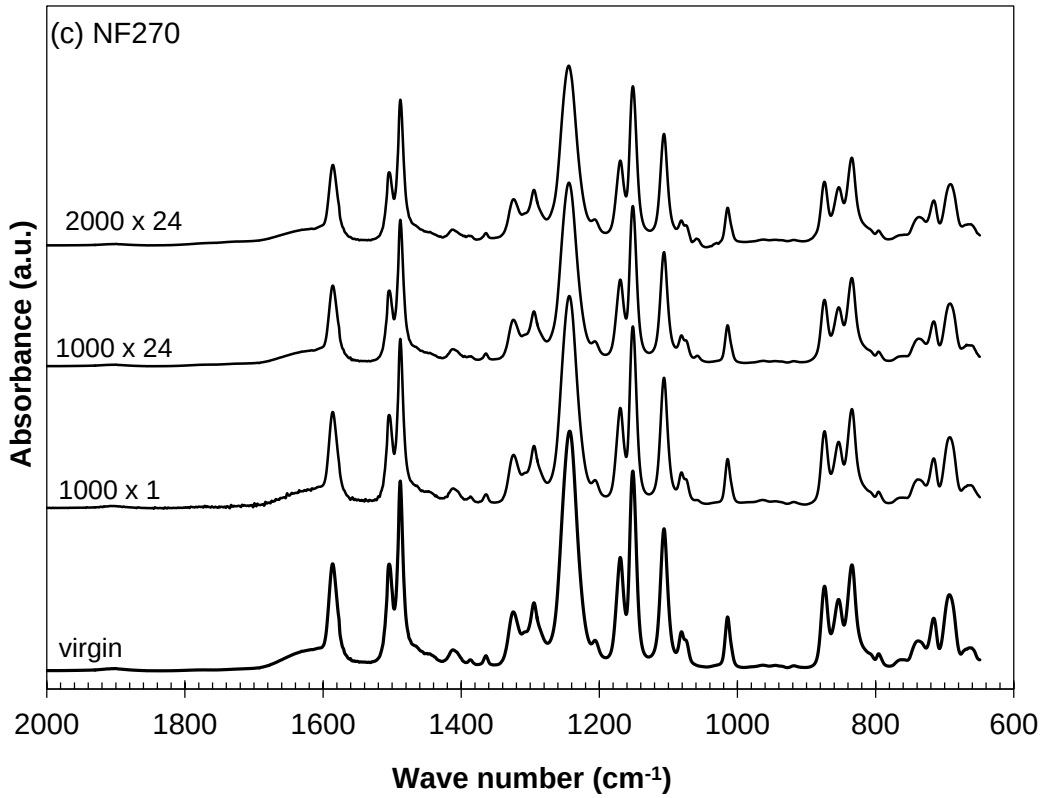

Figure 4-5. ATR-FTIR spectra for (a) NF90, (b) BW30 and (c) NF270 membranes: virgin and chlorinated at pH 5; 2000 ppm × 24 h, 1000 ppm × 24 h and 1000 ppm × 1 h.

In contrast to the obvious spectra changes for the NF90 and BW30 membranes, there was no noticeable change in the FTIR peaks detected for the NF270 PIP membrane (Figure 4-5c). This result is consistent with the XPS survey spectra (Figure 4-2) results in which the nitrogen in the tertiary PA of NF270 was less prone to chlorine attack. Nevertheless, a small amount of chlorine was still incorporated into the PIP PA layer, which was assumed to be at nitrogen atoms of non-crosslinked amine groups.

It is also interesting to compare the XPS and FTIR results for the PVA coated BW30 membrane. Since XPS measures only the top 1-5 nm thickness of a sample, its signal responds mainly to the coating material and exposed surface PA. In contrast, ATR-FTIR has a much deeper sample penetration depth and allows measurement of the PA properties across the entire active layer. Thus, a comparison between the surface XPS and the ATR-FTIR measurements can reveal

important information on the degree of membrane chlorination across the PA rejection layer (Tang et al., 2007). Although the XPS results showed less surface chlorine on the BW30 membrane than on NF90 membrane at short exposure (1000 ppm × 1 h), the FTIR spectra of chlorinated BW30 show a complete disappearance of the amide II band (1541 cm^{-1}) and the aromatic amide peak (1609 cm^{-1}). The latter suggests that the PVA coating did not protect the FA PA matrix from chlorine attack under the severe chlorination conditions applied in this study. Therefore, the lower XPS chlorine signal for the PVA coated membranes (Figure 4-2) was merely a reflection that less PA was exposed at the membrane surface due to the presence of the coating. Chlorine might have penetrated through the coating and caused the damage to the PA underneath. No changes in the polysulfone layer can be observed at a wave band 1145 – 1350 cm^{-1}, which is consistent with the finding of Ettori et al. (2011) that polysulfone was not chemically modified by chlorination. FTIR spectra from 2700 to 3800 cm^{-1} for the three membranes are provided in Appendix B-4. For the NF90 and BW30 FA membranes, the magnitude of the broad peaks centered ~ 3300 cm^{-1}, which are assigned to N–H and/or O–H stretching (Tang et al., 2009a), decreased as the chlorination conditions became more severe. On the other hand, for the NF270 PIP membrane, only a slight reduction in the C–H stretching peak at 2970 cm^{-1} was observed (Tang et al., 2009a).

4.3.3 Changes in membrane surface charge and hydrophilicity

The surface charge of the NF90 and NF270 membranes before and after chlorination is presented in Figure 4-6 and that of BW30 membranes is provided in Appendix B-5. Both the NF90 and NF270 membranes became more negative as the chlorine concentration increased, which agrees with previous observations (Kwon, 2005; Simon et al., 2009). It is useful to note that the magnitude of this negative charge shift within a membrane is not constant; at low pH, the shift magnitude is relatively large. The iso-electrical point of virgin NF90 is at pH ~ 5.5 and the positive charge at low pH is contributed by the protonated amide group (Childress and Elimelech, 1996). All chlorinated membranes were negatively

charged at the lowest measured pH leading to the speculation that due to N–Cl bond formation, the amide nitrogen can no longer form $–NH_2^+$ groups (Simon et al., 2009). Meanwhile, the negative charge at high pH is associated with deprotonation of carboxylic acid (Childress and Elimelech, 1996). The more negative zeta potential at high pH confirms that the number of carboxylic groups on the surface increased, consistent with the chlorine-promoted hydrolysis mechanism.

The hydrophobicity of the membranes evaluated by contact angle measurement is illustrated in Figure 4-7; addition data for other membranes are in Appendix B-6. A higher value of the contact angle denotes greater difficulty in wetting the membrane. Despite the measurement uncertainty, some general trends can be observed. The membrane surfaces became less hydrophilic under severe chlorination conditions. However, the NF270 and BW30 membranes treated at 1000 ppm for 1 h became more hydrophilic. Both trends in wettability might be explained by the competing effects of the N-chlorination and hydrolysis processes. The incorporation of chlorine on the membrane surface can cause an increase in hydrophobicity and inhibition of membrane wetting. On the other hand, an increase in carboxylic/ hydroxyl functional groups can increase membrane wetting.

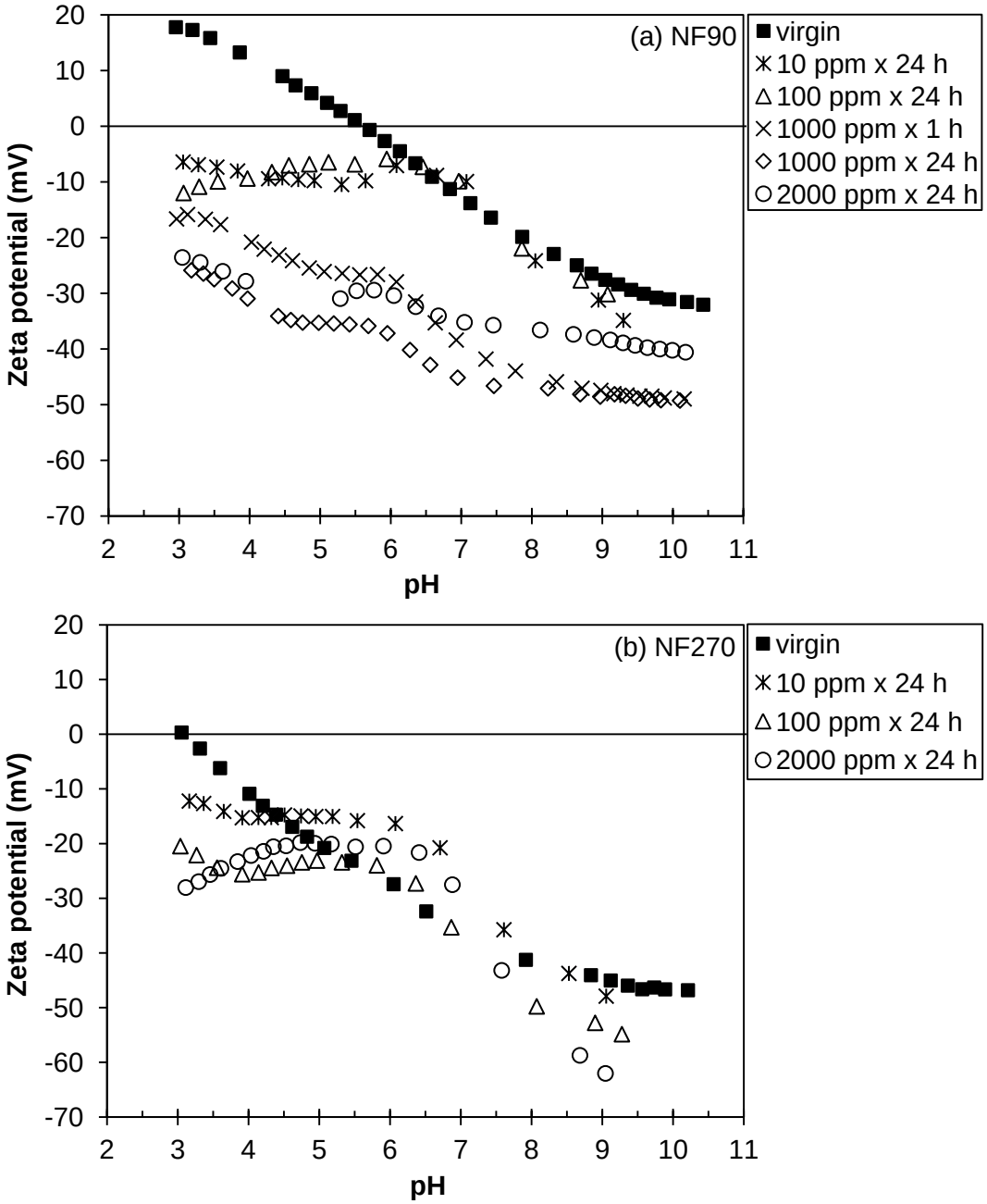

Figure 4-6. Zeta potential for virgin and chlorinated (a) NF90 and (b) NF270 membranes as a function of pH. The background electrolyte was 10 mM NaCl. The uncertainty in the zeta potential measurements is estimated to be ~ +/- 5 mV (Figure B-6 and Tang et. al (2006)).

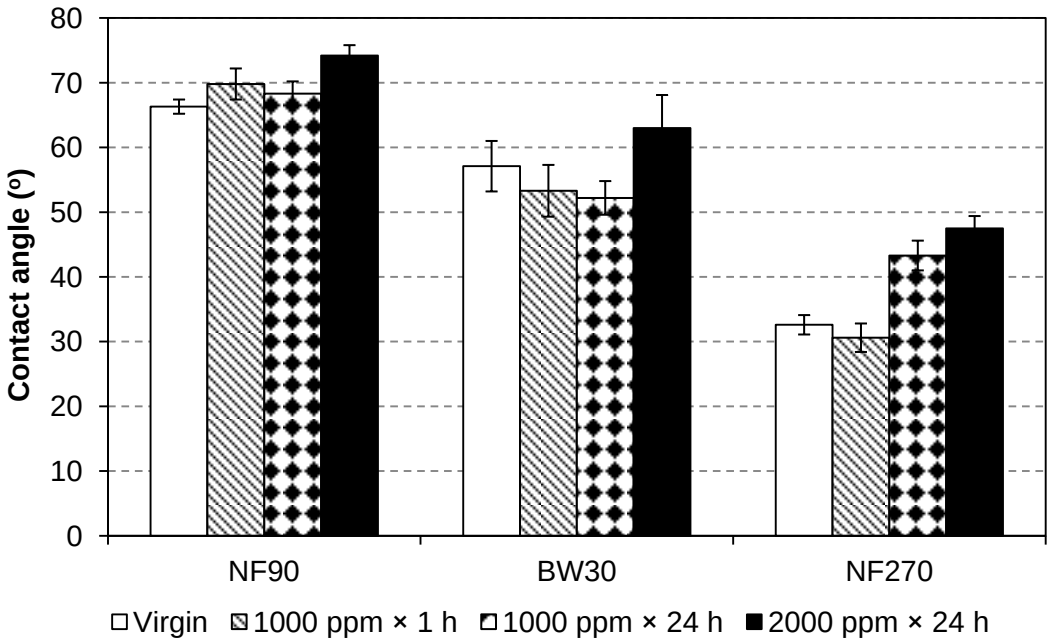

Figure 4-7. Contact angle (°) for virgin and chlorinated membranes. Error bar indicates the standard deviations of 40 measurements (2 independent membrane coupons and 20 different locations for each sample).

4.3.4 Changes in membrane performance

To evaluate the changes in intrinsic membrane properties, the water permeability coefficient, *A* (m/s.Pa), and solute permeability coefficient, *B* (m/s), for virgin and chlorinated membranes are presented in Figure 4-8. Higher *A* and *B* values indicate that the membrane is more permeable to water or solutes (Mulder, 1996). In the current study, chlorination decreased both the *A* and *B* values. The decrease of *A* with increasing exposure to chlorine can be explained by the decrease of membrane wettability due to chlorine incorporation into the membranes (Koo et al., 1986) in addition to any possible changes in the PA polymer conformation (Avlonitis et al., 1992; Soice et al., 2004; Kwon and Leckie, 2006a; b). The decrease in water flux of BW30 membranes treated at 1000 ppm for 1 and 24 h despite a slight increase in hydrophilicity can be attributed to membrane tightening due to formation of azo-compound on the surface (Soice et al., 2004). The more negative membrane surface charge due to increased carboxylic functional groups can enhance electrostatic repulsion between the membrane and

anionic solutes; therefore salt passage through the chlorinated membranes was reduced (Seidel et al., 2001; Simon et al., 2009) despite the reduced degree of cross-linking (Figure 4-3b).

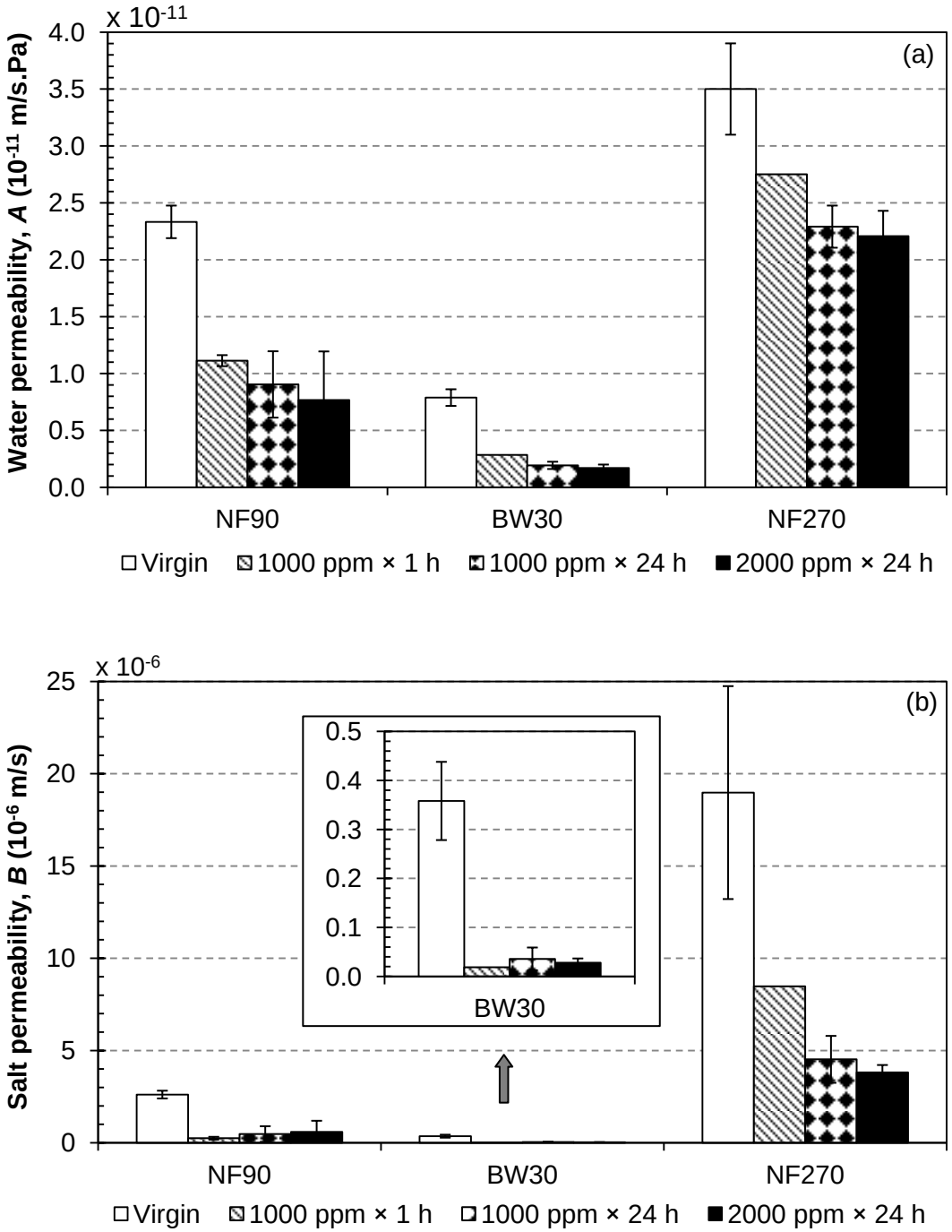

Figure 4-8. Virgin and chlorinated membrane performance: (a) water permeability coefficient, *A* (m/s.Pa) and (b) solute permeability coefficient, *B* (m/s). The operating pressures for the NF90, BW30 and NF270 membranes were set at 0.69, 1.79 and 0.48 MPa (~ 100, 260 and 70 psi), respectively.

4.4 Conclusions

In conclusion, the data presented in this study suggest that the chlorination of FA PA membranes promotes the hydrolysis of the amide C–N bond. The simultaneous occurrence of the N-chlorination and C–N hydrolysis leads to opposing effects. While the incorporation of chlorine into the PA backbone makes the membrane less hydrophilic and less permeable, the hydrolysis of the C–N bond has the potential to make the membrane more hydrophilic. This proposed mechanism could possibly explain the disparate and often contradictory observations reported in the literature.

Chapter 5

Investigation of NF and RO Membrane Performance Changes due to Hypochlorite Degradation

5.1 Introduction

Reverse osmosis (RO) and nanofiltration (NF) membranes have been widely used in desalination and water recycling to meet the increasing demand for fresh water around the world (Drewes et al., 2003; Lee et al., 2010). The past few decades have witnessed remarkable improvements in membrane performance – mainly in the rejection and permeability of PA based TFC membranes (Lee et al., 2010; Li and Wang, 2010). However, the effects of biocides such as chlorine or hypochlorite, which are employed to prevent biofouling or as membrane cleaning agent, on the performance and useful life span of PA TFC membrane are still poorly understood and remain an on-going area of research (Glater et al., 1994; Van der Bruggen et al., 2008; Cran et al., 2011; Ettori et al., 2011; Zhai et al., 2011).

Studies on the response of membrane performance to chlorine contact have led to divergent observations and explanations. Some studies reported that the flux and salt rejection of PA membranes increased after treatment with hypochlorite solutions at high pH (above 9) (Jons et al., 1999; Kwon and Leckie, 2006b; Kang et al., 2007). In other studies, it was observed that changes in the PA structure and surface chemistry caused by chlorine treatment lowered membrane flux (Koo et al., 1986; Soice et al., 2004; Kwon and Leckie, 2006b; Simon et al., 2009; Ettori et al., 2011; Do et al., 2012a). Mechanistic explanations for these contradictory observations are inconsistent (Glater et al., 1981; Koo et al., 1986; Soice et al., 2003). In order to improve membrane resistance to chlorine degradation, a

systematic understanding of membrane chlorination and its consequences on membrane performance is critically needed.

While data about the influence of membrane chlorination on flux and NaCl rejection are readily available, studies of the effects of membrane chlorination on the passage of other solutes through NF and RO membranes are limited. Investigation on the rejection of trace organic compounds by chlorinated NF and RO membranes suggested that changes in rejection are the results of a complex interaction between modified membrane properties and the nature of the solutes at filtration conditions (Urase and Sato, 2007; Simon et al., 2009). Inorganic contaminants, such as boron (in form of boric acid and borate ion) and arsenic (commonly presents as arsenate (V) anion) are also important contaminants of concern in desalination (Macedonio and Drioli, 2008). Taniguchi et al. (2001) found a correlation between the rejection of NaCl and boron for the chlorinated cross-linked fully-aromatic PA UTC-80 membranes (Toray Industries, Japan); however, no explanation was offered to rationalize their observations. Zhai et al. (2011) reported that hypochlorite treated PA RO membranes at pH 9 could experience enhanced boron rejection. However, this study focused on the effects of hypochlorite concentrations and filtration feed pH on rejection rather than on any explanation for the rejection mechanism. To the best of our knowledge, there are no reports in the literature on the effect of chlorine on arsenic rejection and on the molecular weight cut-off (MWCO) determined by PEG.

The goal of this study was to elucidate the impacts of chlorine exposure on different rejection mechanisms of RO and NF membranes. Changes in rejection by size exclusion were investigated by filtration of neutral solutes (PEGs and boron) while changes in rejection by charge repulsion were studied with NaCl and As(V). Furthermore, the importance of chlorination-promoted hydrolysis (Do et al., 2012a) on both major solute (NaCl), PEGs and trace contaminants (boron and As(V)) will be discussed in detail.

5.2 Materials and methods

5.2.1 Materials and chemicals

5.2.1.1 Polyamide membranes

Three different commercial PA-TFC membranes from Dow FilmTec (Minneapolis, MN, USA) were used: NF270, a piperazine (PIP) based semi-aromatic NF membrane, and NF90 and BW30, two fully-aromatic NF and RO membranes, respectively (Tang et al., 2009a). The surface of the BW30 membrane is polyvinyl alcohol (PVA) coated (Tang et al., 2007). All membranes were stored until used at 4 ^{o}C in the dark.

5.2.1.2 Chemicals

Unless specified otherwise, all reagents and chemicals were of analytical grade with a purity over 99%. Sodium thiosulfate used in the chlorine titration, sodium hypochlorite (~ 10% NaOCl, reagent grade) used in the membrane degradation and boric acid used in the filtration tests were purchased from Sigma Aldrich (St. Louis, MO, USA). Disodium hydrogen arsenate heptahydrate was obtained from Alfa Aesar (Ward Hill, MA, USA). Poly(ethylene glycol)s - PEGs standards for the calibration curves were obtained from Varian Inc. (Santa Clara, CA, USA). The PEGs used for the rejection tests, sodium chloride and concentrated hydrochloric acid were purchased from Merck (Darmstadt, Germany). MilliQ water (Millipore, Billerica, MA, USA) was used in all preparations and experiments.

5.2.2 Membrane degradation protocol

Membrane coupons were treated in NaOCl solutions according to the protocol described previously (Do et al., 2012a). Briefly, exact total chlorine concentration of the soaking solution, which is the sum of all active chlorine species (White, 1986), was determined by titration with a sodium thiosulfate standard and reported as ppm of equivalent Cl (Eaton et al., 1995). The pH was adjusted to 5 - a typical set point in plant operation (Bartels and Wilf, 2005) by the

addition of concentrated HCl or NaOH not more than 24 h before use. Since the pK_a of hypochlorous acid is ~ 7.5 (Kwon and Leckie, 2006a), the main active species at this soaking pH 5 is HOCl. Membranes were rinsed and soaked in MilliQ water for 24 h to remove surface impurities and preservatives before degradation tests. The coupons were pre-soaked in NaOCl solution at the same testing conditions for 1 min to remove excess water. The pre-soaked coupons were immersed in Wheaton bottles containing NaOCl solutions of 10, 100, 1000 and 2000 ppm total Cl for 24 h at room temperature (~ 21 ^{o}C) to achieve accelerated laboratory-scale chlorine degradation (Kwon and Leckie, 2006b; Simon et al., 2009; Ettori et al., 2011). The bottles were constantly shaken and covered with aluminum foil to prevent photochemical degradation of chlorine and radical reactions.

5.2.3 Membrane surface analysis

Before the characterization tests, the membrane samples were thoroughly rinsed with MilliQ water and vacuum dried for at least 48 h.

5.2.3.1 X-ray Photoelectron Spectroscopy (XPS)

Elemental analysis of the membrane surface chemistry was performed using a Kratos AXIS Ultra XPS spectrometer (Shimadzu, Columbia, MD, USA) with a monochromatic aluminum Kα X-ray source at 1486.7 eV and a 3.6 eV electron flood gun to compensate for membrane surface charging. Survey spectra were averaged from 3 scans per sample, over the range of 0 – 1000 eV at 1 eV resolution. The elemental binding energy was calibrated with the reference energy of carbon 1s at 285 eV (Beamson and Briggs, 1992). Relative sensitivity factors (RSF) of 0.78, 0.477, 0.278 and 0.891 were used for the O 1s, N 1s, C 1s and Cl 2p peaks, respectively.

5.2.3.2 Contact angle

Contact angle, which indicates the wettability of the membrane surface, was measured using the sessile drop method. Tangent lines to both sides of a 10 µL MilliQ water droplet were measured by a Dataphysics Instruments OCA Goniometer (Filderstadt, Germany). The reported contact angle of each membrane sample was the average of 40 measurements (2 independent membrane coupons and 20 different locations for each sample) with errors indicated by the standard deviations.

5.2.4 Evaluation of membrane performance

5.2.4.1 NF/RO filtration system

The custom-assembled high pressure cross-flow filtration system in Figure 3-2 consists of identical rectangular CF042 cells (Delrin Acetal, Sterlitech, Kent, WA, USA) in a parallel arrangement. The active membrane area was 42 cm^2 (4.6 cm × 9.2 cm); spacers of 1.2 mm thickness from GE Osmonics (Minnetonka, MN, USA) were used for all filtration tests. Both permeate and concentrate were re-circulated back to the feed tank; the temperature of the feed solution was controlled at 21 ± 1 ^oC by a Polysciene chiller (Niles, IL, USA).

5.2.4.2 Water permeability and sodium rejection

Prior to the permeability and rejection (performance) tests, virgin membranes (soaked in MilliQ water for 24 h) and chlorine-treated membranes were cleaned thoroughly with MilliQ water. For all performance tests (including the PEG rejection tests in Section 5.2.4.3 and boron and arsenic rejection tests in Section 5.2.4.4), the cross-flow velocity of the system was 22.6 cm/s; operating pressures for NF90, BW30 and NF270 membranes were set at 0.69, 1.79 and 0.48 MPa (~ 100, 260 and 70 psi), respectively, to obtain similar water fluxes (at around 1.4 to 1.7 × 10^{-5} m/s) for the virgin membranes. A feed solution of 10 mM NaCl in MilliQ water was circulated in the system at a pH ~ 6.5. The reported water permeability and NaCl rejection were recorded after 24 h of membrane

compaction. The permeate flux, J_w was determined by weight. The salt rejection was calculated from the permeate and tank conductivity measured by an Ultrameter II conductivity meter (Myron L Company, Carlsbad, CA, USA). At least two separate runs were performed for each treatment.

The water permeability coefficient, A (m/s.Pa), was determined from the water flux (J_w) measurements and the applied pressure difference (ΔP) using the following equations (Mulder, 1996):

$$A = \frac{J_w}{\Delta P - \Delta \pi} \tag{2-3}$$

$$\Delta \pi = iR_g T(C_b - C_p) \tag{2-4}$$

where $\Delta \pi$ is the osmotic pressure difference across the membrane, i is the dimensionless van't Hoff factor, and C_b and C_p are the bulk and permeate salt concentrations, respectively.

The apparent solute rejection, R was determined from the solute concentrations of the permeate, C_p, and the feed, C_f, using the following equation:

$$R = 1 - \frac{C_p}{C_f} \tag{2-5}$$

A diamond-patterned feed spacer was used together with a relatively high cross flow velocity (~ 22.6 cm/s) to minimize the effect of concentration polarization.

5.2.4.3 PEG rejection

After 24 h of membrane compaction, the system was flushed with MilliQ water for 5 min and the feed was switched to one of three PEG solutions with average molecular weights of 200, 400 and 600 g/mol, each with a concentration of

5.5 g/L. For each PEG feed, 10 mL of PEG samples from both the permeate and feed were taken after a 10 min filtration. After each PEG run, the system was flushed with fresh MilliQ water for 15 min to clean the setup. At least 1 replicate was done for each test condition.

PEG concentrations were determined by gel permeation chromatography (GPC) performed on a Varian Inc. PL-GPC 50 Plus system (Santa Clara, CA, USA) with a refractive index detector. The system, which was set at 30 ^{o}C, used PL Aquagel-OH 20 GPC column (Varian Inc.) with a packing material of 5 µm diameter and MilliQ water as the solvent.

5.2.4.4 Boron and arsenic (V) rejection

After 24 h of membrane compaction, boric acid and disodium hydrogen arsenate heptahydrate were added to achieve a feed concentration of 20 mg B/L and 150 mg As/L. Concentrated HCl and NaOH were used to adjust the feed pH to 7. The boron concentration was determined using a Perkin Elmer Optima 2000 inductively coupled plasma – optical emission spectrometer (ICP-OES) (Zaventem, Belgium). The arsenic concentration was analyzed using an Agilent 7700 inductively coupled plasma – mass spectrometer (ICP-MS) (Tokyo, Japan). The reported rejection was determined after treating the boron and arsenate solutions continuously for 24 h.

5.3 Results and discussion

5.3.1 Membrane surface characterization

5.3.1.1 Surface chlorine composition

In Figure 5-1, the chlorine content on the membrane surface (in atomic percentages, %Cl) obtained using XPS survey scans is plotted against the chlorine exposure (for 24 h at pH 5). The measured Cl content is mainly contributed by chlorine covalently bonded to the polyamide (e.g., N–Cl bonding); there is negligible chloride anion absorbed on the membrane surface (Do et al., 2012a).

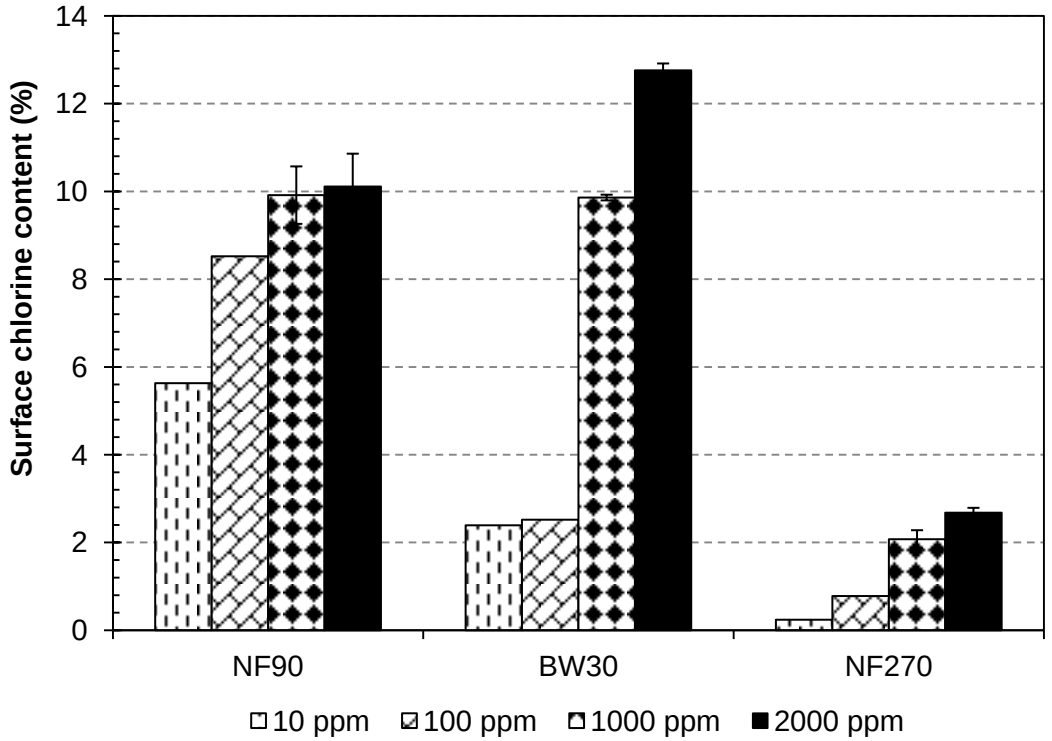

Figure 5-1. Surface chlorine atomic percent of NF90, BW30 and NF270 membranes exposed to different chlorine concentrations for 24 h at pH 5.

Generally, the results show an increase in the chlorine content with increasing exposure with some exceptions. For the NF90 membrane, the chlorine contents after exposure to 1000 and 2000 ppm were near identical, 9.92% and 10.11%, respectively, indicating a saturation point between 100 and 1000 ppm for the chlorine uptake of the uncoated aromatic PA membranes (Soice et al., 2003; Kwon et al., 2008). Compared to NF90, the chlorine uptake of the BW30 membranes after exposure to 10 and 100 ppm for 24 h was lower, which is attributed to their PVA surface coating layers. However, when treated with 1000 and 2000 ppm chlorine, the Cl contents of the BW30 membranes (9.86% and 12.76%, respectively) were equal to and higher than those of the NF90 membranes, indicating that the PVA coating does not protect the BW30 membranes effectively against attack by high chlorine concentrations (Do et al., 2012a). The chlorine uptake by the piperazine-based NF270 membrane increased nearly proportional to the exposure but was always lower than that by the fully-aromatic membranes.

This suggests that the tertiary nitrogen in the semi-aromatic PA does not readily react with chlorine (Jensen et al., 1999; Soice et al., 2003).

The degree of membrane degradation can be evaluated by the atomic O/N ratio, which is an indicator of cross-linking in the PA layer (Tang et al., 2007; Coronell et al., 2008). According to Tang et al. (2007), the O/N ratio is 1.0 for 100% cross-linking when all O and N form amide groups; while a 2.0 ratio indicates fully linear PA chains with one free carboxyl group for every 2 amide groups. Calculation of the O/N ratios for the virgin and treated membranes is given in Table C-1. With increasing chlorine exposure, the O/N ratio increased, indicating that the cross-linkages decreased, which may be attributed to induced membrane hydrolysis due to hypochlorite attack of the amide nitrogen. Loss of cross-linking of the PA rejection layer may lead to the shortening of the membrane life span.

5.3.1.2 Membrane wettability

The wettability of a membrane is assessed by contact angle measurement, whereby a lower contact angle indicates that the surface is more hydrophilic or more polar. The contact angles of all membranes in Figure 5-2 decreased after 10 ppm chlorination, indicating an increased surface wettability. In contrast, exposure to 1000 and 2000 ppm chlorine treatment increased the contact angles, indicating that the membrane surfaces became more hydrophobic and less wettable than the virgin membranes. The different effects of chlorination on wettability are suggested to be the result of two competing processes: chlorination and hydrolysis of the amide groups. A higher contact angle or reduced hydrophilicity is caused by the incorporation of chlorine onto the surface by chlorination (Koo et al., 1986; Kwon and Leckie, 2006a; Simon et al., 2009). In our previous study (Do et al., 2012a), it was observed that N-chlorination can promote hydrolysis of the amide C–N bond to form more hydrophilic carboxyl –COOH groups and thus increased membrane hydrophilicity.

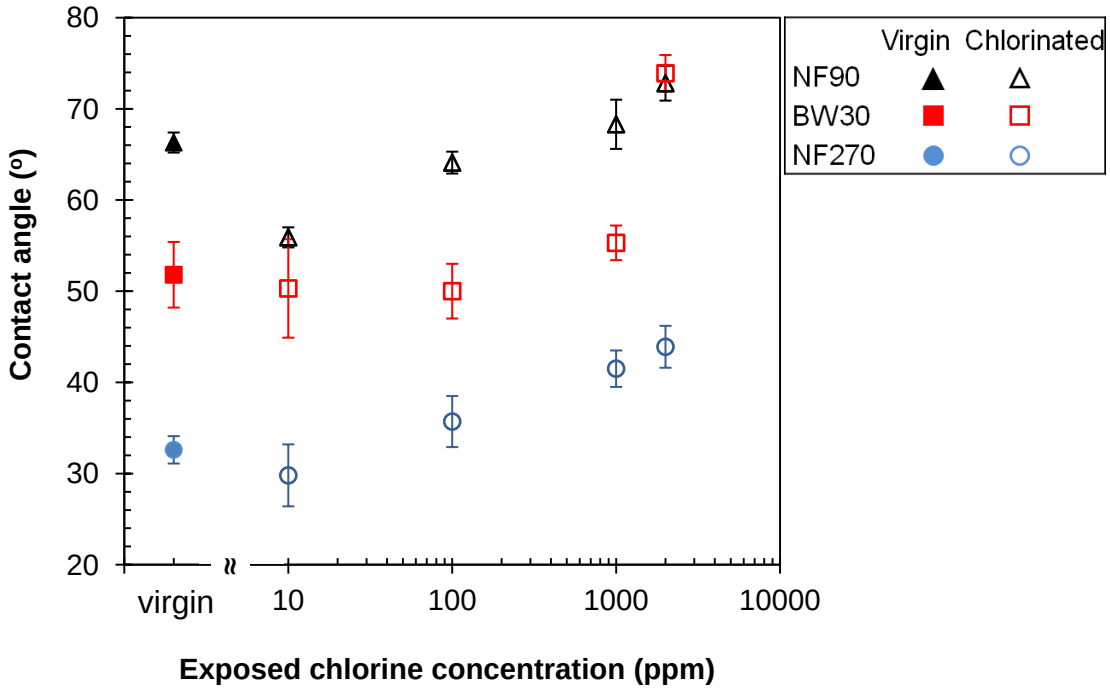

Figure 5-2. Contact angles of NF90, BW30 and NF270 membranes exposed to different chlorine concentrations for 24 h at pH 5.

5.3.2 Membrane performance

5.3.2.1 Water permeability

The effect of membrane chlorination on the water permeability of NF90, BW30 and NF270 membranes is shown in Figure 5-3. The permeability decreased steadily in all cases. For severe degradation conditions (1000 and 2000 ppm), significant permeability decline can be the result of increased hydrophobicity (Figure 3), which made the membrane surface more difficult to be wetted (Koo et al., 1986). Meanwhile, mildly chlorinated membranes (at 10 and 100 ppm) can experience tightening effects, resulting from the formation of additional linkages via azo-compounds on the surface due to chlorination, thereby causing the membrane to be less permeable (Soice et al., 2003; Soice et al., 2004). Alternatively, Kwon et al., suggested that the loss of hydrogen bonds between the amidic hydrogen and the carbonyl groups in the polymer chains due to chlorination can lead to chain compaction and restricted water passage (Kwon and Leckie, 2006b; Kwon et al., 2006).

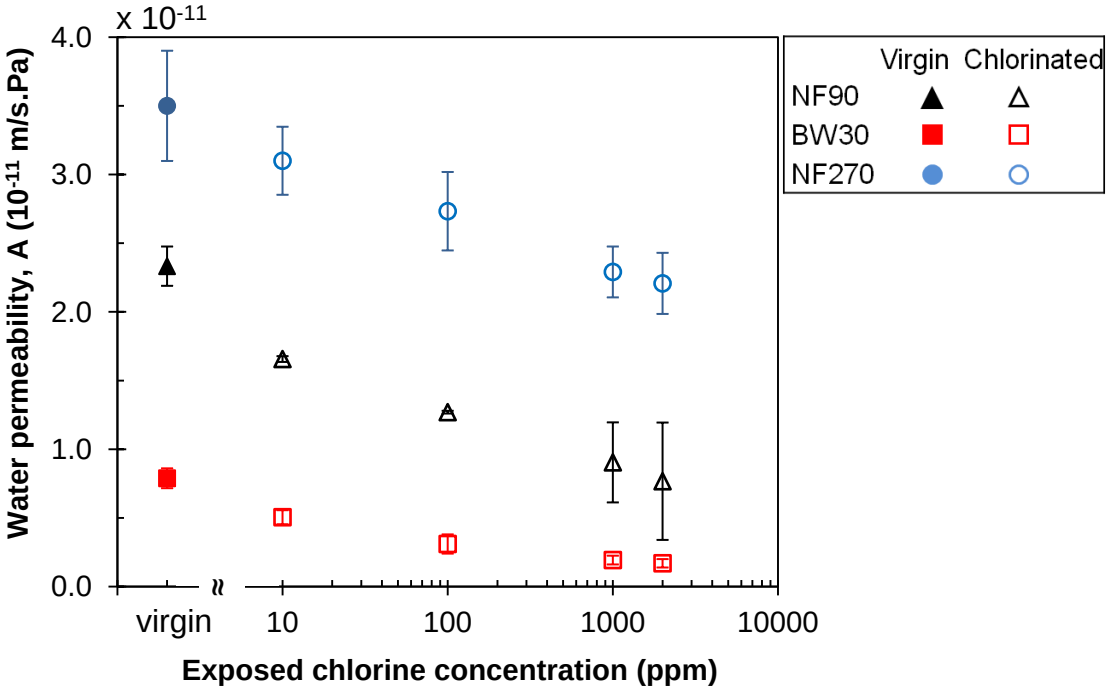

Figure 5-3. Water permeability of NF90, BW30 and NF270 membranes after 24 h filtration. Membranes were exposed to different chlorine concentrations for 24 h at pH 5. Operating pressures for NF90, BW30 and NF270 membranes were set at 0.69, 1.79 and 0.48 MPa (~ 100, 260 and 70 psi).

5.3.2.2 PEG rejection

In order to investigate the impact of chlorination on rejection by size exclusion, PEGs of 3 different molecular weights (200, 400 and 600 Da) were employed in filtration tests. These organic compounds are widely used to determine the MWCO of membranes since they are neutral and non-polar and their rejections are solely by the size exclusion mechanism (Schäfer et al., 2005; López-Muñoz et al., 2009). Rejection of PEGs by virgin and chlorinated NF90 membranes is plotted against the molecular weights of the PEGs in Figure 5-4; the results for BW30 and NF270 membranes are presented in Appendix C-2. The MWCO (corresponding to a 90% PEG rejection) for the virgin NF90 membrane was ~ 200 Da and is within the range reported in literature (López-Muñoz et al., 2009). At mild chlorination conditions (10 and 100 ppm), enhancement in the rejection of NF90 membranes (e.g., 95% compared to 89% PEG 200 rejection of virgin membrane) can be attributed to tightening effects (Section 5.3.2.1). The

PEG 200 rejection of severely degraded NF90 membranes (1000 and 2000 ppm) declined to 78% and 60%, respectively. In the case of 1000 and 2000 ppm chlorine exposure, the MWCO of the chlorinated NF90 membrane increased to ~ 400 and 600 Da, respectively, perhaps due to polymer chain degradation and the creation of a more open polyamide structure in the rejection layer. This result is consistent with the increased O/N elemental ratio from our XPS analysis (and thus reduced polyamide cross-linking degree, see Section 5.3.1.1), which suggests that the membrane structure was damaged as a result of C–N bond cleavage due to chlorination promoted hydrolysis (Do et al., 2012a). Similar changes were observed in case of the BW30 and NF270 membranes.

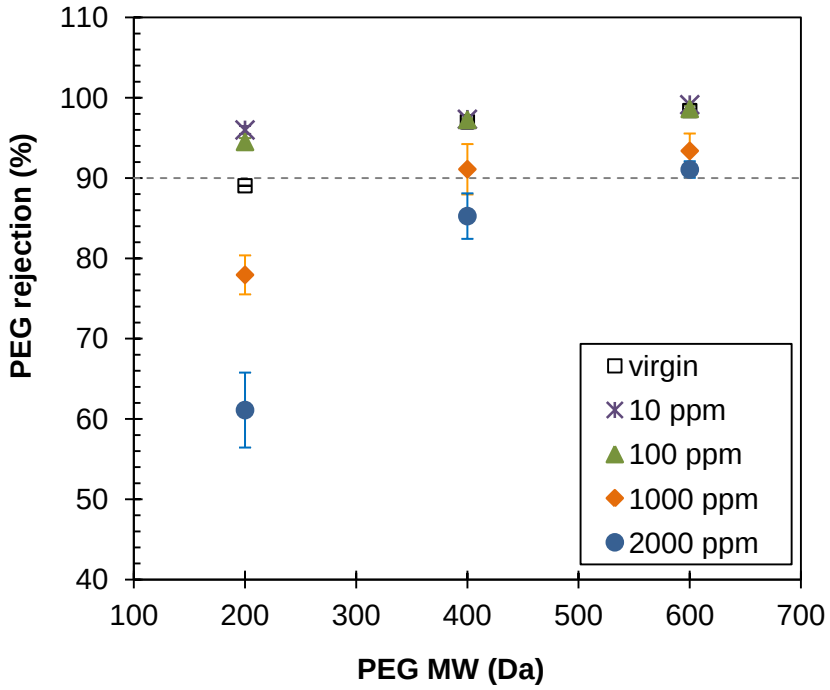

Figure 5-4. PEG rejection of virgin and chlorinated NF90 membranes. Membranes were exposed to 10, 100, 1000 and 2000 ppm of chlorine for 24 h at pH 5. Error bars represent the range of duplicate measurements.

5.3.2.3 NaCl rejection

In our previous study, chlorination promoted hydrolysis of the C–N bond incorporates more –COOH groups on the membrane surface and therefore lowers the surface charge of the membranes (Do et al., 2012a). More negative surface

charges improved rejection of NaCl by charge repulsion in all the membranes, as indicated in Figure 5-5. This is in contrast to the PEG rejection (Section 5.3.2.2), which decreased with increasing chlorine exposure. The enhanced surface negativity, together with the tightening effect, increased rejection of mildly chlorinated NF90 membranes at 10 and 100 ppm to 98.0% and 98.4% compared to 85.3% for the virgin membrane. Highly chlorinated NF90 membranes (1000 and 2000 ppm) rejected NaCl by 93% and 90%, respectively, significantly better than the virgin membrane but not as high as the mildly chlorinated ones. Apparently, the highly chlorinated membranes did not benefit from the tightening effect. In addition, the PEG rejection results revealed an increased MWCO of the chlorinated membrane (Figure 5-4). Therefore, the better rejection is the result of the enhanced negative charged surface. A comparison of the NaCl rejection at mild chlorination condition (10 and 100 ppm) and that at severe chlorination conditions (1000 and 2000 ppm) confirms that the PA polymer structure was damaged at the more severe degradation conditions.

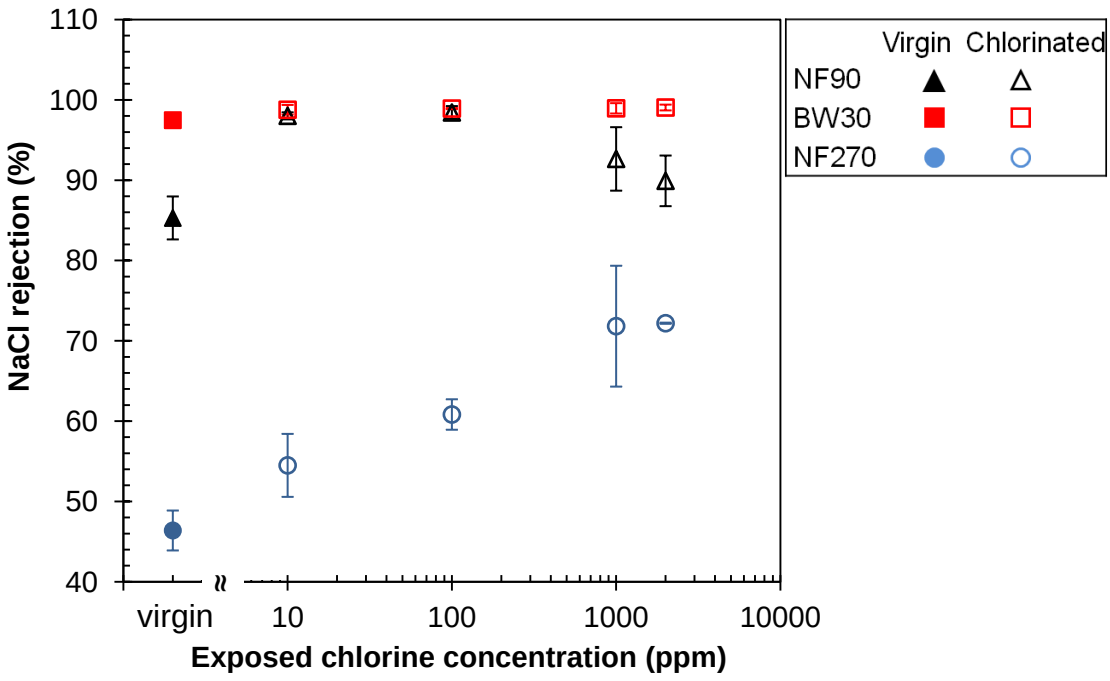

Figure 5-5. NaCl rejection of NF90, BW30 and NF270 membranes after 24 h filtration. Membranes were exposed to different chlorine concentrations for 24 h at pH 5. Operating pressures for NF90, BW30 and NF270 membranes were set at 0.69, 1.79 and 0.48 MPa (~ 100, 260 and 70 psi).

The increased NaCl rejection by the BW30 membrane can be attributed to the enhanced surface charge. However, the increase is marginal, probably due to the presence of the neutral PVA coating layer, which still partially covers the PA rejection layer and moderates the enhanced charge effect. For the loose NF270 membrane, enhanced surface negativity contributes significantly to the rejection by charge repulsion, even at high exposure conditions. The structural damage due to chlorination could not be observed in the case of NaCl filtration as clearly as in the case of the PEGs filtration in Section 5.3.2.2.

5.3.2.4 Arsenic (V) and boron rejection of NF90

Rejection tests of the arsenic (V) anion and boron were performed for virgin and chlorinated NF90 membranes to assess whether the effects of membrane chlorination on trace inorganic contaminant rejection could be correlated with the changes in charge repulsion and size exclusion caused by chlorination observed in Sections 5.3.2.2 and 5.3.2.3. Arsenic acid has a pK_{a1} of 2.2 and pK_{a2} of 7.8 (Macedonio and Drioli, 2008), and boric acid has pK_a value of 9.25 (Koseoglu et al., 2008). At a filtration pH 7, As(V) exists as an anion and is hypothesized to be rejected by charge repulsion effect in addition to size exclusion, while the rejection mechanism for uncharged boron is hypothesized to be by size exclusion. Rejection data obtained after 24 h filtration are presented in Figure 5-6. Data show that boron rejection has similar characteristics to the PEG rejection of chlorinated NF90 membrane – it increased at low chlorine exposure (10 ppm) but was reduced at severe exposure (1000 and 2000 ppm). The severely compromised boron rejection at 2000 ppm chlorine exposure can be attributed to the increased MWCO of the membrane as a result of chlorination induced hydrolysis (Section 5.3.2.2). The rejection of As(V) shares a similar pattern with NaCl rejection, which stayed relatively high in spite of the increased MWCO, and therefore may be interpreted as the effect of enhanced charge repulsion. The slight reduction of As rejection at 2000 ppm chlorine exposure may be attributed to the loss of PA cross-linking due to hydrolysis of the C–N bonds.

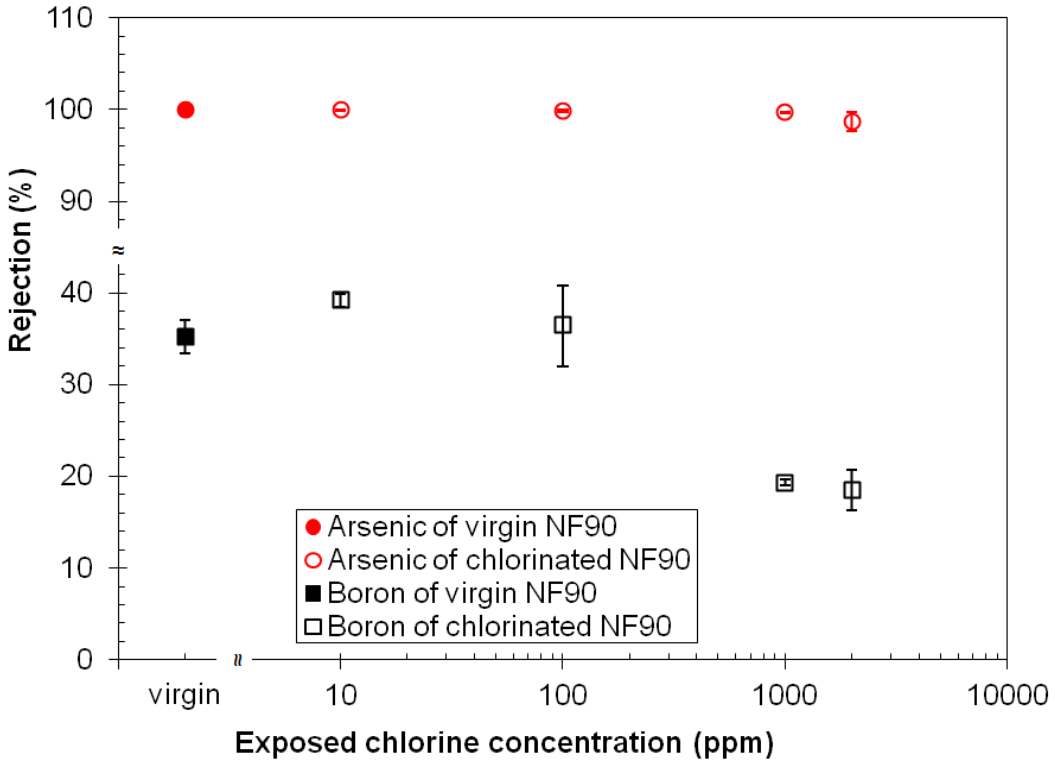

Figure 5-6. Rejection of arsenic (V) and boron of virgin and chlorinated NF90 membranes after 24 h filtration. Chlorinated membranes were exposed to 10, 100, 1000 and 2000 ppm of chlorine for 24 h at pH 5. Error bars represent the range of duplicate measurements.

The results obtained from the current study have major implications in understanding solute rejection by chlorinated membranes. Shifts in membrane rejection are caused by competing mechanisms (tightening effect, charge repulsion, and chlorination induced hydrolysis). Neutral solutes seem to be more adversely affected under severe chlorination due to 1) membrane hydrolysis (which counteracts the size exclusion effect) and 2) the lack of electrostatic repulsion. While NaCl is typically used as a standard test solute for membrane rejection, enhanced NaCl rejection can benefit from charge interaction but does not necessarily suggest improved rejection of other (neutral) trace contaminants, many of which may be of environmental and health concerns. Future research will further explore the role of such competing effects on the rejection of trace organic contaminants.

5.4 Conclusions

Chlorination and chlorination promoted hydrolysis of PA membranes change the physiochemical properties and the chemical structure of the active layer. The type and extent of these changes depend on the chlorine concentration. Importantly, this study suggests that mild chlorination can improve membrane rejection. Analysis of the rejection behavior of charged (NaCl, arsenate (V)) and neutral (boron and PEG) solutes revealed the type of changes caused by chlorination. The data confirmed that neutral solutes are rejected by the size exclusion mechanism while charged species are predominantly rejected by charge repulsion. Membranes chlorinated under mild conditions (100 ppm and below) showed lower flux but better rejection than virgin ones (due to the tightening effect and a slightly enhanced surface charge). The performance of highly chlorinated membranes (1000 ppm and above) was consistent with the previously observed competing effects of chlorination and hydrolysis (Do et al., 2012a). Incorporation of Cl created more hydrophobic surfaces causing the flux to decrease. On the other hand, chlorination promoted hydrolysis introduced more negative carboxyl groups on the membrane surface and improved the rejection of charged solutes. However, it also cleaved the amide bonds and caused polyamide depolymerization, which increased the membrane permeability for neutral species.

Chapter 6

Effects of Chlorine Exposure Conditions on Physiochemical Properties and Performance of a Polyamide Membrane – Mechanisms and Implications

6.1 Introduction

Over the past few decades, reverse osmosis (RO) and nanofiltration (NF) membrane technologies are increasingly used for water and wastewater treatment and seawater desalination. The most widely employed membrane types are thin film composites (TFC) based on aromatic polyamide (PA) chemistries, which provide excellent selectivity (Lee et al., 2010; Li and Wang, 2010). However, the performance of the PA layer is known to degrade during contact with oxidizing agents that are used for biofouling control and water disinfection, such as aqueous chlorine (Glater et al., 1994). It has been reported that exposure to chlorine can cause flux to decline (Glater et al., 1981; Koo et al., 1986; Soice et al., 2003; Kwon and Leckie, 2006b; Kwon et al., 2006; Kang et al., 2007; Simon et al., 2009; Ettori et al., 2011; Do et al., 2012a; b) and either increase (Kwon and Leckie, 2006b; Kwon et al., 2006; Simon et al., 2009; Do et al., 2012a; b) or decrease (Glater et al., 1981; Koo et al., 1986; Soice et al., 2003; Kwon and Leckie, 2006b; Kwon et al., 2006; Kang et al., 2007; Simon et al., 2009; Ettori et al., 2011) the salt rejection. Nonetheless, certain chlorine exposure conditions can improve the flux and salt rejection of PA membranes, and are employed as post-treatment in membrane manufacture (Glater et al., 1981; Jons et al., 1999; Kwon and Leckie, 2006b; Kwon et al., 2006; Kang et al., 2007; Zhai et al., 2011). Different mechanisms for chlorine to attack the PA layer of the membrane have been proposed. Active chlorine species having a partial positive charge can bind with the lone electron pair of the amide nitrogen to form N-chloroamide (Challis and

Challis, 1970; Glater et al., 1994; Jensen et al., 1999; Kwon et al., 2008; Do et al., 2012a). The other mechanism suggests that chlorine can attach to the amide aromatic ring via direct electrophilic substitution (Shafer, 1970; Glater and Zachariah, 1985) or via inter-molecular rearrangement from N-chloroamide (Orton and Jones, 1909; Orton et al., 1928; Kawaguchi and Tamura, 1984a).

The pH of chlorine exposure was reported to affect the extent to which PA membranes are degraded by chlorination (Lowell et al., 1987; Soice et al., 2003; Ettori et al., 2011). Studies have shown that chlorine is more reactive with PA at low pH, at which HOCl is the dominating active chlorine species (Lowell et al., 1987; Soice et al., 2003). Using simple model compounds, Soice et al. (2003; 2004) reported that OCl^- may not react directly with amide and aromatic rings and suggested that a different unknown degradation mechanism occurs at pH 9 and above. In our previous study, we proposed that N-chlorination can promote hydrolysis and cleavage of the amide C–N bonds even at low pH (pH 5) causing loss of membrane performance (Do et al., 2012a; b). It can be predicted that high pH favors hydrolysis due to the abundant availability of hydroxyl groups; however, detailed studies to address this issue have not been carried out yet. The competing effects of chlorine induced hydrolysis and N-chlorination could possibly explain the disparate and often contradictory observations on membrane performance changes reported in the literature.

Although the water permeability and NaCl rejection of chlorinated membranes are well documented, studies that investigated the influence of membrane chlorination on the rejection of other trace organic and inorganic compounds appear to be lacking. The passage of inorganic compounds such as boron and arsenic through membranes affected by chlorine is an important issue because these contaminants are of great concern in desalination operations (Macedonio and Drioli, 2008). Urase and Sato (2007) and Simon et al. (2009) investigated the rejection of trace organic compounds by chlorinated NF and RO membranes and reported that changes in rejection are the result of complex interaction between modified membrane properties and the nature of the solutes at

filtration conditions. Meanwhile, studies on boron rejection of chlorinated membranes by Taniguchi et al. (2001) and Zhai et al. (2011) focused on the correlation between the rejection of NaCl and boron and the effects of feed pH and hypochlorite concentrations on rejection rather than on explaining the rejection mechanism.

The complex impact of chlorine exposure on PA membranes and contradictory explanations prompted us to systematically investigate the chlorination effects on compound rejection as well as major chlorination mechanisms. For the first time, the competing effects of chlorine concentration and pH on chlorination promoted hydrolysis and N-chlorination mechanisms are reported. Their effects on membrane physiochemical and separation properties are systematically analyzed. In addition, the rejection of contaminants of significant environmental and health concern (boric acid, H_3BO_3 and arsenic (V) anion, $H_2AsO_4^-$) was evaluated to highlight the different mechanisms involved in changes in solute rejection upon chlorine exposure.

6.2 Materials and methods

6.2.1 Materials and chemicals

The NF90 nanofiltration membrane used in the current study is a commercial TFC membrane from Dow FilmTec (Minneapolis, MN, USA). The polyamide rejection layer of this membrane is formed by interfacial polymerization of m-phenylene diamine and trimesoyl chloride (Tang et al., 2009a; b). The membrane was stored at 4 ^oC in the dark until used.

Unless specified otherwise, all chemicals were of analytical grade with a purity over 99%. Sodium hypochlorite (~ 10% NaOCl, reagent grade), sodium thiosulfate and boric acid were purchased from Sigma Aldrich (St. Louis, MO, USA). Disodium hydrogen arsenate heptahydrate was obtained from Alfa Aesar (Ward Hill, MA, USA). Calcium chloride dihydrate used in the reaction with the

membrane functional groups was purchased from Merck (Darmstadt, Germany). MilliQ water (Millipore, Billerica, MA, USA) was used in all preparations and experiments.

6.2.2 Membrane chlorination procedures

The membranes were chlorinated in NaOCl solutions following the previously described protocol (Do et al., 2012a; b). The total chlorine concentration – Cl_T, which is defined as the sum of all active chlorine species (White, 1986), was determined from iodometric titration with sodium thiosulfate (Eaton et al., 1995) and reported as ppm of equivalent Cl. The solution pH was prepared at 5, 7 and 9 by adding concentrated HCl or NaOH. The concentrations of HOCl and OCl^- species were calculated from the below equations (Benjamin, 2002) with the acidity constant of hypochlorous acid, $K_a = 2.9 \times 10^{-8}$ (Kwon and Leckie, 2006a; Silberberg, 2006).

$$[HOCl] = \frac{Cl_T [H^+]}{K_a + [H^+]} \quad (2\text{-}9)$$

$$[OCl^-] = \frac{Cl_T K_a}{K_a + [H^+]} \quad (2\text{-}10)$$

Before the chlorination tests, the membrane coupons were rinsed and soaked in MilliQ water for 24 h to remove surface impurities and preservatives. The coupons were pre-soaked in NaOCl solutions at the same testing conditions for 1 min to remove excess water, and then immersed in Wheaton bottles containing NaOCl solutions of different Cl_T and pH for predetermined durations. The bottles were wrapped in aluminum foil to prevent radical reactions and photochemical degradation of chlorine, and were constantly shaken at room temperature (~ 21 ^oC).

6.2.3 Carboxyl functional groups identification by calcium cations

Virgin membranes were prepared by soaking for 24 h in advance and freshly chlorinated membranes were thoroughly rinsed to remove any remained chlorine solution. The membrane coupons were immersed in $CaCl_2$ 0.1 mM solution twice, each time for 10 min. The reaction pH was adjusted to 7 by adding appropriate amounts of 0.1 M HCl or NaOH. The coupons were then rinsed with a 0.001 mM $CaCl_2$ solution at pH 7 for 4 consecutive times (5 min each) to remove calcium ions that were not bound to the membrane surface (adapted from Coronell et. al (2008; 2009)). In order to prevent Ca^{2+} precipitation due to infusion of atmospheric carbon dioxide and maintain a stable pH of the solution, the reactions were performed in 500 mL cylindrical gas-washing bottles, which allowed nitrogen gas to be continuously purged in order to blanket the solution. The coupons were dried with nitrogen gas and kept in a vacuum desiccator.

6.2.4 X-ray Photoelectron Spectroscopy (XPS)

The elemental composition of the membrane surface was quantified from XPS survey spectra obtained using a Kratos AXIS Ultra XPS spectrometer (Shimadzu, Columbia, MD, USA) at 1 eV resolution. The monochromatic aluminum Kα X-ray source was set at 1486.7 eV and a 3.6 eV electron flood gun was used to compensate for surface charging. The relative sensitivity factors (RSF) for O 1s, N 1s, C 1s, Cl 2p and Ca 2p peaks are 0.78, 0.477, 0.278, 0.891 and 1.833, respectively.

6.2.5 Attenuated total reflection-Fourier transform infrared (ATR-FTIR)

FTIR spectra over the range of 650 – 2000 cm^{-1} were obtained using a IRPrestige-21 (Shimadzu, Columbia, MD, USA) with a 45^{o} multi-reflection HATR ZnSe flat plate crystal (PIKE Technologies, Madison, WI, USA) as the ATR element. Each spectrum was averaged from 50 scans at a resolution of 2 cm^{-1}. Baselines were corrected for atmospheric CO_2 and water vapor.

6.2.6 Contact angle measurement

Contact angles between the membrane and the tangent lines to both sides of a 10 µL MilliQ water droplet were measured using a Dataphysics Instruments OCA Goniometer (Filderstadt, Germany) via the sessile drop method. The reported contact angle was the average of 40 measurements (2 independent membrane coupons and 20 different locations for each sample) with errors indicated by the standard deviations.

6.2.7 Zeta potential

The membrane surface charge was measured using a SurPASS electrokinetic analyzer (Anton Paar GmbH, Graz, Austria). An adjustable gap cell with a channel height of ~ 110 ± 5 µm and NaCl electrolyte solution of 10 mM were used. The zeta potential was calculated from the streaming potential using the Fairbrother–Mastin formula (Elimelech et al., 1994) over the pH range from 3 to 9, achieved by auto-titration with 0.1 M HCl and NaOH.

6.2.8 Membrane performance tests

The water permeability and solute rejection of virgin and chlorinated membranes were evaluated by a laboratory-scale high pressure cross-flow filtration system consisting of parallel CF042 cross-flow test cells (Sterlitech, Kent, WA, USA). The details of the setup and filtration protocol were described in Do et al. (2012a) and are briefly summarized here. Before the tests, coupons (4.6 cm × 9.2 cm) of virgin membranes (soaked in MilliQ water for 24 h) and freshly chlorine-treated membranes were cleaned thoroughly with MilliQ water. Feed solution of 10 mM NaCl in MilliQ water, pH ~ 6.5 was circulated in the system at a cross-flow velocity of 1 L/min (corresponding to a superficial velocity of 22.6 cm/s) at a controlled temperature (21 ± 1 ^{o}C). The trans-membrane pressure was set at 0.69 MPa (~ 100 psi) to obtain a virgin membrane flux of ~ 1.2 × 10^{-5} m/s. The permeate flux was determined by a gravimetric method and the NaCl rejection was calculated from the permeate and tank conductivity. The reported water permeability and NaCl rejection were determined after 24 h of membrane

compaction (Do et al., 2012a; b). Subsequently, boric acid and disodium hydrogen arsenate heptahydrate were spiked to achieve a feed concentration of 20 mg B/L and 150 mg As/L; concentrated HCl and NaOH were used to adjust the feed pH to 7. The reported boron and arsenate rejections were recorded after continuous filtration for 24 h. The boron concentration was determined using a Perkin Elmer Optima 2000 inductively coupled plasma – optical emission spectrometer (ICP-OES) (Zaventem, Belgium). The arsenic concentration was analyzed using an Agilent 7700 inductively coupled plasma – mass spectrometer (ICP-MS) (Tokyo, Japan).

6.3 Results and discussion

6.3.1 The roles of chlorination conditions in incorporation of chlorine into the membrane surface

Many studies and manufacturers have reported chlorine exposure or tolerance as a product of time and total chlorine concentration – Cl_T of the treatment solution (ppm Cl_T•h), which implies that exposure time and concentration are equivalent and have a similar effect on membranes. In order to investigate the relevance of this conventional approach to quantify exposure, NF90 membranes were treated with different chlorine concentrations at pH 5 for different exposure durations. Figure 6-1 presents the surface chlorine content, %Cl (atomic percent, based on XPS analysis) as a function of "chlorine exposure" (ppm Cl_T•h) for total chlorine concentrations of 1, 10, 100 and 1000 ppm. As expected, the membrane chlorine uptake increased with ppm Cl_T•h (Soice et al., 2003; Kwon et al., 2008). However, for each fix concentration, the uptake appears to eventually reach saturation after adequate exposure, which may be due to stoichiometric availability of the reactive site (Soice et al., 2003). In addition, at the same ppm Cl_T•h exposure, membranes treated with higher Cl_T appear to achieve a higher surface %Cl. The current study seems to suggest that treatment concentration may play a more important role in the incorporation of chlorine into the membrane than exposure duration. Therefore, further chlorination experiments were performed at a fixed exposure time of 100 h.

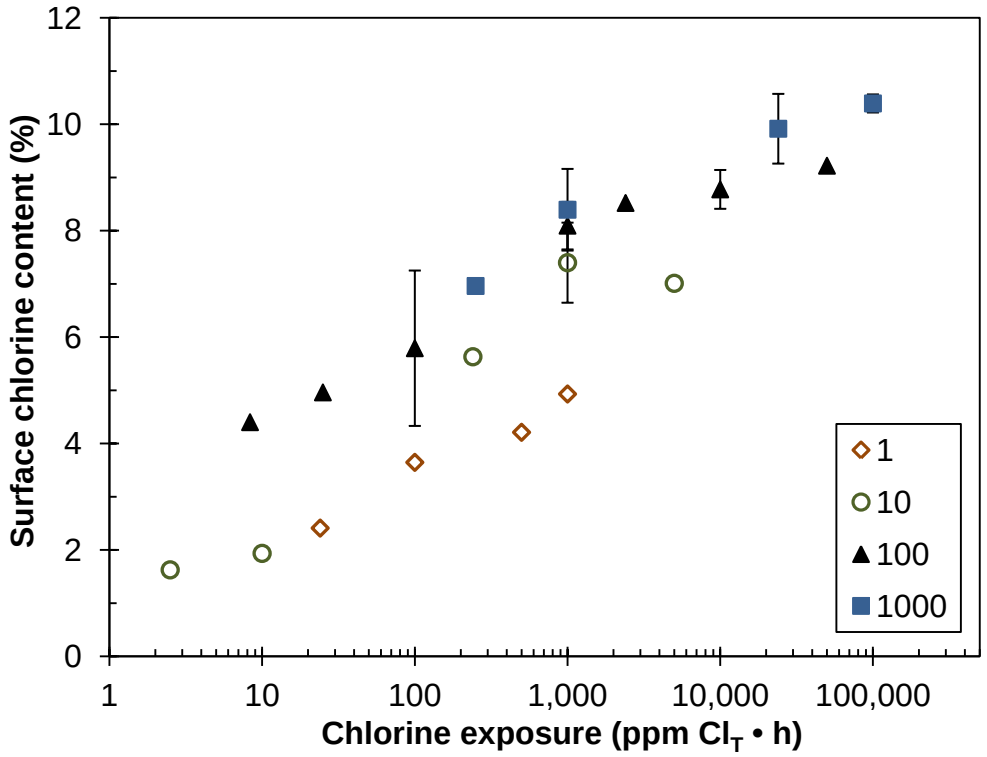

Figure 6-1. Surface chlorine content (atomic % of all surface elements except hydrogen) of NF90 membranes chlorinated at pH 5, total chlorine concentrations of 1, 10, 100 and 1000 ppm Cl_T for different durations. Error bars represent measurement ranges.

The surface %Cl of the NF90 membranes that were exposed to different chlorination solutions for 100 h are presented in Figure 6-2a, where different treatment regions can be divided with regards to the treatment pH and Cl_T indicated by the x and y axes, respectively. The background contours indicate the iso-concentration lines of [HOCl] (ppm Cl, Eq. 2-9) in the exposure solutions. The ranges of HOCl concentrations are given by the color scale. At the same Cl_T, the amount of elemental chlorine on the membranes declined as the exposure pH increased. The available chlorine in the exposure solutions existing in the form of HOCl is approximately ~ 100% at pH 5, ~ 76% at pH 7 but only ~ 3% at pH 9. The result seems to indicate that HOCl has more influence than OCl^- on the incorporation of chlorine into the membrane matrix. This agrees with previous studies on the chlorination of molecular model compounds (Lowell et al., 1987; Soice et al., 2003) and with the literature that reports that HOCl is a stronger

electrophilic chlorinating agent than OCl^- (Voudrias and Reinhard, 1988b; Sivey and Roberts, 2012). To validate this assumption, the surface %Cl is plotted against the HOCl concentrations of the exposure solutions in Figure 6-2b. The plot shows that the surface chlorine content is positively correlated with the active HOCl concentration. However, at an HOCl concentration >100 ppm, the surface %Cl of the membranes exposed to pH 5 is higher than those exposed to pH 7 and 9. At pH 5, in addition to the N-chlorination mechanism by HOCl (Jensen et al., 1999; Kwon et al., 2008; Do et al., 2012a), the formation of trace molecular chlorine (Cl_2) may directly attack the aromatic ring (Voudrias and Reinhard, 1988b; Soice et al., 2003; Sivey and Roberts, 2012). The presence of chloride anion in the chlorine soaking solution is further discussed in Appendix D-1.

In Figure 6-2a, for the membrane that was exposed to a Cl_T of 2000 ppm at pH 9, surface chlorine could not be detected (denoted as N.D.). This condition is further investigated in Section 6.3.2.

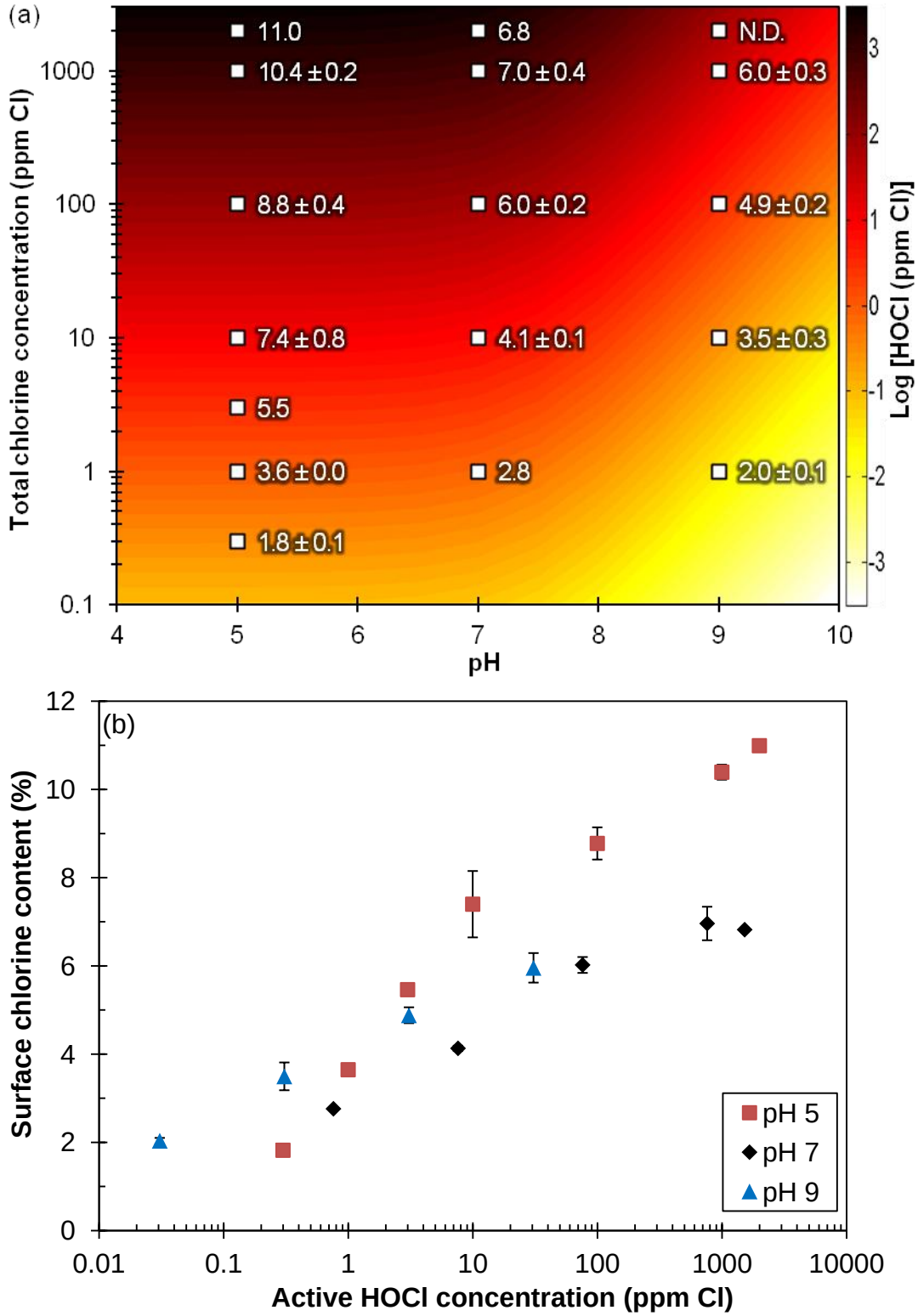

Figure 6-2. Surface chlorine content (atomic %) of NF90 membranes chlorinated for 100 h at different total chlorine concentrations and pH. (a) %Cl data at different chlorination conditions, background color contours represent iso-concentration lines of HOCl. N.D.: not detected. (b) %Cl versus HOCl concentration of the exposure solutions.

6.3.2 Chlorination promoted membrane hydrolysis and the role of pH

In our previous study, it was suggested that the presence of chlorine species in the exposure solution can promote the hydrolysis of the amide C–N bonds in the PA leading to C–N bond cleavage and –COOH group formation (Do et al., 2012a). The increased number of –COOH groups and bond cleavage reduces the cross-linking degree of the PA layer (Do et al., 2012a), which can be evaluated by the atomic O/N ratio (Tang et al., 2007; Coronell et al., 2008). The O/N ratio of 1:1 indicates a 100% cross-linking of the PA layer (all O and N form amide groups); and a 2:1 ratio indicates fully linear PA chains (one free carboxyl group for every two amide groups) (Tang et al., 2007). Figure 6-3a presents the XPS data for the O/N ratios for membranes treated at different Cl_T and pH for 100 h. Within the experimental accuracy, the O/N ratios at a given pH increased at higher Cl_T, which confirms the promoting effect of chlorine species on PA layer hydrolysis. Since HOCl plays a dominant role in the incorporation of chlorine into the PA layer (see Section 6.3.1), the O/N ratio is plotted against the active HOCl concentration for different exposure pHs (pH 5, 7 and 9) in Figure 6-3b. As expected, an increased active HOCl concentration resulted in a higher O/N ratio. In addition, membranes chlorinated at higher pHs (pH 7 and pH 9) had significantly higher O/N ratios than their counterparts at pH 5. These results suggest that higher pH can readily promote hydrolysis due to the abundant OH^- groups. A plausible explanation for the dependence of hydrolysis on both chlorine species and OH^- is as follows: active chlorine species (in this case HOCl) attack the electron-rich N atom of a C–N bond (the N-chlorination mechanism), which weakens the C–N bond as the shared pair of electrons are drawn to the N atom (McMurry, 2004; Do et al., 2012a). The resulting positively charged C atom requires a neucleophile (OH^- in this case) to stabilize the atom. As both HOCl and OH^- are likely involved in the chlorination promoted hydrolysis, one may further hypothesize that the degree of hydrolysis is directly linked to the concentration product of [HOCl] • [OH^-] (or equivalently [OCl^-], see Appendix D-2). The current study suggests that pH plays two essentially roles in chlorination promoted hydrolysis by controlling 1) the speciation of HOCl versus OCl^- and 2) the abundance of OH^-.

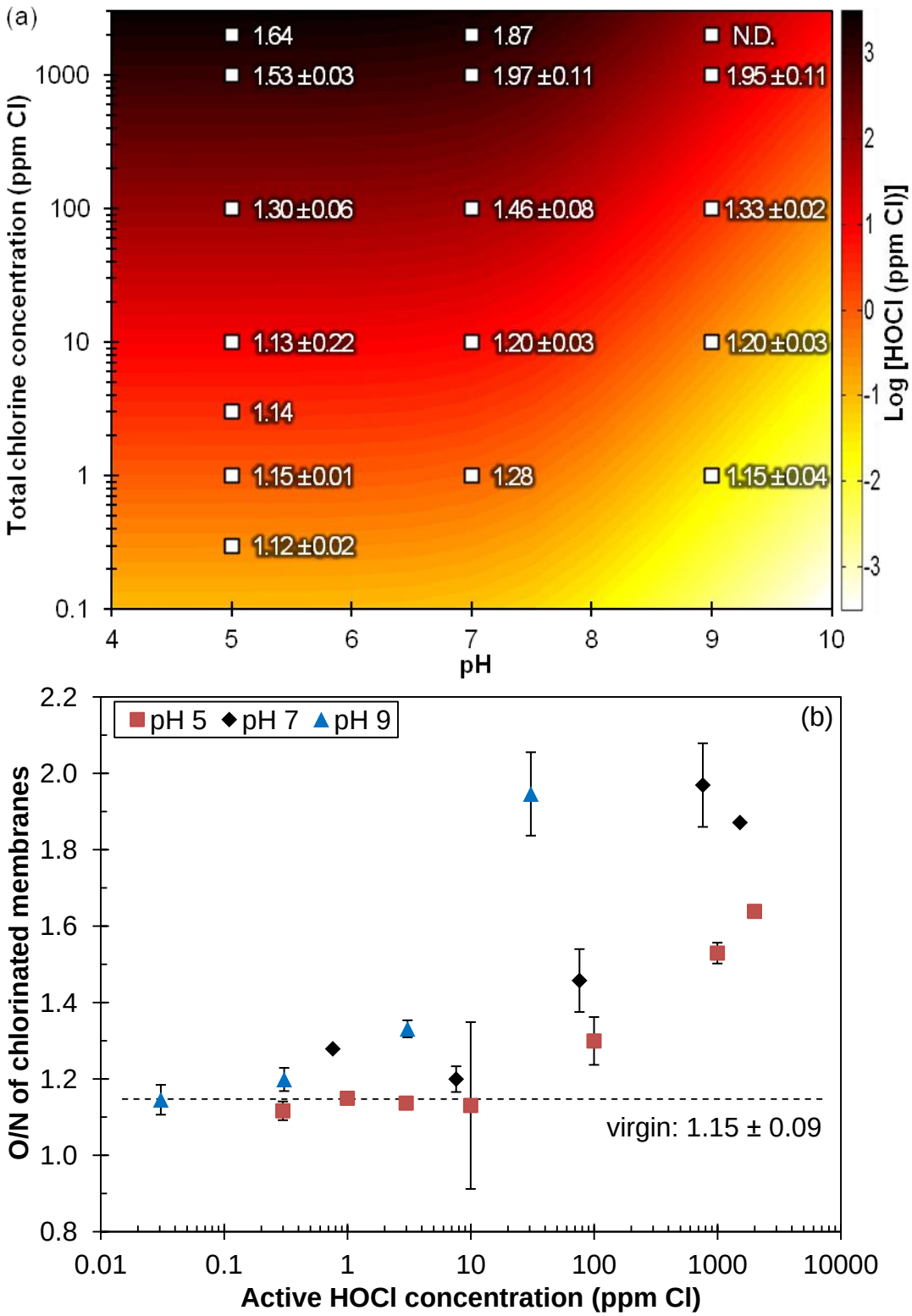

Figure 6-3. O/N ratios of NF90 membranes chlorinated for 100 h at different total chlorine concentrations and pH: (a) O/N data at different chlorination conditions, background color contours represent iso-concentration lines of HOCl. N.D.: not detected; (b) O/N versus HOCl concentration of the exposure solutions.

It is important to highlight that after treating the PA layer with 2000 ppm Cl for 100 h at pH 9, nitrogen and chlorine signals could not be detected on the membrane surface (denoted as N.D.), suggesting that the PA layer was completely removed. ATR-FTIR data shown in Figure 6-4 confirm this supposition. The characteristic peaks for fully aromatic PA, i.e., amide I, aromatic amide and amide II at wave numbers of 1663, 1609 and 1541 cm^{-1} (Tang et al., 2009a), respectively, completely disappeared and only those characteristics of polysulfone remained. The combination of high C_T and high pH completely hydrolyzed the membrane and dissolved the normally insoluble polyamide layer, which directly supports the chlorination promoted hydrolysis mechanism. This experiment also confirmed that chlorine does not bind to the polysulfone layer (Ettori et al., 2011).

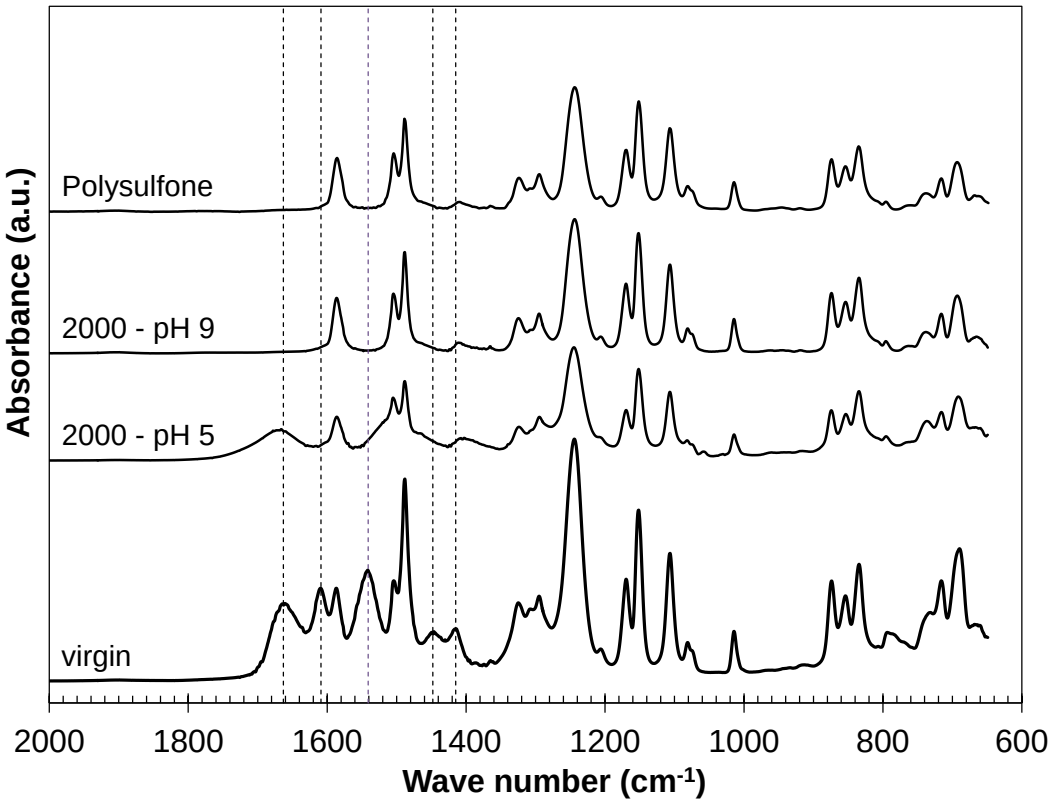

Figure 6-4. ATR-FTIR spectra for polysulfone, NF90 membranes: virgin and chlorinated at 2000 ppm Cl for 100 h at pH 5 and 9.

To further confirm that the increase of oxygen on the membrane is related to increased carboxylate groups as a result of hydrolysis, the chlorinated membranes were exposed to $CaCl_2$ solutions. As Ca^{2+} has a strong tendency to form a complex with carboxylate groups, the surface concentration of Ca (%Ca) can be a useful indicator of the surface concentration of $–COO^-$ (Jin et al., 2009). As shown in Table 6-1, the membrane without chlorine exposure did not show noticeable amount of Ca binding based on XPS measurement, which is likely due to the relatively low XPS detection limit (~ 0.1 atomic%). In addition, the %Ca increased as the Cl_T and pH increased, which is consistent with the more –COOH groups due to severe membrane hydrolysis under the higher Cl_T and higher pH. Nevertheless, the current method is semi-quantitative due to the low XPS detection limit and the possibility of non-specific binding of Ca^{2+} to moieties other than $–COO^-$. Future studies may consider the use of Rutherford backscattering spectroscopy (Coronell et al., 2008; 2009) or uranyl cation binding (Tiraferri and Elimelech, 2012) for more quantitative information on the creation of $–COO^-$ due to chlorine promoted hydrolysis.

Table 6-1. Reaction of calcium cations and membrane carboxylic groups. Surface elemental composition (atomic %) of membranes chlorinated for 100 h. Reaction with Ca^{2+} was performed at pH 7. N.D.: not detected.

[Cl_T] (ppm Cl)	Chlorination pH	Surface elemental composition (at%)				
		O 1s	C 1s	N 1s	Cl 2p	Ca 2p
Virgin		13.37	75.68	10.95	-	N.D.
100	5	14.8	67.3	10.5	7.5	N.D.
100	7	15.1	67.5	11.0	6.3	0.1
100	9	16.2	69.1	10.1	4.4	0.3
1000	5	14.4 ± 1.1	66.0 ± 1.1	9.5 ± 0.3	10.1 ± 0.3	N.D.
1000	7	16.3 ± 0.5	66.9 ± 0.9	9.1 ± 0.6	7.5 ± 0.4	0.3 ± 0.0
1000	9	17.3 ± 0.1	66.5 ± 0.3	9.6 ± 0.3	5.9 ± 0.2	0.8 ± 0.0

6.3.3 Changes in surface properties due to chlorination and hydrolysis

Chlorination can modify surface properties and therefore influence membrane performance. After exposing membranes to different Cl_T and pH for 100 h, the resulting contact angles were significantly different (Figure 6-5a), with lower contact angles generally found at higher pHs (pH 7 and pH 9) and lower Cl_T. In contrast, the largest contact angles were found at pH 5 and high Cl_T (1000 and 2000 ppm). These trends may be attributed to competing effects of chlorine incorporation, which decreases hydrophilicity (Koo et al., 1986; Simon et al., 2009) versus hydrolysis of the C–N bonds, which increases hydrophilicity (Do et al., 2012a). Increased contact angles, i.e., more hydrophobic surface for exposures of 1000 and 2000 ppm for 100 h at pH 5 are the result of chlorine incorporation into the membrane (Koo et al., 1986; Simon et al., 2009). At lower chlorine contents (%Cl), conversion of C=O groups to $–COO^-$ due to amide bond hydrolysis can dominate the effect of chlorine incorporation, thus rendering the surface more hydrophilic (Do et al., 2012a). Figure 6-5b further illustrates these competing effects: the membranes are most hydrophilic at a low exposure active HOCl concentration and high pH (more hydrolysis and less surface chlorine) and become less hydrophilic as the exposed HOCl concentrations increase. It is also worthwhile to note that severe degradation of polyamide may also expose the polysulfone support and thus change the contact angle measurement. In current study, the peeling off polyamide from polysulfone support only happened for 2000 ppm exposure at pH 9 based on XPS and FTIR measurements.

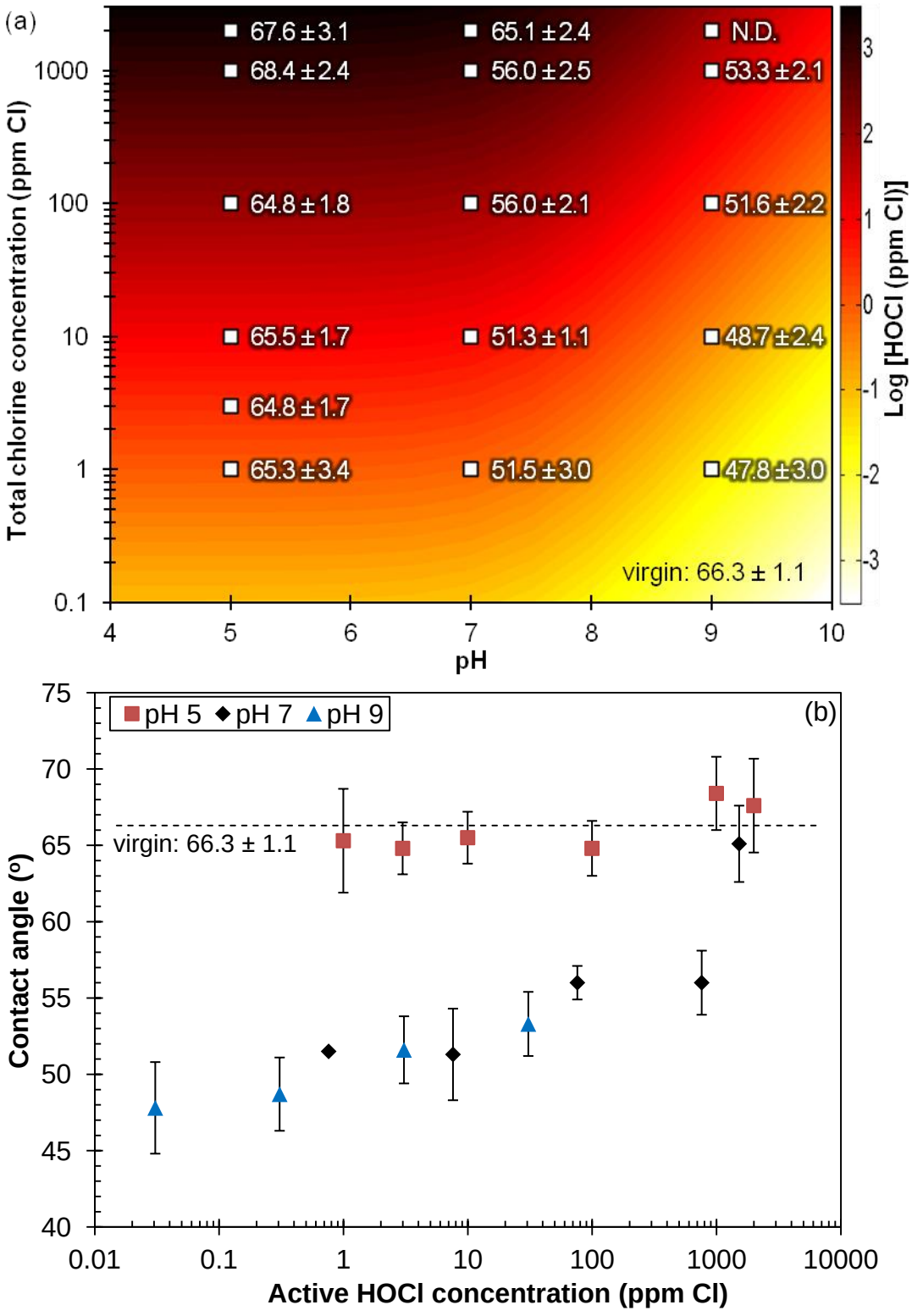

Figure 6-5. Contact angles (degree) of NF90 membranes chlorinated for 100 h at different total chlorine concentrations and pH: (a) Contact angle data at different chlorination conditions, background color contours represent iso-concentration lines of HOCl; (b) Contact angle versus HOCl concentration of the exposure solutions.

The surface charge of virgin and chlorinated membranes (1000 ppm, 100 h, pH 5 and 9) were measured with NaCl 10 mM over pH 3 to 9 and provided in Figure D-2, Appendix D-3. The virgin NF90 membrane has its iso-electrical point (IEP) at pH ~ 5.5 and is possitively charged at a pH below the IEP due to the protonation of amide groups (Childress and Elimelech, 1996). Chlorinated membranes became negatively charged at a pH below the IEP of the virgin membrane. These results agreed with previous studies (Kwon and Leckie, 2006a; Simon et al., 2009; Do et al., 2012a) and support the N-chlorination mechanism, where chlorine displaces the hydrogen of the amide nitrogen and inhibits the formation of $–NH_2^+$ groups (Do et al., 2012a). The increased negative charge density at high pH can be attributed to an increased surface density of $–COO^-$ groups, consistent with the chlorination promoted hydrolysis mechanism.

6.3.4 Changes in membrane water permeability, rejection of major solutes (NaCl), and rejection of trace contaminants (B and As(V)) due to chlorination and hydrolysis

The influence of chlorination and hydrolysis on membrane performance was appraised by studying the water permeability, the rejection of major solutes (NaCl), and the rejection of trace contaminants (boric acid and arsenic (V) anion). The water permeability values and NaCl rejection of membranes chlorinated at different Cl_T and pH for 100 h are presented in Figure 6-6. At the same Cl_T, the increase of the water permeability as the pH increases can be attributed to hydrolysis effects, which create a more open PA structure (Figure 6-3) and make the membrane surface more hydrophilic (Figure 6-5). At pH 9 where the chlorinated membrane were generally very hydrophilic (contact angle ~ or < 50º), the increased Cl_T led to increased water permeability as a result of reduced degree of cross-linking (Figure 6-3). Indeed, the permeability of the membrane chlorinated at 1000 ppm Cl_T and pH 9 was too large to be quantified in the current study. In contrast, at pH 5 where the chlorinated membranes were relatively more hydrophobic, the increased Cl_T resulted in a reduced water permeability as the surface became more difficult to wet. Mixed trends were observed at pH 7 (water

permeability first reduced and then increased with increasing Cl_T) due to the competing hydrophobicity and reduced cross-linking effects.

The rejection of the major solute, NaCl, can be understood by considering both the size exclusion and charge repulsion mechanisms. At low Cl_T (e.g., 10 ppm) and pH 5, a higher salt rejection (99.6 ± 0.4%) compared to the virgin membrane (87.1 ± 6.3%) can be explained by the tightening effects due the formation of azo compounds on the membrane surface (Soice et al., 2003; Soice et al., 2004). Our prior rejection study with poly(ethylene glycol) (PEG) revealed a reduced molecular weight cutoff for NF90 chlorinated at 10 ppm Cl_T and pH 5 (PEG 200 Da rejection of 95% for the chlorinated membrane compared to that of 90% for the virgin membrane) (Do et al., 2012b). Another important mechanism is charge repulsion. Since NaCl is a charged solute, its rejection is affected not only by the tightness of the membrane rejection layer but also by the membrane surface charge. Under most treatment conditions, NaCl rejection by chlorinated membranes is better compared to the virgin membrane partly due to the enhanced negative surface charge (Appendix D-3). However, at high pH and Cl_T, where hydrolysis gets more servere, the enhanced charge repulsion does not compensate for the opening of the rejection layer. This is shown in the cases of chlorination at 1000 ppm at pH 7 and 9, for which the cross-linking ratios (Figure 6-3) indicate almost linear PA layers: the rejection of the membrane exposed to pH 7 was only 55.2% compared to 87.1% for the virgin membrane; and the rejection of the membrane exposed to pH 9 diminished to ~ 0% (denoted as N.P.). The data for the salt permeability coefficient, *B* (m/s), which is an intrinsic property of the rejection layer was provided in Appendix D-4.

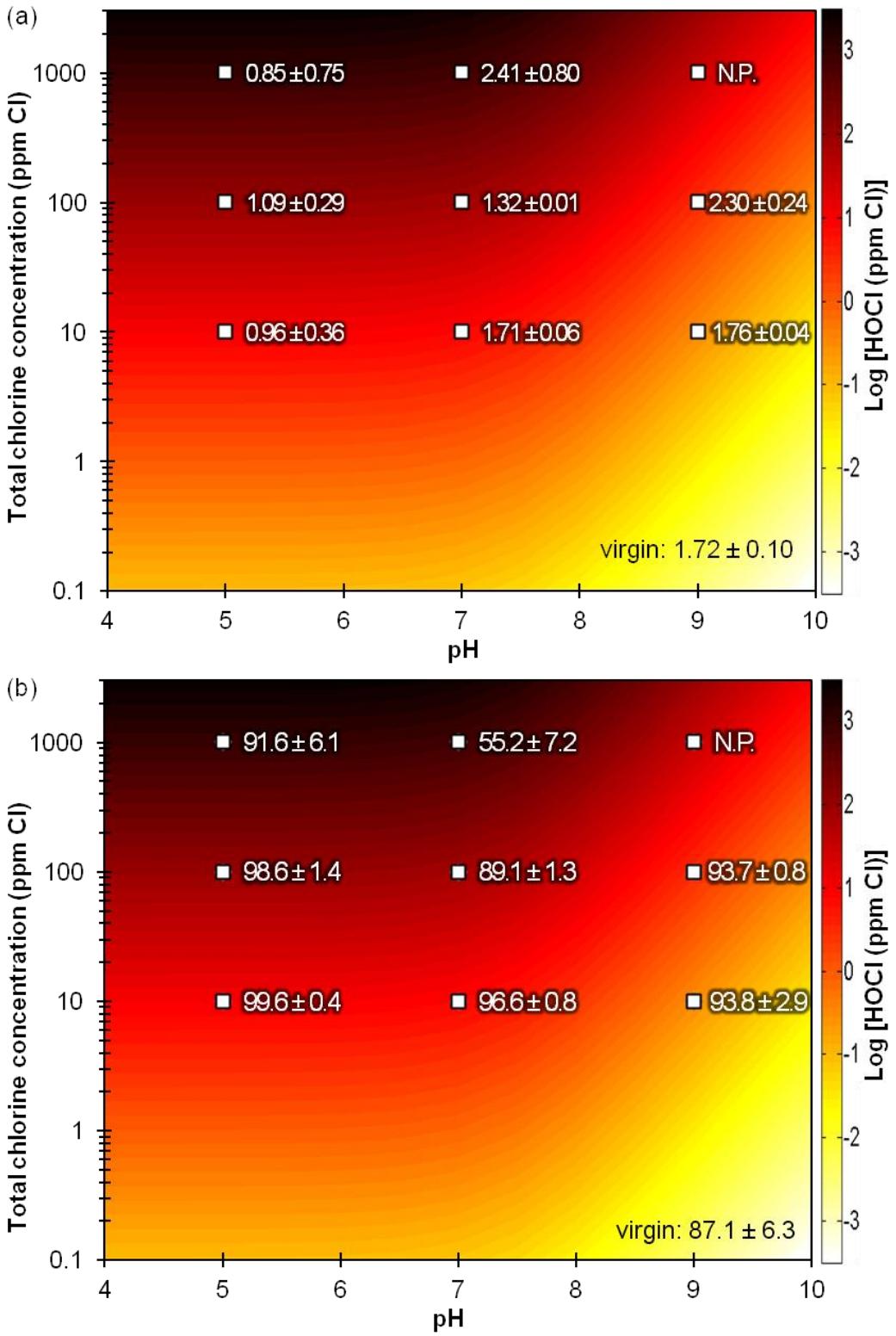

Figure 6-6. Performance of NF90 membranes, virgin and chlorinated for 100 h at different total chlorine concentrations and pH: (a) water permeability values (× 10^{-11} m/s•Pa); and (b) NaCl rejection (%) data at different chlorination conditions, background color contours represent iso-concentration lines of HOCl. N.P.: membrane failed to perform.

Solutions of arsenic (V) anion, which exists as $H_2AsO_4^-$ at feed pH 7 were filtrated at feed pH 7 to verify the chlorination and hydrolysis effects on the rejection of charged solutes. The performance of chlorinated membranes in terms of As(V) rejection in Figure 6-7a follows the patterns for NaCl rejection. The rejection of As(V) plotted against that of NaCl in Figure D-4a, Appendix D-5 shows a very high correlation coefficient ($R^2 = 0.97$).

The rejection of boric acid presented in Figure 6-7b reveals different trends. Boric acid, H_3BO_3 is neutral at feed pH 7; therefore, its rejection is solely by size exclusion mechanism and does not benefit from the enhanced surface negativity. The decreased boron rejection under most treatment conditions reveals that bond cleavage by hydrolysis results in a more open membrane structure. Significantly, at 1000 ppm, pH 7 or 9, the membrane almost completely lost its boron rejection. Even at 10 ppm Cl_T, boron retention decreases considerably at pH 7 and 9, whereas the As(V) rejection did not change significantly as pH increases. The exceptional increase in rejection occurred at a chlorination condition of 10 ppm, pH 5, which can be attributed to the tightening effects (Soice et al., 2003; Soice et al., 2004) and the corresponding reduced MWCO (Do et al., 2012b). The poor correlation between the rejection of uncharged boric acid with that of charged NaCl is illustrated in Figure D-4b, Appendix D-5.

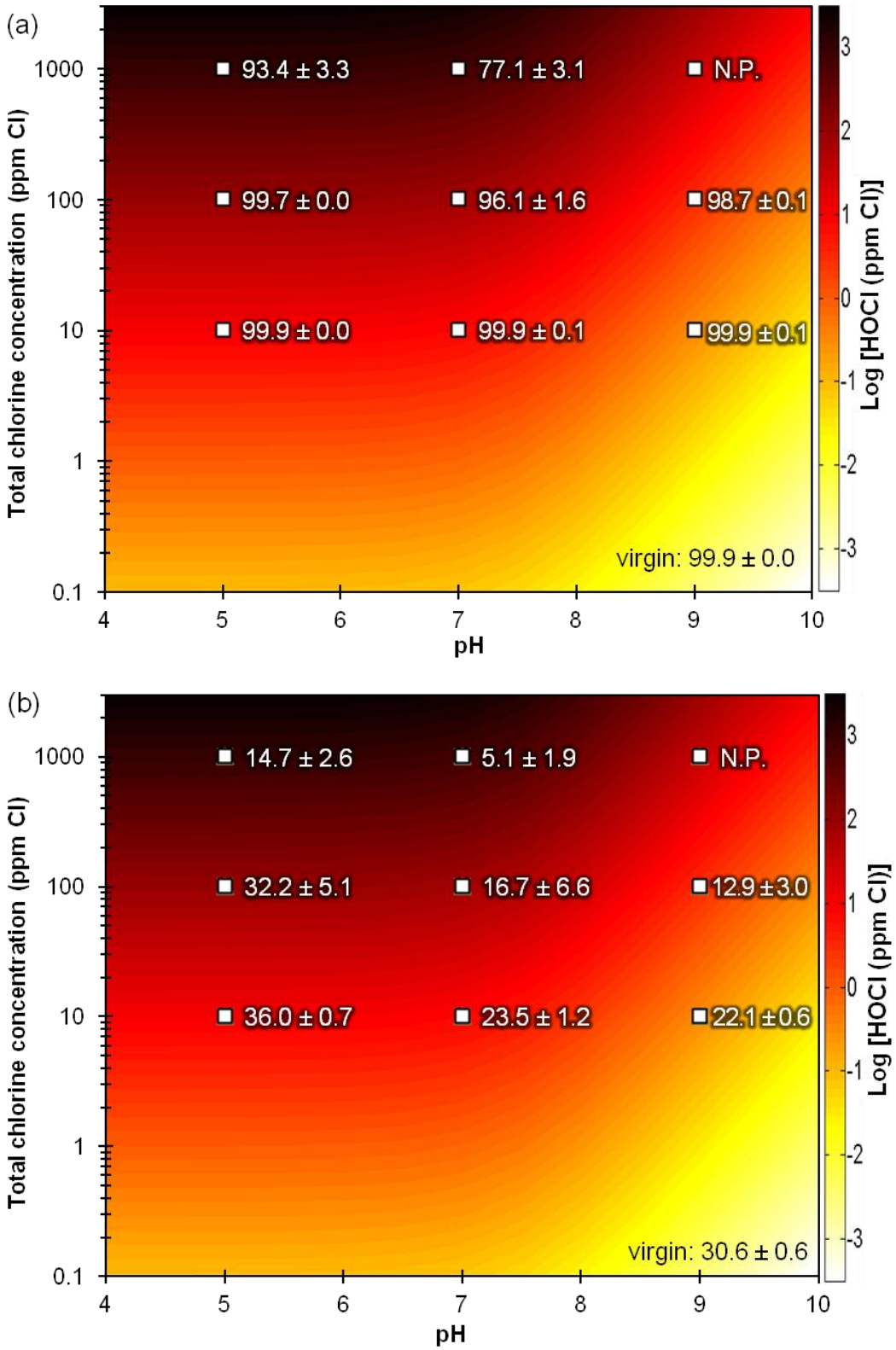

Figure 6-7. Trace inorganic rejection of NF90 membranes, virgin and chlorinated for 100 h at different total chlorine concentrations and pH: (a) arsenic (V) and (b) boron rejection data at different chlorination conditions, background color contours represent iso-concentration lines of HOCl. N.P.: membrane failed to perform.

6.4 Conclusions

This study demonstrates the concurrence of competing processes of chlorine exposure: (1) chlorine incorporation into the membrane matrix is largely governed by the HOCl concentration and it increases at lower pH and higher Cl_T; (2) chlorination induced hydrolysis of the polyamide depends on the concentrations of both HOCl and OH^-. The degree of polyamide cross-linking can be greatly reduced at higher pH and higher Cl_T. Additional mechanisms include direct ring attack by molecular chlorine species (favored at low pH and high Cl_T) and the tightening effects due to the formation of azo-compounds (favored at low pH and low Cl_T). The competing effects of these processes result in opposing trends in terms of physiochemical properties and membrane performance. The incorporation of chlorine into the membrane matrix results in more hydrophobic and less water permeable membranes. On the other hand, chlorination promoted hydrolysis of amide bonds creates additional surface carboxylic groups, enhances membrane hydrophilicity and surface charge density, and increases the membrane water permeability.

The current study clearly contrasts the rejection behavior of charged solutes versus that of neutral compounds by the chlorinated membranes. The size exclusion mechanism plays a dominant role in the rejection of neutral solutes (e.g., boron at pH 7); the rejection value tends to decrease as a result of reduced polyamide cross-linking upon chlorination. For charged solutes such as NaCl and As(V), electrostatic interaction also plays an important role in addition to the size exclusion mechanism. This can lead to a very different rejection behavior for charged solutes compared to that of neutral solutes for chlorinated membranes. For example, chlorination promoted hydrolysis increases the membrane surface charge density and enhances the charge repulsion mechanism, which explains the increased NaCl rejection under most chlorination conditions (even if the corresponding boron rejection decreases). Whereas most existing membrane chlorination studies have focused on NaCl rejection behavior, the design of a membrane plant can often be governed by the rejection of other contaminants (e.g., boron in seawater desalination). Thus, future membrane chlorination studies are

recommended to include contaminants of environmental and health significance (e.g., pharmaceutically active compounds and endocrine disruptors for wastewater reclamation applications by RO).

The current study reveals opportunities for membrane performance enhancement by using chlorination post-treatment. Improved water permeability and NaCl rejection can be obtained by carefully optimizing chlorination conditions. For example, membranes chlorinated at pH 9 and moderate Cl_T (100 ppm) had greatly increased water permeability (2.30 L/m^2h) and rejection (93.7%) compared to the virgin NF90 membrane (1.72 L/m^2h and 87.1%). In addition, the chlorinated membrane surface is more hydrophilic compared to the virgin membrane, which tends to minimize membrane fouling (Tang et al., 2011). When the rejection of NaCl is of primary concern relative to other contaminants, controlled chlorine exposure has considerably potential for improving the performance of polyamide based RO and NF membranes.

Chapter 7

Conclusions, Contributions and Recommendations

7.1 Conclusions and contributions

This research presents a comprehensive study on the impacts of chlorination conditions on the mechanisms of polyamide membrane degradation and membrane structure, properties and performance. Different membrane chemistries involving fully aromatic and piperazine based polyamides (PA) and the effects of treatment conditions, including concentrations, pH and durations were investigated. The changes in elemental composition and bonding chemistry at the surface of rejection layers after the membranes were exposed to different chlorine treatment conditions were determined using XPS. The nature of chemical bonding across the rejection layer and polysulfone supporting layer was elucidated from ATR-FTIR data. This research was the first to prove the increase of carboxylic groups on the chlorine treated membrane surface, using the calcium treatment technique. Zeta potential and sessile drop contact angle measurements were employed to determine the changes in the surface charge and wettability of the membranes. The combination of these characterization techniques to comprehensively investigate the nature of chlorine attack on fully aromatic and semi-aromatic polyamide membranes is a novel contribution of this thesis.

As a result of these coordinated characterization techniques, this research has successfully identified and demonstrated a new chlorination promoted hydrolysis mechanism that occurs simultaneously with the incorporation of chlorine into the PA matrix. The different steps involved in the mechanism include: chlorine attaches to and withdraws the lone electron pair of the amide nitrogen, causing the weakening and cleavage of the amide C–N bond; and the positively charged C atom is in turn stabilized by the hydroxyl group. This

hydrolysis mechanism was supported by the increased oxygen content of the rejection layer (XPS), the decrease of C–N bonds (XPS, ATR-FTIR), and the increase in surface negative charge (zeta potential measurement) and –COOH groups (Ca^{2+} reaction).

Chlorine treatment conditions influence the two chlorination and hydrolysis processes as follows:

- Chlorine incorporation into the membrane matrix is largely governed by the HOCl concentration and pH. This effect increases as the pH decreases and the total chlorine concentration increases.

- Chlorination induced hydrolysis depends on the concentrations of both HOCl and OH^-. The C–N bond hydrolysis increases with increasing pH and total chlorine concentration.

This study identified that although the tertiary amide nitrogen of the semi-aromatic PA was less prone to chlorine attack, chlorine may still bind to the non cross-linked amino groups and hydrolysis of the PA could still occur. The observed degradation of the membrane performance is attributed to the hydrolysis of the C–N bonds.

In contrast to the common belief that the polyvinyl alcohol coating can inhibit chlorine attack on the membrane, chlorine was still found to bind to the PA layer underneath the coating. Moreover, the coating can be partially or fully detached under severe chlorine treatment conditions.

The effects of chlorine exposure on the PA structure were correlated with membrane performance, which was evaluated in terms of water permeability, rejection of charged (NaCl, arsenic (V) anion) and neutral (polyethylene glycols - PEGs and boric acid) solutes. N-chlorination and C–N bond hydrolysis cause opposite effects on membrane physiochemical properties and performance; their simultaneous occurrence offers coherent explanations to the disparate and often

contradictory observations on chlorination effects reported in the literature, which are summarized below:

- Incorporation of chlorine into the PA layer causes the membrane surface to be more hydrophobic. Chlorine also inhibits the formation of $–NH_2^+$ groups, thereby increasing negative charge density.

- Hydrolysis of C–N bonds leads to bond cleavage and increased $–COO^-$ groups, which renders the membrane surface more hydrophilic and more negatively charged.

- The water permeability declines when the membrane surface is more hydrophobic due to domination of chlorine incorporation, and increases when the membrane surface is more hydrophilic due to domination of OH^- incorporation.

- Both chlorination and hydrolysis enhance the negative surface charge, which enhances rejection of charged solutes (e.g., NaCl, As(V) anion) due to increased charge repulsion. However, hydrolysis simultaneously causes PA bond cleavage. When the bond cleavage dominates the increase in negative surface charge (at high pH and high chlorine concentration), the rejection will be adversely affected.

- Rejection of neutral solutes (e.g., PEGs and boric acid) does not benefit from charge repulsion and therefore is significantly diminished by hydrolysis, which creates a more open PA structure.

7.2 Recommendations for future work

In order to gain further understanding of the effects of chlorine exposure on membranes, the following research is suggested:

1. Determining the optimum conditions for post-treating membrane with chlorine. This thesis has shown the potential to obtain membranes with better flux and rejection of both charged and uncharged solutes by chlorine treatment. However, the exposure conditions still need to be further optimized.

2. Investigating the changes in surface roughness due to chlorine exposure for a more accurate determination of membrane hydrophilicity. In contact angle measurement, the ridge-and-valley structure of the membranes may cause air to be trapped in the troughs as the droplet is deposited on the surface and reduce the hydrophilicity. Therefore, the changes in surface wettability measured by the contact angle method may not be solely attributed to the changes in membrane chemical groups but also to the topography alteration. The Cassie–Baxter model may be employed to obtain a more accurate evaluation of the membrane wettability.

3. Further studies of the effects of chlorine exposure on the rejection of compounds with special and complex characteristics such as polar compounds, surfactants, pharmaceutically active compounds and endocrine disruptors. These classes of chemicals are of environmental and health concern. Their retention by chlorinated membranes is of great interest in desalination and wastewater reclamation and their rejection mechanisms are still poorly understood.

4. Appraisal of the effects of other chlorine-based agents such as chlorine dioxide (ClO_2) and chloramines on membrane performance. They are suggested to be less harsh on PA membranes and could be used as alternative membrane cleaning agents.

5. Assessing the role of chloride and bromine anion in chlorination. Chloride anion can favor the formation of molecular chlorine (Cl_2), bromine (Br_2) and mixed ClBr which have stronger reactivity than HOCl and may directly attack the aromatic ring and cause further changes on the membrane physiochemical properties and performance. The presence of bromide was reported to cause more severe membrane degradation. However, the role of bromide in hydrolysis has not been investigated yet.

Appendix A.

A-1. Polyethylene glycol (PEG) concentrations by gel permeation chromatography (GPC)

Typical GPC chromatograms for three PEGs having concentrations of 2.5 g/L are combined in Figure A-1. The retention times for PEG 600, 400 and 200 Da are 8.5, 8.7 and 9.3 min, respectively.

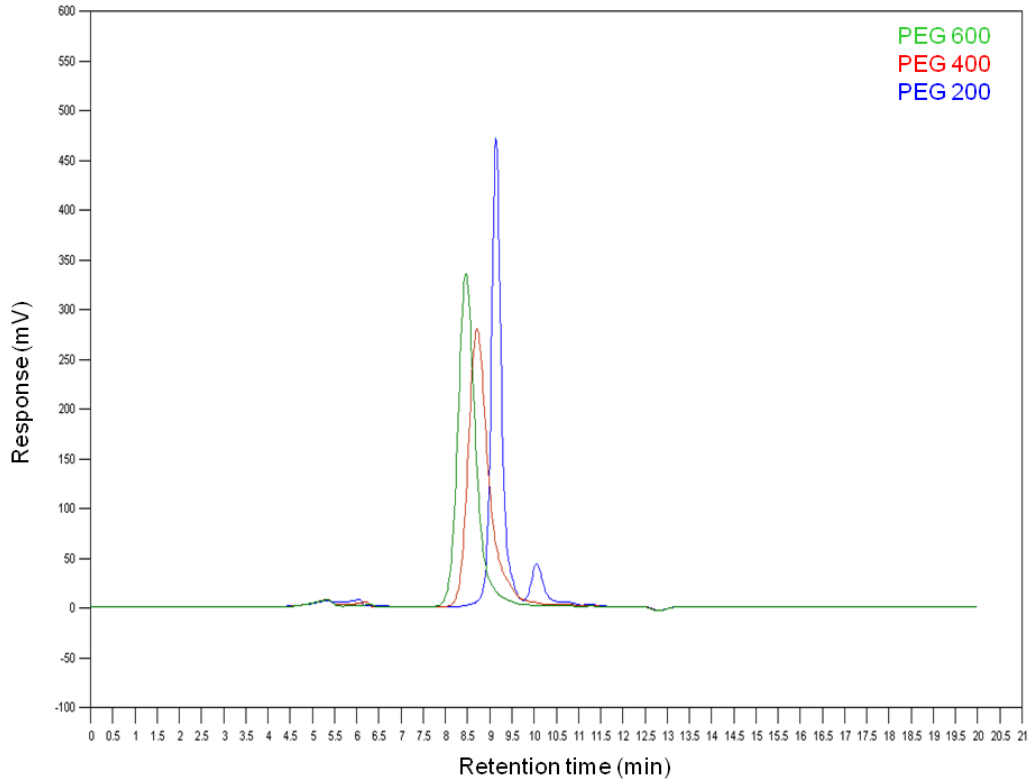

Figure A-1. Chromatograms for PEG 600, 400 and 200 (from left to right). Concentration: 2.5 g/L.

A seven-point calibration covering a 0.1 – 7.5 g/L range was run at the beginning of each batch. The PEG concentration was calibrated with the peak height (mV). The coefficient of determination (R^2) was greater than 0.99 for all runs (Figure A-2).

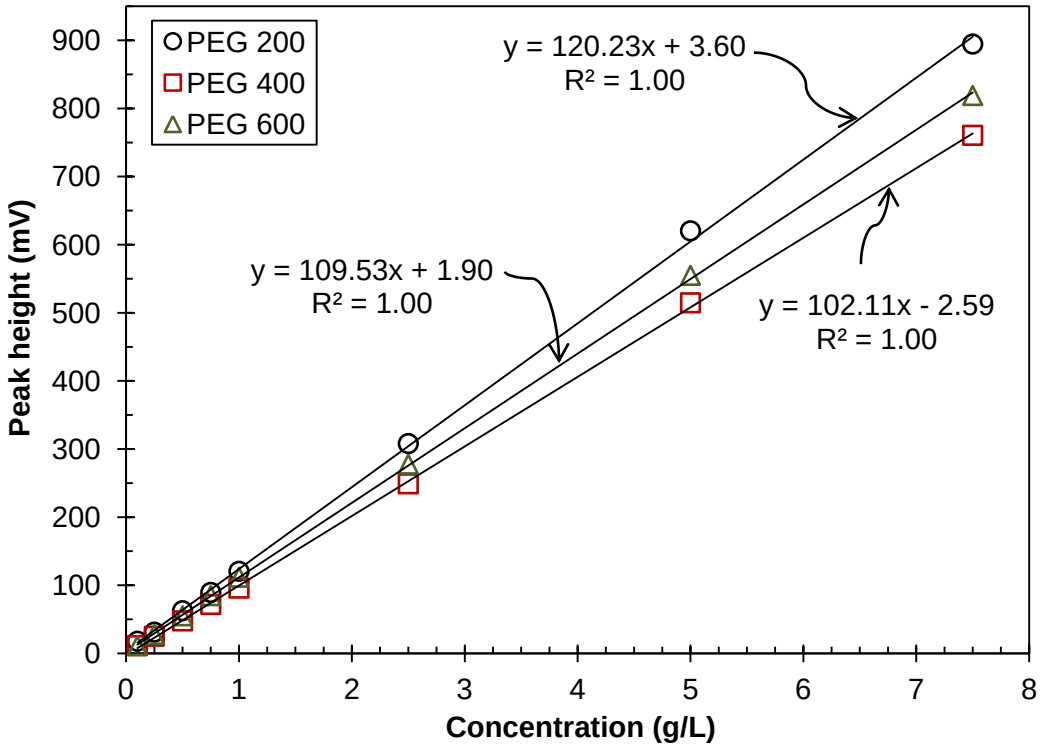

Figure A-2. Calibration for PEG 200, 400 and 600 Da.

Appendix B. Supplemental Data for Chapter 4

B-1. Elemental compositions of virgin and chlorinated membranes by XPS

The elemental compositions of virgin and chlorinated membranes obtained from XPS survey scans are tabulated in Table B-1. In addition, the O/C and O/N ratios were calculated. Errors reported for the atomic concentration are measurement ranges from 2 to 5 measurements.

Table B-1. Elemental compositions of virgin and chlorinated membranes.

Mem-brane	[HOCl] (ppm)	Soaking time (h)	Atomic Concentration %					Atomic ratios	
			O 1s	C 1s	N 1s	Cl 2p	S 2p	**O÷C**	**O÷N**
NF90	virgin		12.0 ± 0.9	77.6 ± 0.1	10.4 ± 0.9	-	-	0.15 ± 0.01	1.15 ± 0.02
	1000	1	12.6 ± 1.2	69.6 ± 2.3	9.4 ± 0.6	8.4 ± 0.7	-	0.18 ± 0.02	1.34 ± 0.02
	1000	24	14.0 ± 1.3	65.8 ± 0.9	10.3 ± 0.6	9.9 ± 0.9	-	0.21 ± 0.02	1.36 ± 0.02
	2000	24	14.1 ± 1.1	66.0 ± 0.5	9.8 ± 0.5	10.1 ± 1.1	-	0.21 ± 0.02	1.44 ± 0.02
XLE	virgin		12.2 ± 0.8	77.0 ± 0.2	10.8 ± 0.9	-	-	0.16 ± 0.01	1.13 ± 0.02
	1000	1	12.1	68.7	11.2	8.0	-	0.18	1.08
	2000	24	13.9	65.1	9.0	11.9	-	0.21	1.54
BW30	virgin		25.9 ± 3.4	72.3 ± 0.6	2.7 ± 3.4	-	-	0.36 ± 0.05	9.72 ± 0.46
	1000	1	28.7 ± 2.0	68.3 ± 2.9	1.4 ± 0.3	1.6 ± 0.5	-	0.42 ± 0.03	20.89 ± 0.11
	1000	24	20.4 ± 0.1	63.3 ± 0.0	6.5 ± 0.2	9.8 ± 0.1	-	0.32 ± 0.00	3.15 ± 0.01
	2000	24	19.4 ± 1.4	61.3 ± 0.9	5.6 ± 0.7	12.8 ± 0.2	-	0.32 ± 0.02	3.47 ± 0.05
SW30HR	virgin		27.9	71.5	0.6	-	-	0.39	46.47
	1000	1	24.8	71.5	2.3	1.4	-	0.35	10.74
NF270	virgin		14.2 ± 0.9	74.4 ± 1.6	11.4 ± 0.7	-	-	0.19 ± 0.01	1.24 ± 0.02
	1000	1	17.0 ± 3.1	70.4 ± 3.5	11.6 ± 0.4	0.6 ± 0.1	0.4 ± 0.1	0.24 ± 0.05	1.47 ± 0.05
	1000	24	17.7 ± 0.5	68.1 ± 0.1	11.8 ± 0.3	2.1 ± 0.3	0.3 ± 0.0	0.26 ± 0.01	1.51 ± 0.01
	2000	24	19.5 ± 1.5	66.0 ± 0.8	11.5 ± 0.5	2.7 ± 0.2	0.4 ± 0.0	0.29 ± 0.02	1.69 ± 0.03
HL	virgin		13.0	74.4	12.6	-	-	0.18	1.03
	1000	1	12.1	75.9	11.7	0.4	-	0.16	1.04

B-2. Surface oxygen content for chlorinated BW30 membrane

The oxygen content of BW30 decreased at higher chlorine percentages, which is consistent with the assumption that the oxygen-rich PVA coating layer was detached from the PA layer under severe chlorination conditions.

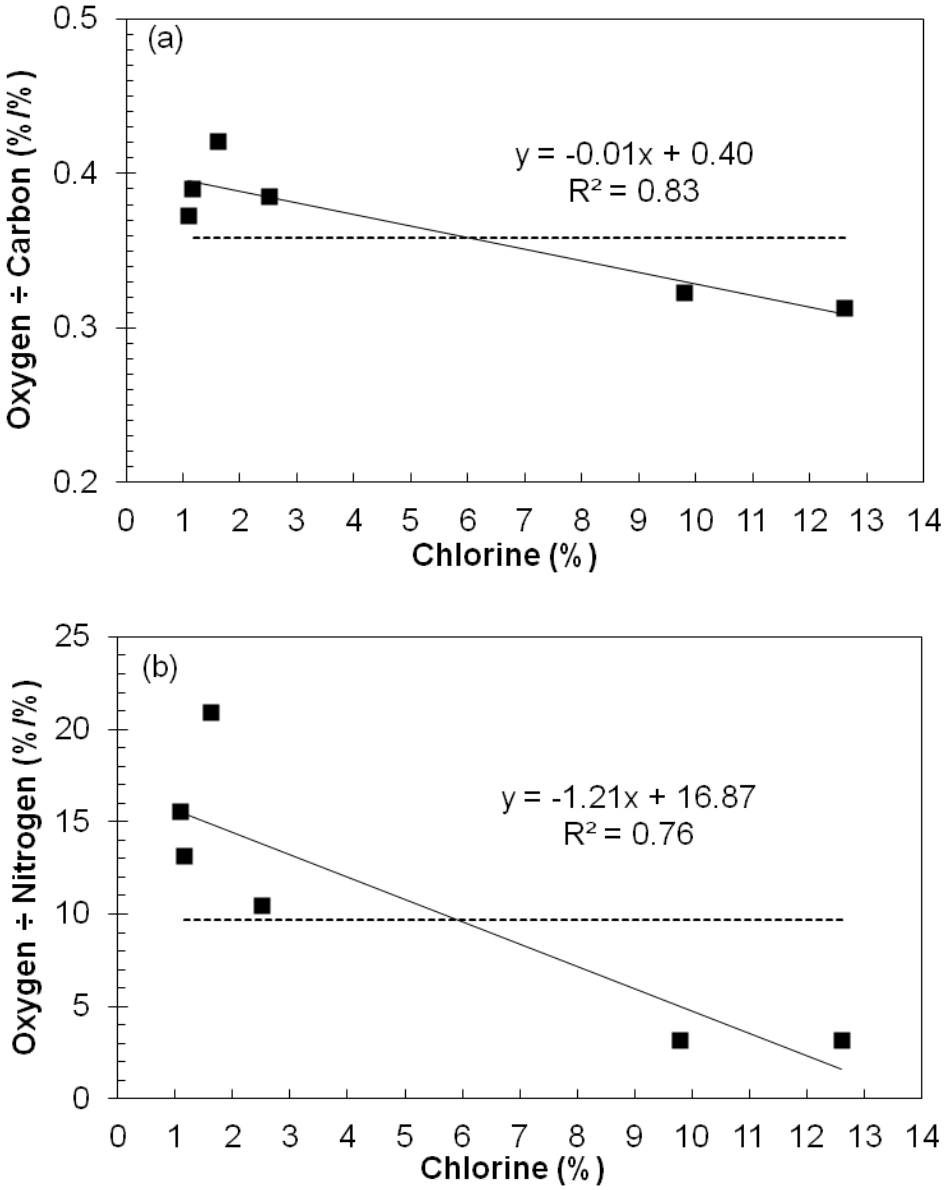

Figure B-1. Ratio of (a) oxygen to carbon and (b) oxygen to nitrogen as a function of the atomic percent of bound chlorine for BW30 at different chlorination conditions: pH 5; 2000 ppm × 24 h, 1000 ppm × 24 h, 1000 ppm × 1 h, 100 ppm × 24 h, 100 ppm × 10 h and 10 ppm × 100 h. The dotted lines represent the (a) O/C and (b) O/N ratio for virgin membranes.

B-3. High resolution XPS spectra for virgin and chlorinated BW30 and NF270 membranes

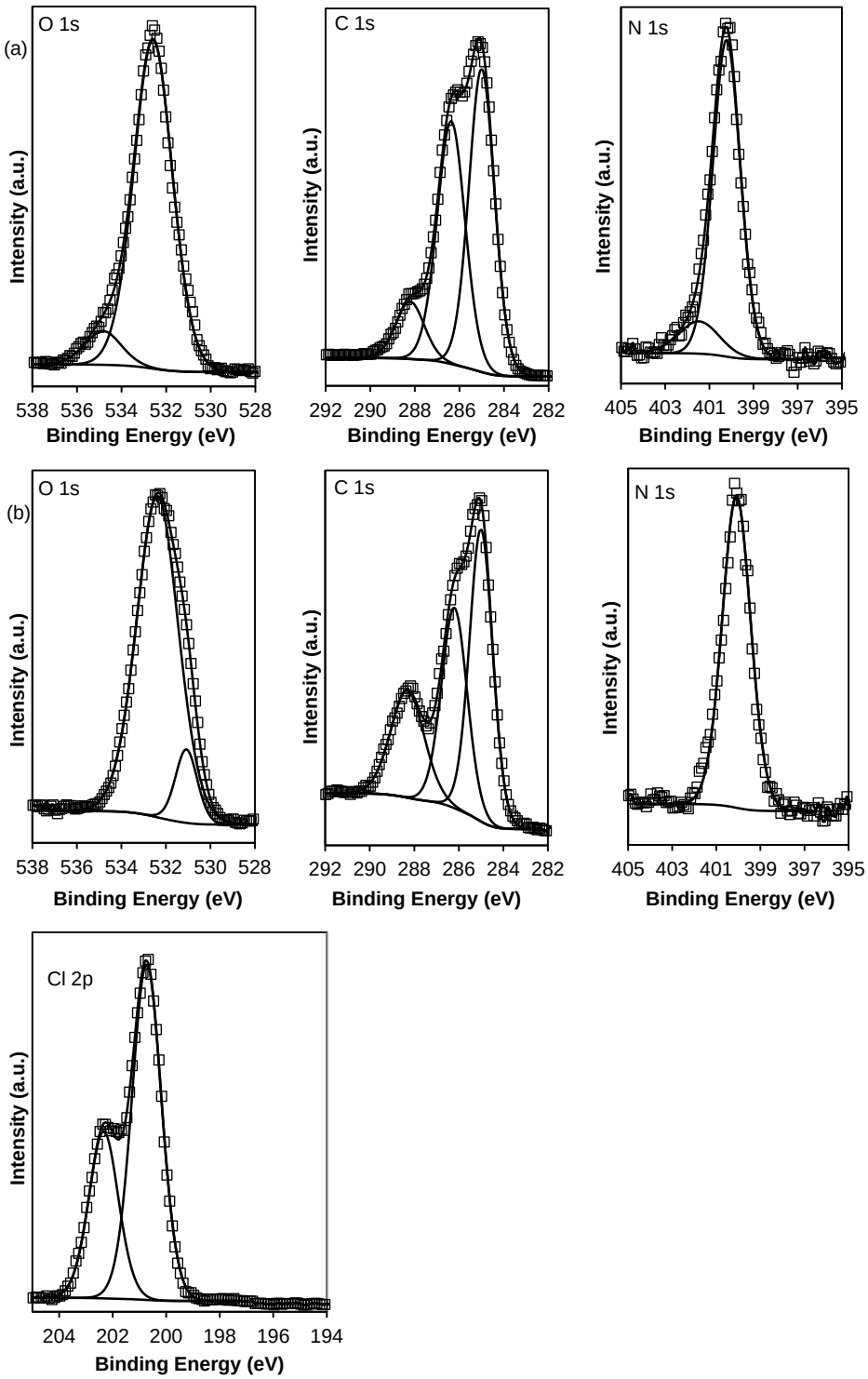

Figure B-2. High resolution XPS spectra of (a) O 1s, C 1s, N 1s for virgin and (b) O 1s, C 1s, N 1s, Cl 2p for chlorinated BW30 (2000 ppm × 24 h, pH 5).

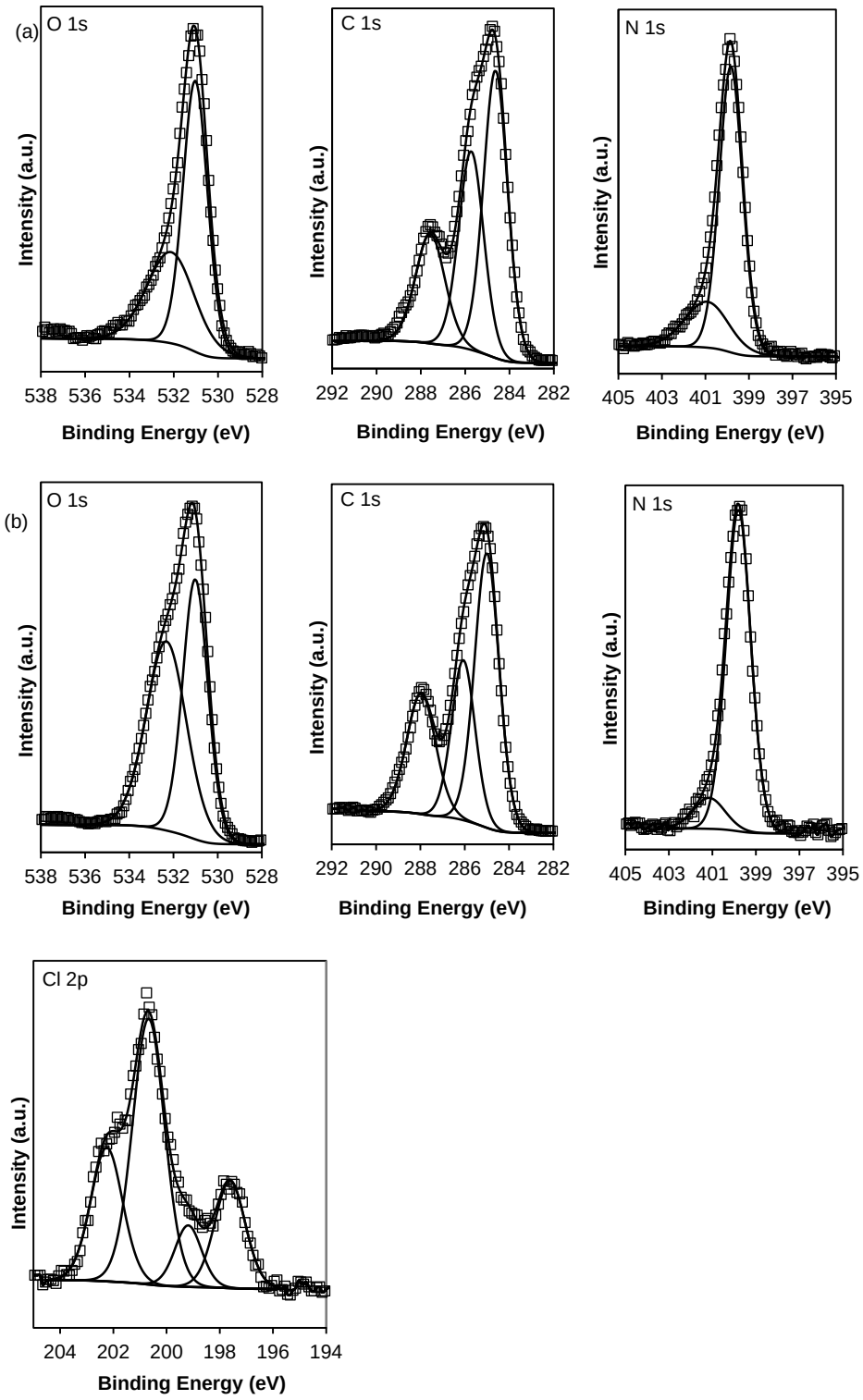

Figure B-3. High resolution XPS spectra of (a) O 1s, C 1s, N 1s for virgin and (b) O 1s, C 1s, N 1s, Cl 2p for chlorinated NF270 (2000 ppm × 24 h, pH 5).

B-4. ATR-FTIR spectra at wave number 2700 – 3800 cm^{-1}

FTIR spectra from 2700 to 3800 cm^{-1} for the three membranes are provided in Figure B-4 below. For the NF90 and BW30 FA membranes, the magnitude of the broad peaks centered ~ 3300 cm^{-1}, which are assigned to N–H and/or O–H stretching (Tang et al., 2009a), were reduced as chlorination conditions became more severe. On the other hand, for the NF270 PIP membrane, only a slight reduction in the C–H stretching peak at 2970 cm^{-1} was observed (Tang et al., 2009a).

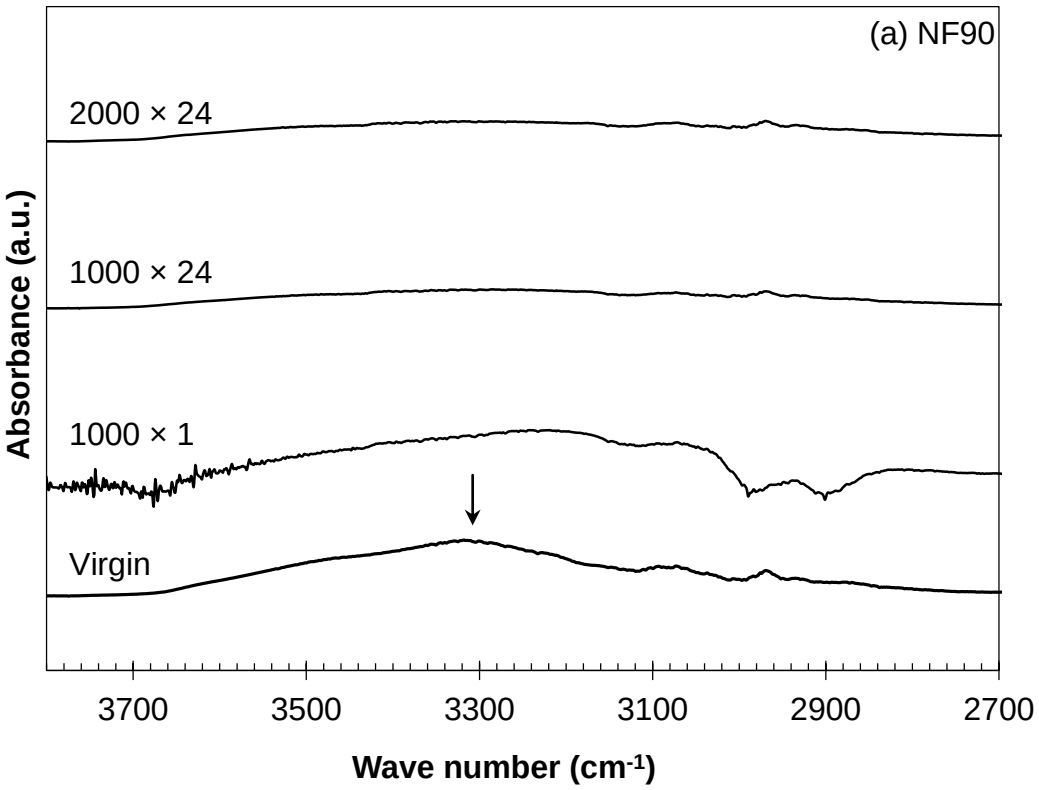

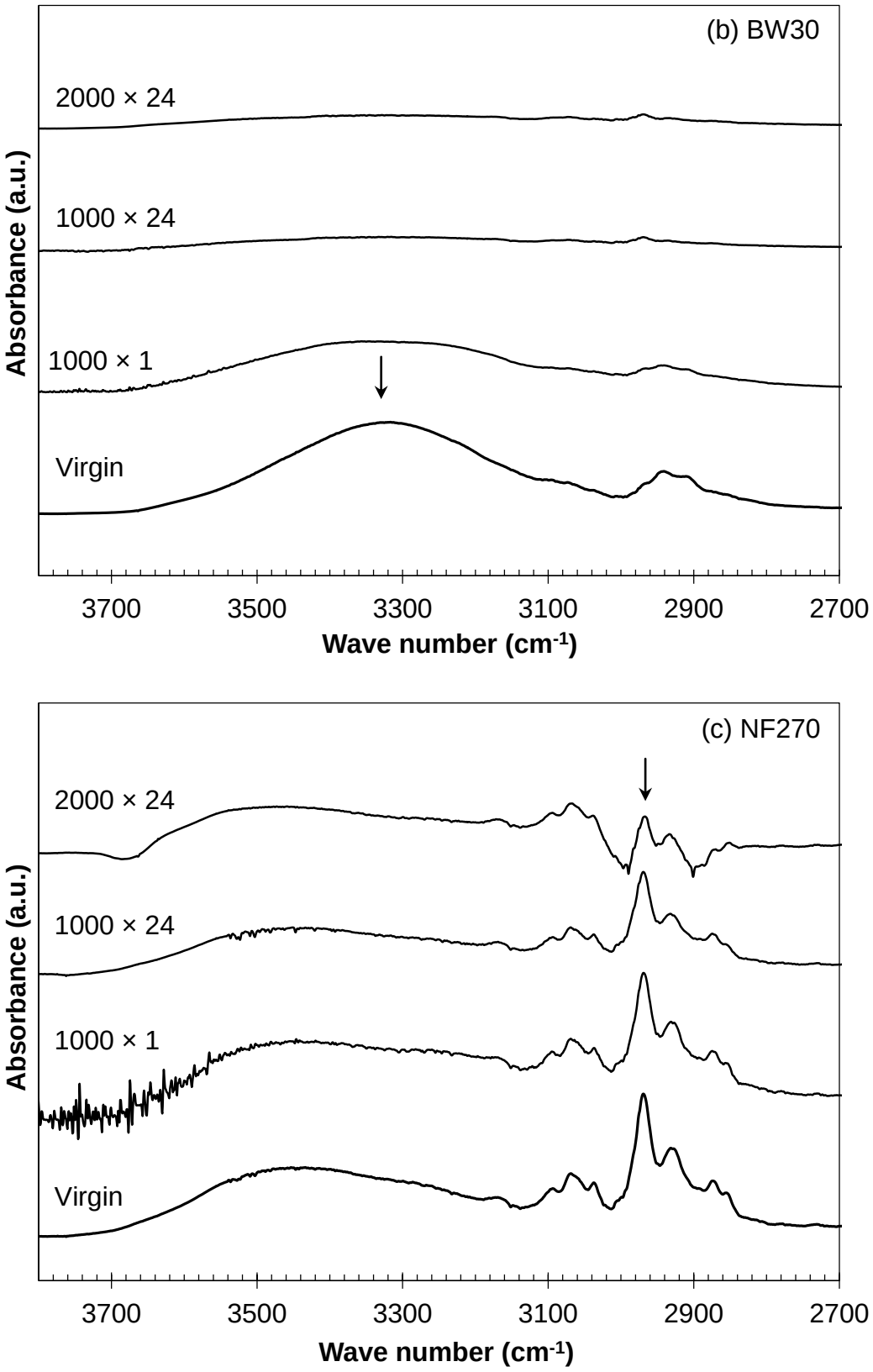

Figure B-4. ATR-FTIR spectra for (a) NF90, (b) BW30 and (c) NF270: virgin and chlorinated at pH 5; 2000 ppm × 24 h, 1000 ppm × 24 h and 1000 ppm × 1 h.

B-5. Surface charge of virgin and chlorinated BW30 and replicates for virgin membranes

The surface charge of virgin and chlorinated BW30 is presented in Figure B-5. A consistent surface charge for more severe chlorination conditions could not be obtained, probably due to the detachment of the PVA coating.

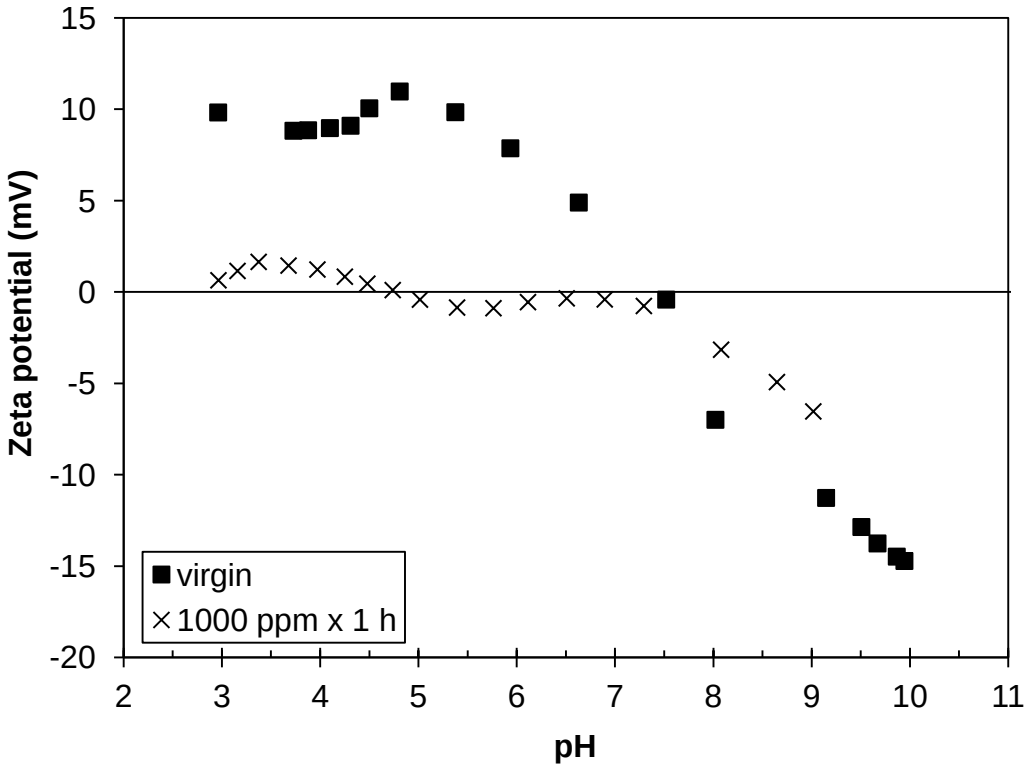

Figure B-5. Zeta potential for virgin and chlorinated BW30 as a function of pH. Background electrolyte was 10 mM NaCl.

A representative zeta potential replicate for virgin coupons is shown as below.

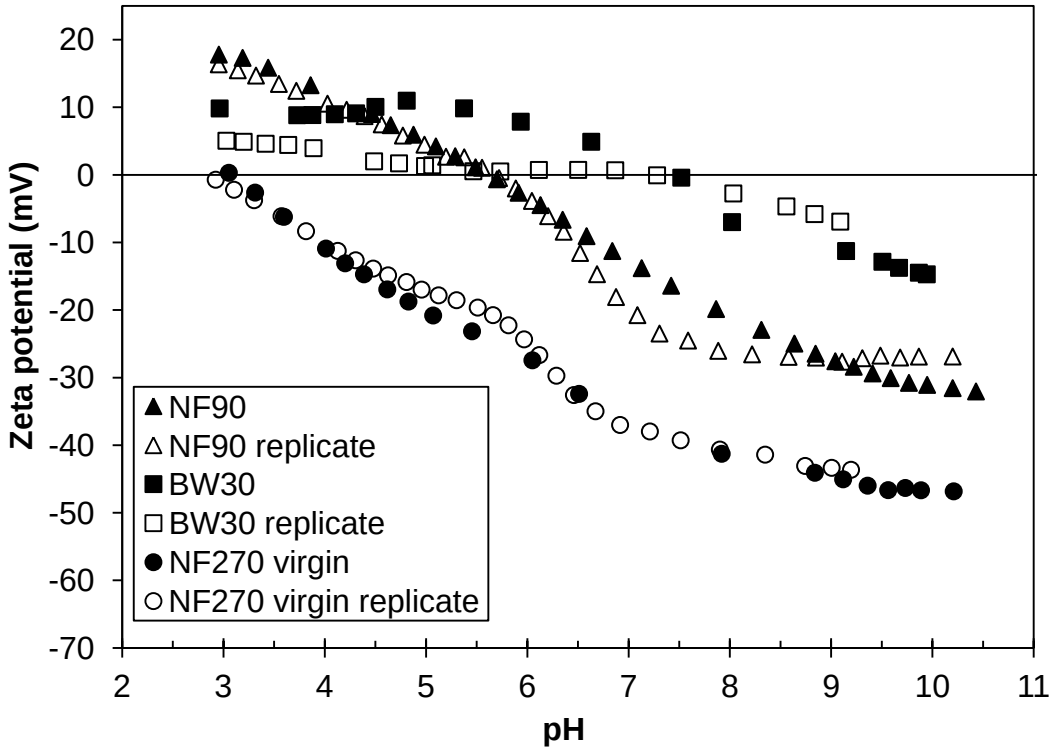

Figure B-6. Zeta potential of two different virgin coupons for NF90, BW30 and NF270.

B-6. Hydrophilicity of virgin and chlorinated membranes

The contact angles of virgin and chlorinated membranes are tabulated in Table B-2 below. The error bars indicate the standard deviations for 40 measurements (2 independent membrane coupons and 20 different locations for each sample).

Table B-2. Contact angles (^{o}) for virgin and chlorinated membranes.

Membrane treatment		Contact angle (^{o})					
[HOCl] (ppm)	Soaking time (h)	NF90	XLE	BW30	SW30HR	NF270	HL
Virgin		66.3 ± 1.1	66.2 ± 2.0	57.1 ± 3.9	61.9 ± 4.4	32.6 ± 1.5	40.5 ± 3.7
1000	1	69.8 ± 2.4	73.5 ± 1.9	53.3 ± 4.0	56.9 ± 3.4	30.6 ± 2.2	31.6 ± 5.5
1000	24	68.3 ± 1.9	-	52.2 ± 2.6	-	43.3 ± 2.3	-
2000	24	74.2 ± 1.6	79.3 ± 2.8	63 ± 5.1	-	47.5 ± 1.9	-

Appendix C. Supplemental Data for Chapter 5

C-1. Cross-linking degree - O÷N ratios of virgin and chlorinated membranes

According to Tang et al. (2007) and Coronell et al. (2008), the O/N ratio indicates the degree of cross-linking of the PA layer. When all the O and N form amide groups and the PA layer is fully cross-linked, the O/N ratio is 1.0. Meanwhile, a 2:1 ratio indicates a fully linear PA layer (Tang et al., 2007). It is observed from Table C-1 that the O/N ratios of uncoated PA membranes (NF90 and NF270) became higher, indicating that the membranes were less cross-linked as the chlorine concentration increased. The reduced degree of cross-linking may be attributed to induced membrane hydrolysis due to chlorine attack on the amide nitrogen. In case of BW30, due to the oxygen-rich surface PVA coating, the O/N ratios are not in the range of 1 to 2 (Tang et al., 2007). The reduced O/N ratios at high chlorine concentrations (1000 and 2000 ppm) can be attributed to the partial detachment of the coating (Do et al., 2012a).

Table C-1. O÷N ratios of virgin and chlorinated membranes.

Chlorine concentration (ppm)	O÷N		
	NF90	BW30	NF270
virgin	*1.15 ± 0.09*	*9.72 ± 8.88*	*1.24 ± 0.08*
10	1.04	4.89	1.34
100	1.19	10.48	1.28
1000	1.36 ± 0.10	3.15 ± 0.08	1.51 ± 0.04
2000	1.44 ± 0.09	3.18 ± 0.31	1.69 ± 0.10

C-2. PEG rejection of virgin and chlorinated BW30 and NF270 membranes

The rejection of virgin and chlorinated BW30 and NF270 membranes was plotted against the molecular weights of the PEGs in Figure C-1. Due to the tightness of the RO membrane, the MWCO of BW30 could not be determined. However, there was a slight but consistent decrease in PEG rejection of severely chlorinated BW30 at 1000 and 2000 ppm. These data support the argument in Appendix C-1 that the coating did not completely protect the underlying PA layer from chlorine attack.

The MWCO of the virgin NF270 in Figure C-1b is interpolated to be ~ 300 Da, which is consistent with the value (340 Da) reported by López-Muñoz et al. (2009). Similar to NF90 performance discussed in Section 5.3.2.2, the PEG rejection of mildly chlorinated NF270 (at 10 and 100 ppm) benefited from a tightening effect and slightly increased. The severely chlorinated NF270 (2000 ppm) had a lower PEG rejection than the virgin, which indicates that its PA structure was more open and agrees with the less cross-linking data in Table C-1.

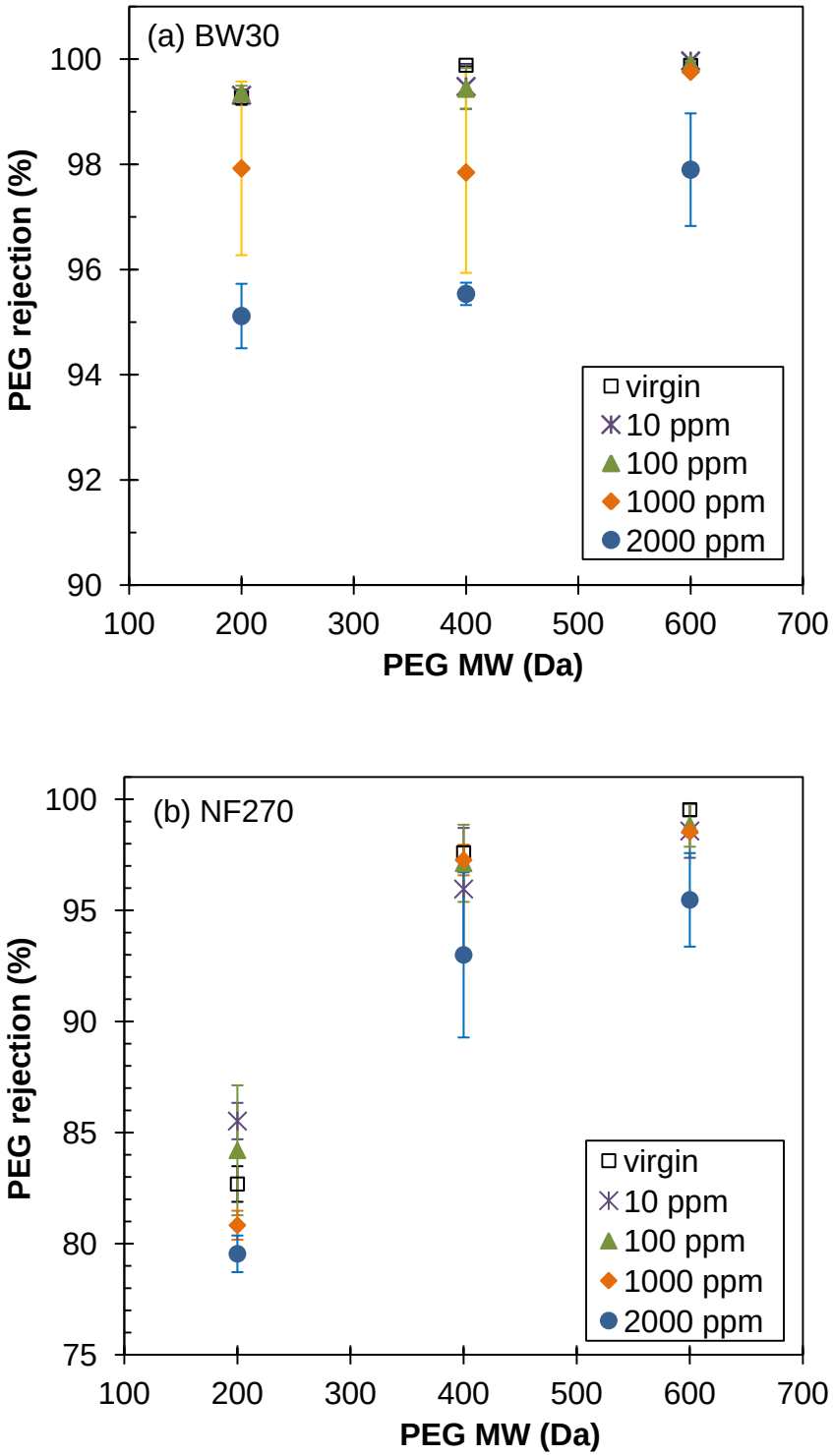

Figure C-1. PEG rejection of virgin and chlorinated (a) BW30 and (b) NF270. Membranes were exposed to 10, 100, 1000 and 2000 ppm of chlorine for 24 h at pH 5. Error bars represent the range of replicate measurements.

Appendix D. Supplemental Data for Chapter 6

D-1. Concentration of chloride ion in chlorine treatment solution

The presence of chloride anion in the chlorine soaking solution was investigated for chlorine concentration of 100 ppm Cl, pH 5. The active elemental chlorine ($[Cl_2]$ + [HOCl] + $[OCl^-]$) was determined from iodometric titration with sodium thiosulfate (Eaton et al., 1995) and reported as ppm of equivalent Cl. Then, the total elemental chlorine and chloride anion was determined by ion chromatography. The concentration of chloride anion, which was introduced by addition of HCl for pH control, was ~ 37.7% of the active elemental chlorine.

D-2. O/N ratios of chlorinated NF90 membranes as a function of [HOCl] • $[OH^-]$ and $[OCl^-]$

The O/N ratios indicating the degree of cross-linking of chlorinated membranes are plotted against the [HOCl] • $[OH^-]$ product in Figure D-1a. The O/N ratios seem to correlate with [HOCl] • $[OH^-]$ better than only [HOCl] as shown in Figure 6-3b, which demonstrates the influence of both HOCl and pH in the chlorination promoted hydrolysis process.

Since $K_a = \dfrac{[H^+] \times [OCl^-]}{[HOCl]}$, the O/N ratios can be equivalently correlated to the $[OCl^-]$ as shown in Figure D-1b, using the below equation:

$$[HOCl] \bullet [OH^-] = K_w / K_a \times [OCl^-]$$

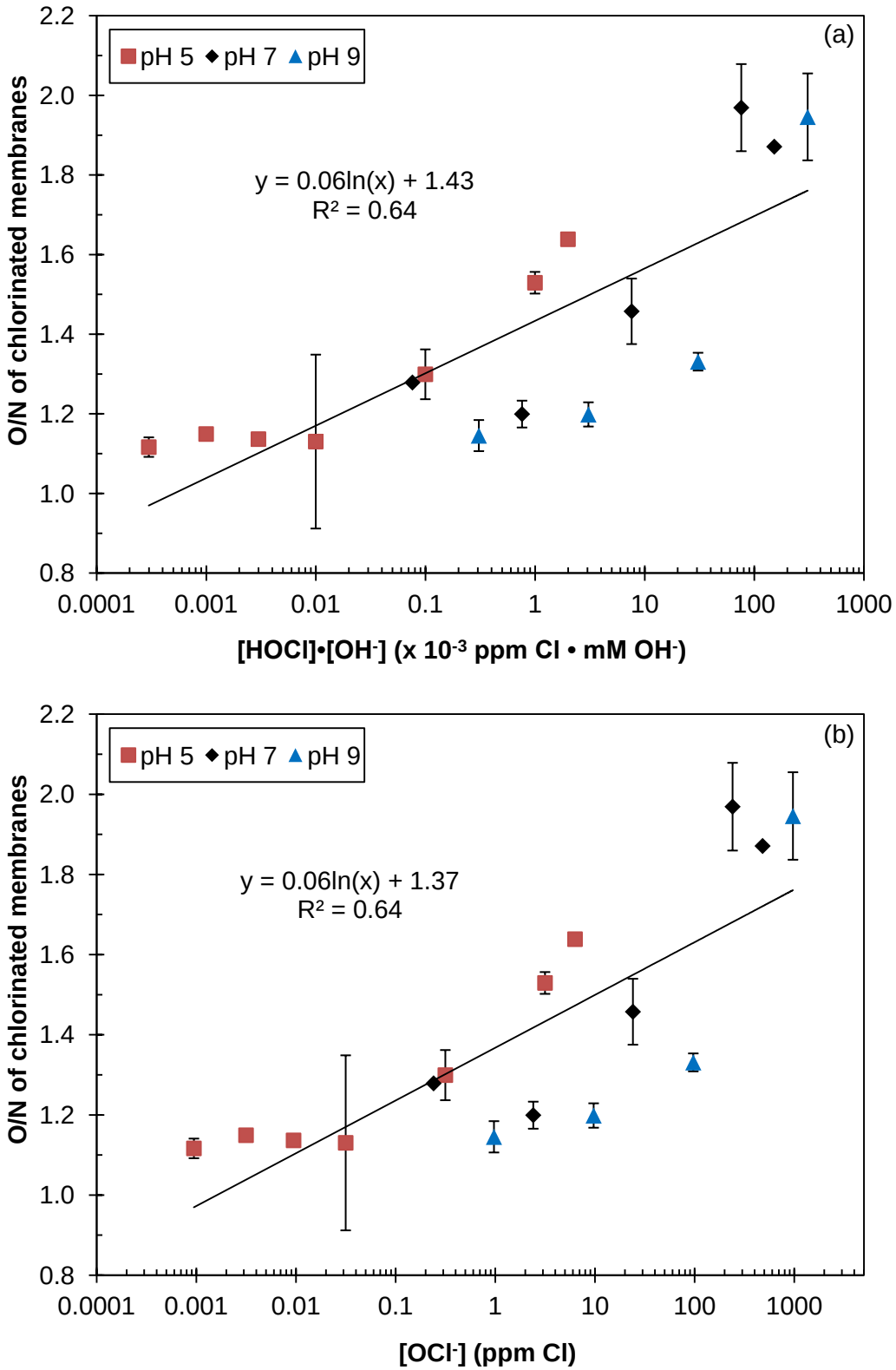

Figure D-1. O/N ratios of NF90 membranes chlorinated for 100 h at different total chlorine concentrations and pH as a function of: (a) [HOCl] • [OH^-] and (b) [OCl^-].

D-3. Zeta potential of virgin and chlorinated NF90 membranes

Figure D-2 presents the surface charge of the virgin and chlorinated membranes (1000 ppm, 100 h, pH 5 and 9) measured with 10 mM NaCl as the electrolyte at pH from 3 to 9. According to our previous studies, the uncertainty in zeta potential measurements is ~ ± 5 mV (Tang et al., 2006; Do et al., 2012a). At pH < 5.5, the positive charge of the virgin membrane is attributed to the formation of $–NH_2^+$ groups (Childress and Elimelech, 1996) and the negative charge of chlorinated membranes is due to amide hydrogen displacement by chlorine (Do et al., 2012a). The enhanced negative charge of chlorinated membranes at high pH can be explained by the increased surface density of the $–COO^-$ groups, consistent with the chlorination promoted hydrolysis mechanism (Do et al., 2012a).

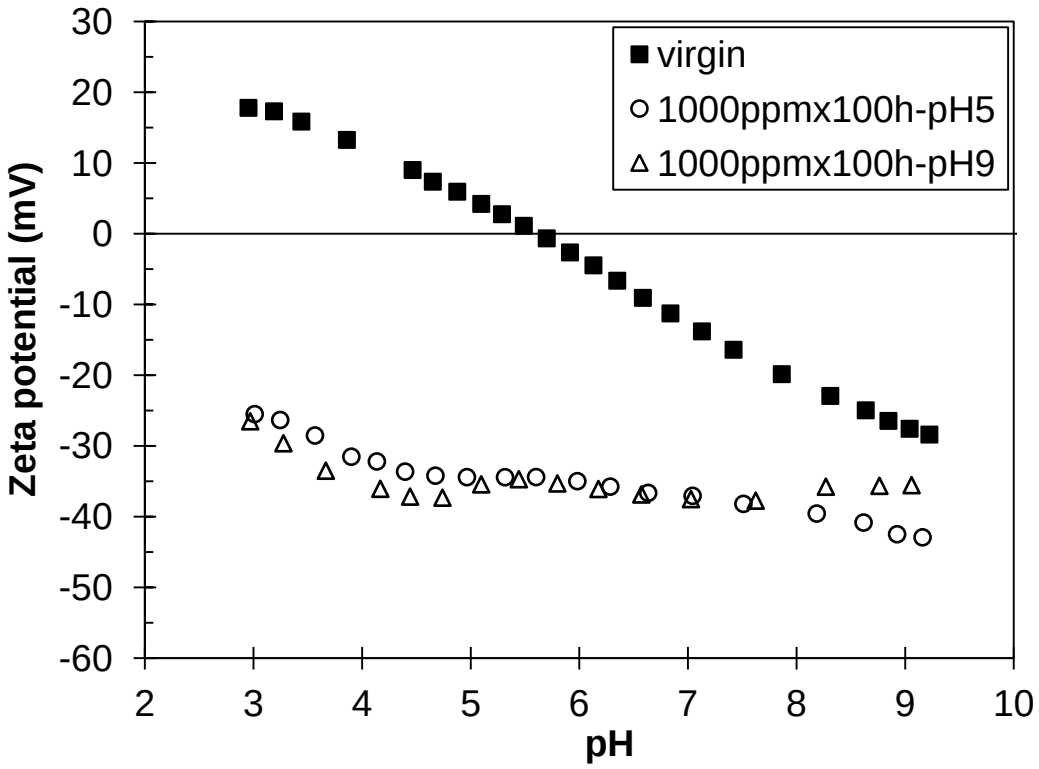

Figure D-2. Zeta potential of the virgin and chlorinated NF90 membranes.

D-4. Permeability of sodium chloride

The salt permeability coefficient, B (m/s), which is an intrinsic property of the rejection layer was determined from the water flux (J_w) and rejection (R) from the following equation (Mulder, 1996):

$$B = J_w \times (\frac{1}{R} - 1)$$

The trends of salt permeability coefficients in Figure D-3 agree well with those of the apparent salt rejection.

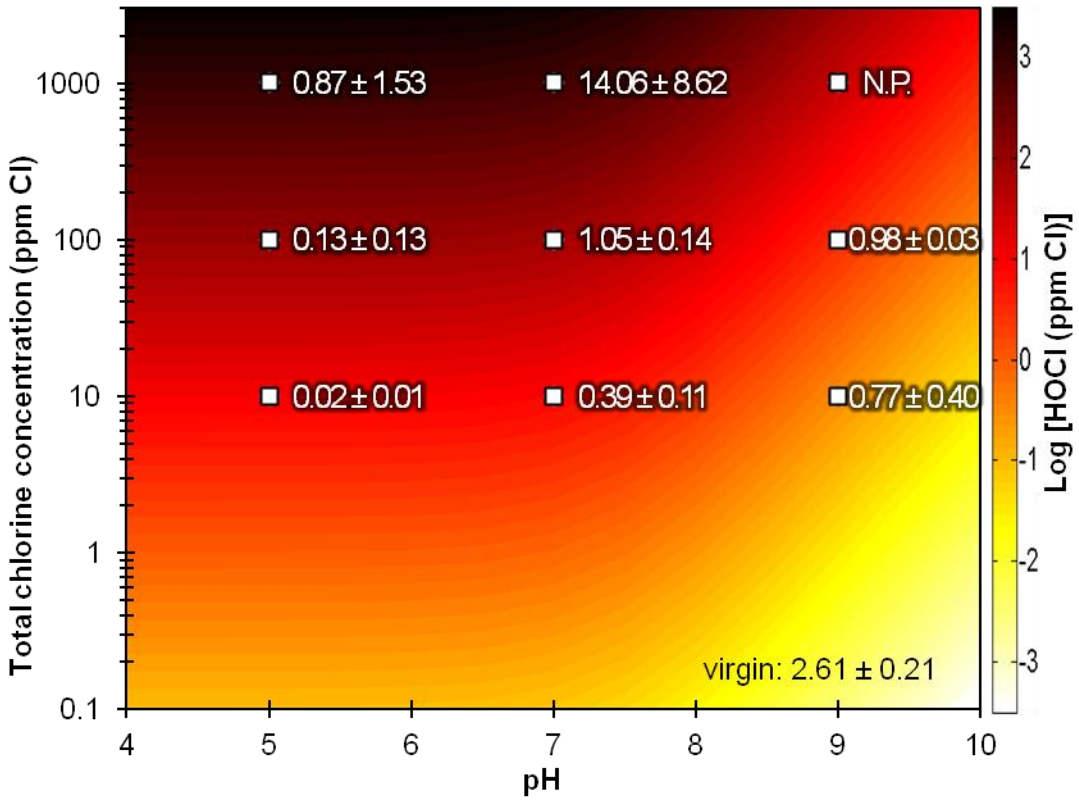

Figure D-3. Salt permeability coefficient, B × 10^{-6} (m/s) of the NF90 membranes: virgin and chlorinated for 100 h at different total chlorine concentrations and pH. Background color contours represent iso-concentration lines of HOCl. N.P.: membrane failed to perform.

D-5. Correlation between trace inorganic contaminants and NaCl rejection

In Figure D-4a, the rejection of arsenic (V) anion highly correlates with that of NaCl, showing that the effects of chlorine exposure on the rejection of charged solutes are similar. However, the boric acid rejection does not correlate well with the NaCl rejection in Figure D-4b because boric acid was neutral at the filtration conditions and did not benefit from the enhanced charge repulsion.

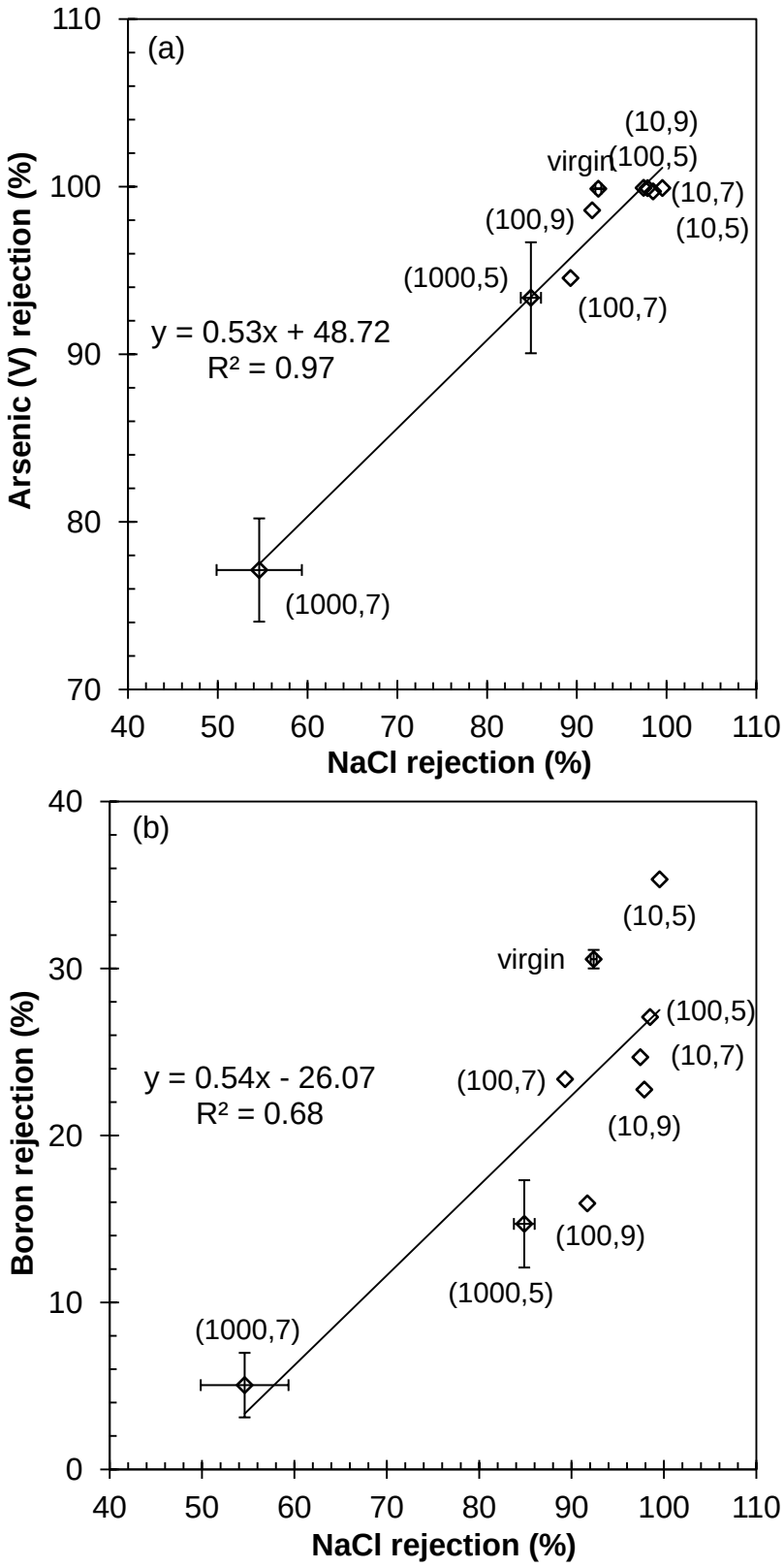

Figure D-4. Correlation between (a) As(V) rejection and (b) boric acid rejection and NaCl rejection of virgin and chlorinated NF90 membranes. The data in the brackets denote: (chlorine concentration, treatment pH).

References

Antony, A., Fudianto, R., Cox, S. and Leslie, G. (2010) Assessing the oxidative degradation of polyamide reverse osmosis membrane-Accelerated ageing with hypochlorite exposure. Journal of Membrane Science 347(1-2), 159-164.

Antony, A., Low, J.H., Gray, S., Childress, A.E., Le-Clech, P. and Leslie, G. (2011) Scale formation and control in high pressure membrane water treatment systems: A review. Journal of Membrane Science 383(1-2), 1-16.

Ariza, M.J., Cañas, A. and Benavente, J. (2000a) Electrical and surface chemical characterizations of the active layer of composite polyamide/polysulphone nanofiltration commercial membranes. Surface and Interface Analysis 30(1), 425-429.

Ariza, M.J., Rodríguez-Castellón, E., Rico, R., Benavente, J., Muñoz, M. and Oleinikova, M. (2000b) Surface characterization of di-(2-ethylhexyl)dithiophosphoric acid-activated composite membranes by x-ray photoelectron spectroscopy. Surface and Interface Analysis 30(1), 430-433.

Avlonitis, S., Hanbury, W. and Hodgkiess, T. (1992) Chlorine degradation of aromatic polyamides. Desalination 85, 321-334.

Barassi, G. and Borrmann, T. (2012) N-chlorination and Orton Rearrangement of Aromatic Polyamides, Revisited. Journal Membrane Science & Technology 2(2), 115.

Bartels, C.R. and Wilf, M. (2005) Design considerations for wastewater treatment by reverse osmosis. Water Science & Technology 51(6-7), 473-482.

Beamson, G. and Briggs, D. (1992) High Resolution XPS of Organic Polymers: the Scienta ESCA 300 database, Wiley New York.

Bellona, C. and Drewes, J.E. (2005) The role of membrane surface charge and solute physico-chemical properties in the rejection of organic acids by NF membranes. Journal of Membrane Science 249, 227.

Bellona, C., Drewes, J.E., Xu, P. and Amy, G. (2004) Factors affecting the rejection of organic solutes during NF/RO treatment - a literature review. Water Research 38, 2795–2809.

Benjamin, M.M. (2002) Water chemistry, 1st ed, McGraw-Hill, Boston.

Bieron, J.F. and Dinan, F.J. (1970) Rearrangement and elimination of the amido group. The Chemistry of Amides. Zabicky, J. (ed), Wiley Interscience, New York, 263-266.

Boussu, K., Baerdemaeker, J.D., Dauwe, C., Weber, M., Lynn, K.G., Depla, D., Aldea, S., Vankelecom, I.F.J., Vandecasteele, C. and Van der Bruggen, B. (2007) Physico-chemical characterization of nanofiltration membranes. ChemPhysChem 8(3), 370-379.

Bowen, W.R. and Doneva, T.A. (2000) Atomic force microscopy studies of nanofiltration membranes: surface morphology, pore size distribution and adhesion. Desalination 129(2), 163-172.

Braghetta, A., DiGiano, F.A. and Ball, W.P. (1997) Nanofiltration of Natural Organic Matter: pH and Ionic Strength Effects. Journal of Environmental Engineering 123(7), 628-641.

Briggs, D. (1998) Surface analysis of polymers by XPS and static SIMS, Cambridge University Press, Cambridge.

Buch, P.R., Jagan Mohan, D. and Reddy, A.V.R. (2008) Preparation, characterization and chlorine stability of aromatic-cycloaliphatic polyamide thin film composite membranes. Journal of Membrane Science 309(1-2), 36-44.

Cadotte, J.E. (1981) Interfacially synthesized reverse osmosis membrane, US Patent 4,277,344.

Cadotte, J.E. (1985) Evolution of composite reverse osmosis membranes. Materials science of synthetic membranes. Lloyd, D.R. (ed), American Chemical Society, Washington, D.C., 273-294.

Cadotte, J.E. and Petersen, R.J. (1980) A new thin-film composite seawater reverse osmosis membrane. Desalination 32, 25-31.

Challis, B.G. and Challis, J.A. (1970) Reactions of the carboxamide group. The Chemistry of Amides. Zabicky, J. (ed), Wiley Interscience, New York, 731-857.

Childress, A.E. and Elimelech, M. (1996) Effect of solution chemistry on the surface charge of polymeric reverse osmosis and nanofiltration membranes. Journal of Membrane Science 119(2), 253-268.

Childress, A.E. and Elimelech, M. (2000) Relating Nanofiltration Membrane Performance to Membrane Charge (Electrokinetic) Characteristics. Environmental Science & Technology 34(17), 3710-3716.

Coronell, O., Mariñas, B.J. and Cahill, D.G. (2009) Accessibility and Ion Exchange Stoichiometry of Ionized Carboxylic Groups in the Active Layer of FT30 Reverse Osmosis Membrane. Environmental Science & Technology 43(13), 5042-5048.

Coronell, O., Mariñas, B.J., Zhang, X. and Cahill, D.G. (2008) Quantification of Functional Groups and Modeling of Their Ionization Behavior in the Active Layer

of FT30 Reverse Osmosis Membrane. Environmental Science & Technology 42(14), 5260-5266.

Cran, M.J., Bigger, S.W. and Gray, S.R. (2011) Degradation of polyamide reverse osmosis membranes in the presence of chloramine. Desalination 283, 58-63.

Do, V.T., Tang, C.Y., Reinhard, M. and Leckie, J.O. (2012a) Degradation of Polyamide Nanofiltration and Reverse Osmosis Membranes by Hypochlorite. Environmental Science & Technology 46(2), 852-859.

Do, V.T., Tang, C.Y., Reinhard, M. and Leckie, J.O. (2012b) Effects of hypochlorous acid exposure on the rejection of salt, polyethylene glycols, boron and arsenic(V) by nanofiltration and reverse osmosis membranes. Water Research 46(16), 5217-5223.

Drewes, J.E., Reinhard, M. and Fox, P. (2003) Comparing microfiltration-reverse osmosis and soil-aquifer treatment for indirect potable reuse of water. Water Research 37(15), 3612-3621.

Eaton, A.D., Clesceri, L.S. and Greenberg, A.E. (1995) Standard Methods for Examination of Water and Wastewater, APHA, AWWA and WEF, Washington DC, US.

Elimelech, M., Chen, W.H. and Waypa, J.J. (1994) Measuring the zeta (electrokinetic) potential of reverse osmosis membranes by a streaming potential analyzer. Desalination 95(3), 269-286.

Ettori, A., Gaudichet-Maurin, E., Schrotter, J.-C., Aimar, P. and Causserand, C. (2011) Permeability and chemical analysis of aromatic polyamide based membranes exposed to sodium hypochlorite. Journal of Membrane Science 375(1-2), 220-230.

Fair, G.M., Morris, J.C., Chang, S.L., Weil, I. and Burden, R.P. (1948) The behavior of chlorine as a water disinfectant. Journal American Water Works Association 40, 1051-1061.

Fairbrother, F. and Mastin, H. (1924) Studies in electro-endosmosis. I. Journal of the Chemical Society 125, 2319-2330.

Fane, A.G., Tang, C.Y. and Wang, R. (2011) Membrane Technology for Water: Microfiltration, Ultrafiltration, Nanofiltration, and Reverse Osmosis. Treatise on Water Science. Wilderer, P. (ed), Elsevier, Oxford, 4, 301-335.

FAO (2009) AQUASTAT 2009: Water and Food Security. http://www.fao.org/nr/water/aquastat/main/index.stm (accessed September 2010)

Glater, J., Hong, S.-k. and Elimelech, M. (1994) The search for a chlorine-resistant reverse osmosis membrane. Desalination 95 (3), 325-345.

Glater, J., McCutchan, J.W., McCray, S.B. and Zachariah, M., R. (1981) The effect of halogens on the performance and durability of reverse-osmosis membranes. Synthetic Membranes. Turbak, A.F. (ed), American Chemical Society, 153, 171-190.

Glater, J. and Zachariah, M.R. (1985) Mechanistic study of halogen interaction with polyamide reverse-osmosis membranes. ACS Symposium Series, 345-358.

Glater, J., Zachariah, M.R., McCray, S.B. and McCutchan, J.W. (1983) Reverse osmosis membrane sensitivity to ozone and halogen disinfectants. Desalination 48(1), 1-16.

Goosen, M., Sablani, S., Al-Hinai, H., Al-Obeidani, S., Al-Belushi, R. and Jackson, D. (2004) Fouling of reverse osmosis and ultrafiltration membranes: a critical review. Separation Science and Technology 39(10), 2261-2298.

Gray, S., Semiat, R., Duke, M., Rahardianto, A. and Cohen, Y. (2011) Seawater Use and Desalination Technology. Treatise on Water Science. Wilderer, P. (ed), Elsevier, Oxford, 4, 73-109.

Hardy, F.E. and Robson, P. (1967) The formation and hydrolysis of substituted N-chloro-N-methylbenzamides in aqueous alkali. Journal of the Chemical Society B: Physical Organic, 1151-1154.

Ingold, C. (1953) Structure and mechanism in organic chemistry, Cornell University Press.

Jensen, J.S., Lam, Y.-F. and Helz, G.R. (1999) Role of amide nitrogen in water chlorination: Proton NMR evidence. Environmental Science & Technology 33(20), 3568-3573.

Jin, X., Huang, X. and Hoek, E.M.V. (2009) Role of Specific Ion Interactions in Seawater RO Membrane Fouling by Alginic Acid. Environmental Science & Technology 43(10), 3580-3587.

Jons, S.D., Stutts, K.J., Ferritto, M.S. and Mickols, W.E. (1999) Treatment of composite polyamide membranes to improve performance, US Patent 5,876,602.

Kang, G.-D., Gao, C.-J., Chen, W.-D., Jie, X.-M., Cao, Y.-M. and Yuan, Q. (2007) Study on hypochlorite degradation of aromatic polyamide reverse osmosis membrane. Journal of Membrane Science 300(1-2), 165-171.

Kawaguchi, T. and Tamura, H. (1984a) Chlorine-resistant membrane for reverse osmosis. I. Correlation between chemical structures and chlorine resistance of polyamides. Journal of Applied Polymer Science 29(11), 3359-3367.

Kawaguchi, T. and Tamura, H. (1984b) Chlorine-resistant membrane for reverse osmosis. II. Preparation of chlorine-resistant polyamide composite membranes. Journal of Applied Polymer Science 29(11), 3369-3379.

Kimura, K., Amy, G., Drewes, J. and Watanabe, Y. (2003a) Adsorption of hydrophobic compounds onto NF/RO membranes-an artifact leading to overestimation of rejection. Journal of Membrane Science 221, 89-101.

Kimura, K., Amy, G., Drewes, J.E., Heberer, T., Kim, T.U. and Watanabe, Y. (2003b) Rejection of organic micropollutants (disinfection by-products, endocrine disrupting compounds, and pharmaceutically active compounds) by NF/RO membranes. Journal of Membrane Science 227, 113.

Kiso, Y., Sugiura, Y., Kitao, T. and Nishimura, K. (2001) Effects of hydrophobicity and molecular size on rejection of aromatic pesticides with nanofiltration membranes. Journal of Membrane Science 192(1-2), 1-10.

Koo, J.-Y., Petersen, R.J. and Cadotte, J.E. (1986) ESCA characterization of chlorine-damaged polyamide reverse osmosis membrane. ACS Polym. Prepr. 27(2), 391-392.

Koseoglu, H., Kabay, N., Yüksel, M., Sarp, S., Arar, Ö. and Kitis, M. (2008) Boron removal from seawater using high rejection SWRO membranes - impact of pH, feed concentration, pressure, and cross-flow velocity. Desalination 227(1-3), 253-263.

Kwon, Y.-N. (2005) Change of surface properties and performance due to chlorination of crosslinked polyamide membranes. PhD Thesis, Stanford University, Stanford.

Kwon, Y.-N. and Leckie, J.O. (2006a) Hypochlorite degradation of crosslinked polyamide membranes: I. Changes in chemical/morphological properties. Journal of Membrane Science 283(1-2), 21-26.

Kwon, Y.-N. and Leckie, J.O. (2006b) Hypochlorite degradation of crosslinked polyamide membranes: II. Changes in hydrogen bonding behavior and performance. Journal of Membrane Science 282(1-2), 456-464.

Kwon, Y.-N., Tang, C.Y. and Leckie, J.O. (2006) Change of membrane performance due to chlorination of crosslinked polyamide membranes. Journal of Applied Polymer Science 102, 5895.

Kwon, Y.-N., Tang, C.Y. and Leckie, J.O. (2008) Change of chemical composition and hydrogen bonding behavior due to chlorination of crosslinked polyamide membranes. Journal of Applied Polymer Science 108(4), 2061-2066.

Lee, K.P., Arnot, T.C. and Mattia, D. (2010) A review of reverse osmosis membrane materials for desalination - Development to date and future potential. Journal of Membrane Science 370(1-2), 1-22.

Leverenz, H.L. and Asano, T. (2011) Wastewater Reclamation and Reuse System. Treatise on Water Science. Wilderer, P. (ed), Elsevier, Oxford, 4, 63-71.

Li, D. and Wang, H. (2010) Recent developments in reverse osmosis desalination membranes. Journal of Materials Chemistry 20(22), 4551-4566.

Lonsdale, H.K., Merten, U. and Riley, R.L. (1965) Transport properties of cellulose acetate osmotic membranes. Journal of Applied Polymer Science 9(4), 1341-1362.

López-Muñoz, M.J., Sotto, A., Arsuaga, J.M. and Van der Bruggen, B. (2009) Influence of membrane, solute and solution properties on the retention of phenolic compounds in aqueous solution by nanofiltration membranes. Separation and Purification Technology 66(1), 194-201.

Lowell, J.R., Friesen, D.T., McCray, S.B., McDermot, S.D., Brose, D.J. and Ray, R.J. (1987) Model compounds as predictors of chlorine sensitivity of interfacial polymer reverse osmosis membranes, Tokyo.

Macedonio, F. and Drioli, E. (2008) Pressure-driven membrane operations and membrane distillation technology integration for water purification. Desalination 223(1-3), 396-409.

Mänttäri, M., Pihlajamäki, A. and Nyström, M. (2006) Effect of pH on hydrophilicity and charge and their effect on the filtration efficiency of NF membranes at different pH. Journal of Membrane Science 280(1-2), 311-320.

McMurry, J. (2004) Organic Chemistry, 6th ed, Brooks/Cole Publishing Company, Belmont.

Mehdizadeh, H. (2006) Membrane desalination plants from an energy-exergy viewpoint. Desalination 191(1-3), 200-209.

Mulder, M. (1996) Basic principles of membrane technology, 2nd Kluwer Academic Publishers, Dordrecht, the Netherlands.

Ng, H.Y. and Elimelech, M. (2004) Influence of colloidal fouling on rejection of trace organic contaminants by reverse osmosis. Journal of Membrane Science 244, 215.

Nghiem, L.D. and Schäfer, A.I. (2005) Trace contaminant removal with nanofiltration. Nanofiltration: Principles and Applications. Schafer, A.I., Fane, A.G. and Waite, T.D. (eds), Elsevier, Oxford, 480-502.

Nghiem, L.D., Schäfer, A.I. and Elimelech, M. (2004) Removal of natural hormones by nanofiltration membranes: Measurement, modeling, and mechanisms. Environmental Science & Technology 38, 1888.

Nghiem, L.D., Schäfer, A.I. and Elimelech, M. (2006) Role of electrostatic interactions in the retention of pharmaceutically active contaminants by a loose nanofiltration membrane. Journal of Membrane Science 286, 52.

Nghiem, L.D., Schäfer, A.I. and Waite, T.D. (2002) Adsorptive interactions between membranes and trace contaminants. Desalination 147, 269-274.

Orton, K.J.P. and Jones, W.J. (1909) CLXIII.—Primary interaction of chlorine and acetanilides. Journal of the Chemical Society, Transactions (95), 1456-1464.

Orton, K.J.P., Soper, F.G. and Williams, G. (1928) CXXXII.-The chlorination of anilides. Part III. N-chlorination and C-chlorination as simultaneous side reactions. Journal of the Chemical Society (Resumed), 998-1005.

Petersen, R.J. (1993) Composite reverse osmosis and nanofiltration membranes. Journal of Membrane Science 83(1), 81-150.

Petersen, R.J. and Cadotte, J.E. (1990) Thin film composite reverse osmosis membranes. Handbook of Industrial Membrane Technology. Porter, M.C. (ed), Noyes Publications, New Jersey, 307-348.

Raval, H.D., Trivedi, J.J., Joshi, S.V. and Devmurari, C.V. (2010) Flux enhancement of thin film composite RO membrane by controlled chlorine treatment. Desalination 250(3), 945-949.

Roeges, N.P.G. (1994) A guide to the complete interpretation of infrared spectra of organic structures, Wiley, New York.

Schäfer, A.I., Fane, A.G. and Waite, T.D. (2005) Nanofiltration: Principles and Applications, Elsevier, Oxford.

Seidel, A., Waypa, J.J. and Elimelech, M. (2001) Role of Charge (Donnan) Exclusion in Removal of Arsenic from Water by a Negatively Charged Porous Nanofiltration Membrane. Environmental Engineering Science 18(2), 105-113.

Shafer, J.A. (1970) Directing and activating effects of the amido group. The Chemistry of Amides Zabicky, J. (ed), Wiley Interscience, New York, 685-729.

Silberberg, M.S. (2006) Chemistry: the molecular nature of matter and change, 3rd ed, McGraw-Hill, New York.

Simon, A., Nghiem, L.D., Le-Clech, P., Khan, S.J. and Drewes, J.E. (2009) Effects of membrane degradation on the removal of pharmaceutically active compounds (PhACs) by NF/RO filtration processes. Journal of Membrane Science 340(1-2), 16-25.

Singh, R. (1994) Polyamide polymer solution behavior under chlorination conditions. Journal of Membrane Science 88 285-287.

Sivey, J.D. and Roberts, A.L. (2012) Assessing the Reactivity of Free Chlorine Constituents Cl2, Cl2O, and HOCl Toward Aromatic Ethers. Environmental Science & Technology 46(4), 2141-2147.

Soice, N.P., Greenberg, A.R., Krantz, W.B. and Norman, A.D. (2004) Studies of oxidative degradation in polyamide RO membrane barrier layers using pendant drop mechanical analysis. Journal of Membrane Science 243(1-2), 345-355.

Soice, N.P., Maladono, A.C., Takigawa, D.Y., Norman, A.D., Krantz, W.B. and Greenberg, A.R. (2003) Oxidative degradation of polyamide reverse osmosis membranes: Studies of molecular model compounds and selected membranes. Journal of Applied Polymer Science 90(5), 1173-1184.

Soltanieh, M. and Gill, W.N. (1981) Review of reverse osmosis membranes and transport models. Chemical Engineering Communications 12(4), 279 - 363.

Sourirajan, S. and Matsuura, T. (1985) Reverse Osmosis/Ultrafiltration Principles, National Research Council Canada.

Steinle-Darling, E. (2008) Rejection of Trace Organics - Nitrosamines, Perfluorochemicals, and Others - via Reverse Osmosis and Nanofiltration. Ph.D Thesis, Stanford University, Stanford.

Tang, C.Y., Chong, T.H. and Fane, A.G. (2011) Colloidal interactions and fouling of NF and RO membranes: A review. Advances in Colloid and Interface Science 164(1-2), 126-143.

Tang, C.Y., Fu, Q.S., Robertson, A.P., Criddle, C.S. and Leckie, J.O. (2006) Use of reverse osmosis membranes to remove perfluorooctane sulfonate (PFOS) from semiconductor wastewater. Environmental Science & Technology 40(23), 7343-7349.

Tang, C.Y., Kwon, Y.-N. and Leckie, J.O. (2007) Probing the nano- and micro-scales of reverse osmosis membranes: A comprehensive characterization of physiochemical properties of uncoated and coated membranes by XPS, TEM, ATR-FTIR, and streaming potential measurements. Journal of Membrane Science 287(1), 146-156.

Tang, C.Y., Kwon, Y.-N. and Leckie, J.O. (2009a) Effect of membrane chemistry and coating layer on physiochemical properties of thin film composite polyamide RO and NF membranes: I. FTIR and XPS characterization of polyamide and coating layer chemistry. Desalination 242(1-3), 149-167.

Tang, C.Y., Kwon, Y.-N. and Leckie, J.O. (2009b) Effect of membrane chemistry and coating layer on physiochemical properties of thin film composite polyamide RO and NF membranes: II. Membrane physiochemical properties and their dependence on polyamide and coating layers. Desalination 242(1-3), 168-182.

Taniguchi, M., Kurihara, M. and Kimura, S. (2001) Boron reduction performance of reverse osmosis seawater desalination process. Journal of Membrane Science 183(2), 259-267.

Tiraferri, A. and Elimelech, M. (2012) Direct quantification of negatively charged functional groups on membrane surfaces. Journal of Membrane Science 389, 499-508.

Uemura, T., Fujimaki, H. and Ikeda, T. (1991) Process of producing composite semipermeable membrane, US Patent 5,051,178.

Uemura, T., Himeshima, Y. and Kurihara, M. (1988) Interfacially synthesized reverse osmosis membrane, US Patent 4,761,234.

Urase, T. and Sato, K. (2007) The effect of deterioration of nanofiltration membrane on retention of pharmaceuticals. Desalination 202(1-3), 385-391.

Van der Bruggen, B., Mänttäri, M. and Nyström, M. (2008) Drawbacks of applying nanofiltration and how to avoid them: A review. Separation and Purification Technology 63(2), 251-263.

Van der Bruggen, B., Schaep, J., Maes, W., Wilms, D. and Vandecasteele, C. (1998) Nanofiltration as a treatment method for the removal of pesticides from ground waters. Desalination 117(1-3), 139-147.

Van der Bruggen, B., Vandecasteele, C., Gestel, T.V., Doyen, W. and Leysen, R. (2003) A review of pressure-driven membrane processes in wastewater treatment and drinking water production. Environmental Progress 22(1), 46-56.

Voudrias, E.A. and Reinhard, M. (1988a) A kinetic model for the halogenation of p-xylene in aqueous hypochlorous acid solutions containing chloride and bromide. Environmental Science & Technology 22(9), 1056-1062.

Voudrias, E.A. and Reinhard, M. (1988b) Reactivities of hypochlorous and hypobromous acid, chlorine monoxide, hypobromous acidium ion, chlorine, bromine, and bromine chloride in electrophilic aromatic substitution reactions with p-xylene in water. Environmental Science & Technology 22(9), 1049-1056.

Wade, L.G. (2006) Organic Chemistry, 6th ed, Pearson Prentice Hall, Upper Saddle River, New Jersey.

Watanabe, Y. and Kimura, K. (2011) Membrane Filtration in Water and Wastewater Treatment. Treatise on Water Science. Wilderer, P. (ed), Elsevier, Oxford, 4, 23-61.

White, G.C. (1986) The handbook of chlorination, 2nd ed, Van Nostrand Reinhold Co., New York.

White, G.C. (2010) White's Handbook of Chlorination and Alternative Disinfectants, 5th ed/ Black & Veatch Corporation, John Wiley & Sons Inc., New Jersey.

Wijmans, J.G. and Baker, R.W. (1995) The solution-diffusion model: a review. Journal of Membrane Science 107(1-2), 1-21.

Wilf, M. and Alt, S. (2000) Application of low fouling RO membrane elements for reclamation of municipal wastewater. Desalination 132, 11.

Wintgens, T., Melin, T., Schäfer, A., Khan, S., Muston, M., Bixio, D. and Thoeye, C. (2005) The role of membrane processes in municipal wastewater reclamation and reuse. Desalination 178(1-3), 1-11.

Zhai, X., Meng, J., Li, R., Ni, L. and Zhang, Y. (2011) Hypochlorite treatment on thin film composite RO membrane to improve boron removal performance. Desalination 274(1-3), 136-143.

Zhou, H. and Smith, D.W. (2001) Advanced technologies in water and wastewater treatment. Canadian Journal of Civil Engineering 28(1), 49-66.